

EMBRYONIC DEVELOPMENT IN VIRTUAL REALITY



Melek Rousian

EMBRYONIC DEVELOPMENT IN VIRTUAL REALITY

Melek Rousian

Embryonic development in virtual reality

Thesis, Erasmus University Rotterdam, The Netherlands

The research described in this thesis has been performed at the department of Obstetrics and Gynaecology, Subdivision of Obstetrics and Prenatal Medicine, Erasmus MC, Rotterdam, The Netherlands.

The printing of this thesis has been financially supported by the Department of Obstetrics and Gynaecology and the Department of Bioinformatics, Erasmus MC, Rotterdam, The Netherlands, Nederlandse Vereniging voor Obstetrie en Gynaecologie and the J.E. Jurriaanse Stichting.

Further support for this dissertation was kindly provided by:



life sciences
redefined



Medical Dynamics
Sorg-Saem

Cover: I-Space virtual reality image of an early foetus at 11 weeks gestational age, by Melek Rousian and Anton Koning. It is remarkable how outer structures can be visualized.

Lay-out and printing: Off page, www.offpage.nl

Copyright © 2011 Melek Rousian, Alblasterdam, The Netherlands, m.rousian@erasmusmc.nl. All rights reserved. No parts of this thesis may be published or transmitted in any form or by any means, electronic, or mechanical, including photocopying, recording or reproduced without written permission of the copyright owner.

EMBRYONIC DEVELOPMENT IN VIRTUAL REALITY

Embryonale ontwikkeling en virtuele realiteit

Proefschrift

ter verkrijging van de graad van doctor aan de
Erasmus Universiteit Rotterdam
op gezag van de rector magnificus

Prof. Dr. H.G. Schmidt

en volgens besluit van het College van Promoties.
De openbare verdediging zal plaatsvinden op
donderdag 24 november om 11.30 uur

door

Melek Rousian
geboren te Alblasserdam



PROMOTIECOMMISSIE

Promotoren: Prof. Dr. E.A.P. Steegers
Prof. Dr. P.J. van der Spek

Overige leden: Prof. Dr. R.M.H. Wijnen
Prof. Dr. W.J. Niessen
Prof. Dr. D. Oepkes

Copromotoren: Dr. N. Exalto
Dr. A.H.J. Koning

Paranimfen: Drs. J.C. van den Beukel
Drs. C.C. Zijderhoudt

Let love lead your soul.
Make it a place to retire to,
a kind of cave, a retreat
for the deep core of being.

(From: The soul of Rumi)

CONTENTS

PART 1	GENERAL INTRODUCTION	11
Chapter 1.1	Introduction	13
Chapter 1.2	Biometry, volumetry and staging in virtual reality	19
PART 2	REPRODUCIBILITY OF <i>IN VIVO</i> AND <i>IN VITRO</i> VOLUME MEASUREMENTS	31
Chapter 2.1	Early pregnancy volume measurements: validation of ultrasound techniques and new perspectives	33
PART 3	AUTOMATED EMBRYONIC VOLUME MEASUREMENTS TO IMPROVE OUR KNOWLEDGE ABOUT <i>IN VIVO</i> EMBRYOGENESIS	49
Chapter 3.1	An innovative virtual reality technique for automated human embryonic volume measurements	51
Chapter 3.2	Gestational sac fluid volume measurements in virtual reality	67
PART 4	NORMAL GROWTH DESCRIPTION OF NON-STANDARD BIOMETRIC MEASUREMENTS	81
Chapter 4.1	First trimester umbilical cord and vitelline duct measurements using virtual reality	83
Chapter 4.2	Virtual reality for embryonic measurements requiring depth perception	99
PART 5	EMBRYONIC BRAIN DEVELOPMENT, BIOMETRY AND VOLUMETRY	105
Chapter 5.1	First trimester embryonic brain development and volumetry using virtual reality	107
Chapter 5.2	Human embryonic growth and development of the cerebellum using three-dimensional ultrasound and virtual reality	125

PART 6	A SYSTEMATIC TOOL FOR DIAGNOSING FIRST TRIMESTER CONJOINED TWINS	143
Chapter 6.1	Diagnostic techniques and criteria for first trimester conjoined twin documentation: a review illustrated by case reports	145
PART 7	GENERAL DISCUSSION	169
PART 8	SUMMARY/SAMENVATTING	181
PART 9	AUTHORS AND AFFILIATIONS	191
	PUBLICATIONS AND AWARDS	192
	PORTFOLIO	194
	WORD OF THANKS/DANKWOORD	197

All movies can be found on the following webpage: <http://phdrouisian.erasmusmc.nl>

PART 1

GENERAL INTRODUCTION

PART 2



CHAPTER 1.1 INTRODUCTION

Organogenesis, which represents first trimester growth and development of the embryo, gestational sac and trophoblast, is a fast and complex process. Many adverse exposures can disturb embryogenesis, affecting both subsequent fetal as well as postnatal health¹⁻³. Before investigating the impact of different factors on first trimester growth and development, it is of great importance to define normal embryonic growth and development.

Human embryogenesis has been studied for centuries using *in vitro* specimen. Ronan O’Rahilly and Fabiola Müller revised three milestone text volumes in which human embryology was systematically described by Wilhelm His (1880-1885), Franklin Mall (1910-1912) and George Streeter (1942-1957), and updated their studies on the staging of human embryos⁴. Franklin Mall started collecting embryos (miscarriage specimen) in 1887 and this became the basis of the Carnegie Collection (Mall and Meyer, 1921). O’Rahilly and Müller’s book ‘Developmental stages in human embryos’ included a revision of Streeter’s work and a survey of the Carnegie Collection⁴. In their book the first 57 post-ovulatory days are described in detail using internal morphological, external morphological and histological criteria. This period is divided into 23 stages, and the last stage, stage 23 represents the end of the embryonic period, as at that moment all essential organ systems are present. Although the embryonic development has been studied in great detail using these stages, they are based on descriptions of *in vitro* specimen which is a marked disadvantage. Nowadays, *in vivo* visualization of the embryo is of vital importance for clinical care and *in vivo* research projects.

It was not until 1957 when it became possible to visualize the embryo *in vivo*. After the introduction of medical ultrasound and the visualization of the first fetus with ultrasound, the resolution improved, transvaginal ultrasound was developed and growth parameters and growth charts were constructed rapidly, resulting in a new era for *in vivo* diagnosis and follow-up from early pregnancy onwards.

These days, two-dimensional (2D) ultrasound examinations are performed routinely in the 2nd trimester of pregnancy, when all organ systems of the fetus are screened for abnormalities⁵. In the early first trimester ultrasound examinations are performed to confirm pregnancy location, viability and duration⁶. The early fetus can be screened for a number of abnormalities in the first trimester NT screening period (between 11+6 and 13+6 weeks GA)⁷⁻¹⁰. Studies are performed to find out what the detection rates are of abnormalities during the early and late first trimester¹¹⁻¹². Secondly, these improvements facilitate the construction of new charts and standards regarding embryonic and early fetal growth and development.

Another impressive development in the embryonic and fetal visualization has been the introduction of three-dimensional (3D) ultrasound in the 1980s. So far, the advantages seem mainly in the detection of external morphological abnormalities during the fetal period¹³. Due to the small size of an embryo and early fetus the whole pregnancy fits in a single transabdominal or transvaginal 3D ultrasound sweep. The relative large amount of amniotic fluid surrounding

the embryo ensures high quality 3D ultrasound datasets, showing the embryo in great detail. Although it offers many advantages, 3D ultrasound datasets are still assessed using 2D media (like computer screens), which implies that the information concerning the third dimension is not presented and used optimally.

Using a stereoscopic display or a virtual reality (VR) system allows optimal presentation of all three dimensions. A high-end VR system, like the Cave Automatic Virtual Environment (CAVE)¹⁸ immerses viewers in a virtual environment, allowing depth perception and interaction with the displayed 'hologram'. This technique can be a major step forward in visualizing 3D data.

In this thesis the use of VR in the assessment of human embryonic growth and development is described for which we have tentatively introduced the name 'virtual embryoscopy'. The research objectives were:

1. To establish the reproducibility of new embryonic biometric and especially volumetric measurements performed using VR (**part 2**).
2. To study embryonic development (such as the embryonic brain) in more detail and to provide growth charts in relation to GA and the CRL for newly introduced biometric and especially automated volumetric measurements (**parts 3 till 5**).
3. To describe the possibility of *in vivo* staging of the embryo based on internal and external morphologic characteristics and to relate this to GA, CRL, embryonic volume and brain ventricle volume (**part 5**).
4. To evaluate the applicability of this technology for diagnosing congenital anomalies such as first trimester conjoined twins (**part 6**).

REFERENCES

1. Barker DJ. The fetal and infant origins of adult disease. *BMJ*. 1990;301:1111.
2. Gluckman PD, Hanson MA, Cooper C, Thornburg KL. Effect of in utero and early-life conditions on adult health and disease. *NEJM*. 2008;359:61-73.
3. Mook-Kanamori DO, Steegers EA, Eilers PH, Raat H, Hofman A, Jaddoe VW. Risk factors and outcomes associated with first-trimester fetal growth restriction. *JAMA*. 2010;303:527-34.
4. O'Rahilly R, Muller F. Developmental stages in human embryos. Washington: Carnegie Institution of Washington Publication 1987.
5. Chervenak F, Isaacson G, Campbell S. The obstetric ultrasound examination Boston: Little Brown 1993.
6. Bottomley C, Van Belle V, Mukri F, Kirk E, Van Huffel S, Timmerman D, Bourne T. The optimal timing of an ultrasound scan to assess the location and viability of an early pregnancy. *Hum Reprod*. 2009;24:1811-7.
7. Nicolaides KH, Azar G, Byrne D, Mansur C, Marks K. Fetal nuchal translucency: ultrasound screening for chromosomal defects in first trimester of pregnancy. *BMJ*. 1992;304:867-9.
8. Nicolaides KH, Brizot ML, Snijders RJ. Fetal nuchal translucency: ultrasound screening for fetal trisomy in the first trimester of pregnancy. *BJOG*. 1994;101:782-6.
9. Brizot ML, Snijders RJ, Bersinger NA, Kuhn P, Nicolaides KH. Maternal serum pregnancy-associated plasma protein A and fetal nuchal translucency thickness for the prediction of fetal trisomies in early

- pregnancy. *Obstet Gynecol* 1994;84:918-22.
10. Brizot ML, Snijders RJ, Butler J, Bersinger NA, Nicolaides KH. Maternal serum hCG and fetal nuchal translucency thickness for the prediction of fetal trisomies in the first trimester of pregnancy. *BJOG*. 1995;102:127-32.
 11. Timor-Tritsch IE, Fuchs KM, Monteagudo A, D'Alton M E. Performing a fetal anatomy scan at the time of first-trimester screening. *Obstet Gynecol*. 2009;113:402-7.
 12. Ebrashy A, El Kateb A, Momtaz M, El Sheikhah A, Aboulghar MM, Ibrahim M, Saad M. 13-14-week fetal anatomy scan: a 5-year prospective study. *Ultrasound Obstet Gynecol*. 2010;35:292-6.
 13. Timor-Tritsch IE, Platt LD. Three-dimensional ultrasound experience in obstetrics. *Curr Opin Obstet Gynecol*. 2002;14:569-75.
 14. Falcon O, Peralta CF, Cavoretto P, Faiola S, Nicolaides KH. Fetal trunk and head volume measured by three-dimensional ultrasound at 11 + 0 to 13 + 6 weeks of gestation in chromosomally normal pregnancies. *Ultrasound Obstet Gynecol*. 2005;26:263-6.
 15. Lee W, Deter RL, McNie B, Goncalves LF, Espinoza J, Chaiworapongsa T, Romero R. Individualized growth assessment of fetal soft tissue using fractional thigh volume. *Ultrasound Obstet Gynecol*. 2004;24:766-74.
 16. Rousian M, Verwoerd-Dikkeboom CM, Koning AH, Hop WC, van der Spek PJ, Exalto N, Steegers EA. Early pregnancy volume measurements: validation of ultrasound techniques and new perspectives. *BJOG*. 2009;116:278-85.
 17. Blaas HG, Eik-Nes SH, Berg S, Torp H. In-vivo three-dimensional ultrasound reconstructions of embryos and early fetuses. *Lancet* 1998;352:1182-6.
 18. Cruz-Neira C SD, DeFanti T. Surround-screen projection-based virtual reality: the design and implementation of the CAVE (tm). *Proceedings of the 20th annual conference on computer graphics and interactive techniques*. 1993:135-42.



CHAPTER 1.2 BIOMETRY, VOLUMETRY AND STAGING IN VIRTUAL REALITY

Melek Rousian, Christine M. Verwoerd-Dikkeboom, Anton H.J. Koning,
Peter J. van der Spek, Niek Exalto, Eric A.P. Steegers

Partly based on the article 'Innovative three-dimensional imaging: opportunities
for virtual embryoscopy'

Ned Tijdschr Geneeskd. 2010; 154:A1606.

Three-dimensional ultrasound

Since the introduction of three-dimensional (3D) ultrasound during the 1980s hundreds of articles have been published in medical literature describing the application of this technique in obstetrics and prenatal medicine. A single 3D dataset acquired in the end first trimester allows for full off-line evaluation of standard anatomical landmarks¹. The multiplanar sectional plane mode is used, allowing the examiner to rotate the 3D dataset around three orthogonal axes, and to scroll through the datasets in order to obtain the required plane for checking and measuring the structure of interest (figure 1). The possibility of evaluating additional anatomical landmarks, besides the already used growth parameters (like the crown-rump length, gestational sac diameter, yolk sac diameter) during the early first trimester is nowadays being studied in detail; especially using 2D techniques²⁻⁴.

Once a 3D ultrasound dataset has been acquired and stored (figure 2) unique information can be collected by performing off-line volume calculations. Both hypoechoic and hyperechoic structures can be measured manually and hypoechoic structures even semi-automatically, immediately on the ultrasound machine or later on a personal computer using specialized software. Examples of volume measurements in the first trimester are placental volume, amniotic fluid volume, yolk sac volume and fetal body volume (usually without including the volume of the limbs)²⁻⁵. The brain cavities can also be segmented and visualized,

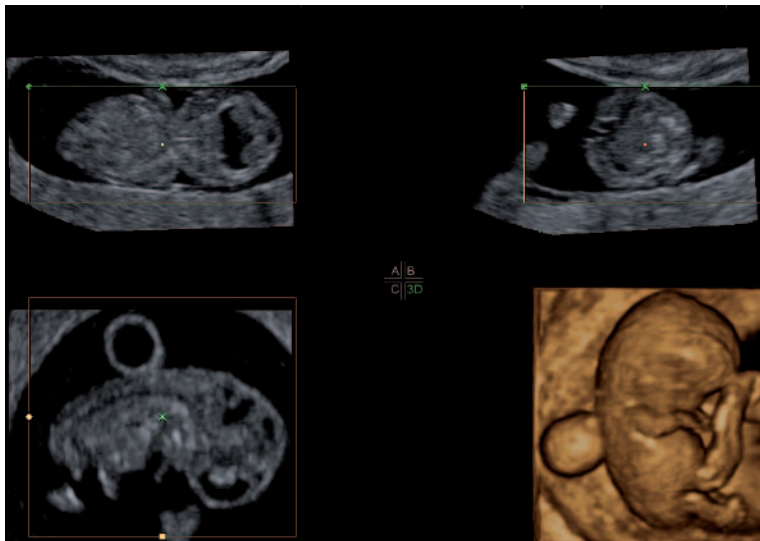


Figure 1. A 3D ultrasound dataset, obtained using a transvaginal probe, of an embryo at 10+1 weeks gestational age (GA) is shown in the multiplanar sectional plane mode of the 4D View application. The A plane represents the coronal view, the B plane the axial view and the C plane the sagittal view of the embryo. The final image shows a 3D rendering of the embryo.



Figure 2. A 3D rendering by 4D View of a nine-week old embryo.

although most applications can not determine their volume due to the small size⁵⁻⁶. Blaas *et al.* were able to measure the brain ventricle volume in the first trimester of pregnancy with an in-house developed system⁷.

The I-Space virtual reality system

Three-dimensional ultrasound has many advantages compared to two-dimensional (2D) ultrasound. Unfortunately the 3D images are currently viewed and assessed using 2D media like ordinary computer screens. These 2D media do not offer depth perception, which is required for optimal interpretation of 3D and four-dimensional (4D) ultrasound images. On March 24th, 2005 the department of Bioinformatics of the Erasmus MC in Rotterdam opened a Barco I-Space virtual reality (VR) system. The Erasmus MC I-Space uses passive 3D projection (i.e. based on polarization) to offer different images to the left and right eye. The two images show the same objects, but viewed from a slightly different angle. The brain is capable of constructing a single 3D image out of these two 2D projected images (figure 3).

In the Erasmus MC eight Barco SIM5 projectors are installed behind or above the four projection screens (2.60 x 1.95 meters), which form the floor, left, right and front walls of the I-Space (figure 4). In every corner of this room an infrared camera (four in total) is installed for tracking purposes. The tracking system registers the position and orientation of the user's head, in order to provide him with the correct perspective, and a joystick. The wireless four-button plus hat-switch joystick is used to operate a specialized volume rendering application called V-Scope, which was developed to allow visualization of and interaction

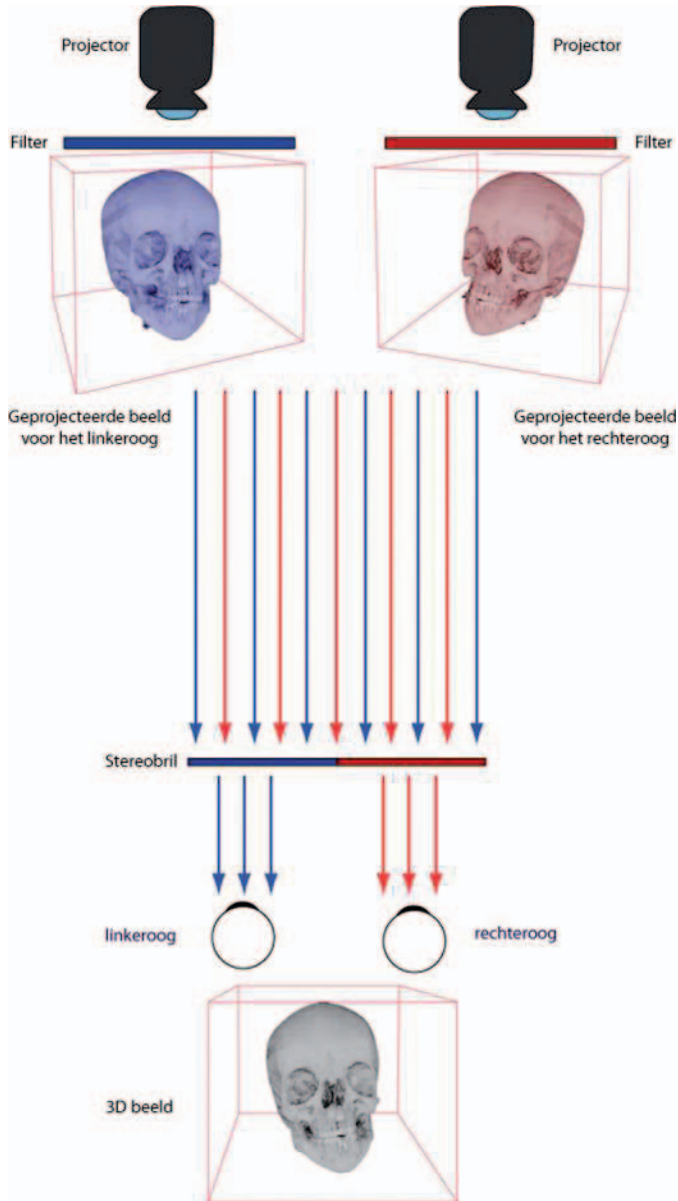


Figure 3. Illustration of stereoscopic imaging in the I-Space. The two images are projected through two different filters, illustrated as a red filter and a blue filter. The observer wears glasses, and in these glasses similar filters (red and blue) have been placed. With the right (red) filter, only the light from the right projector is visible. With the left (blue) filter only the light of the left projector is visible. This forces the viewer to see a different image with each eye. Since it is in fact the same object, but viewed in a slightly different angle, this results in depth perception. The I-Space does not use red and blue filters, but circular polarizing filters, which have the same effect, but allow full color images to be viewed.

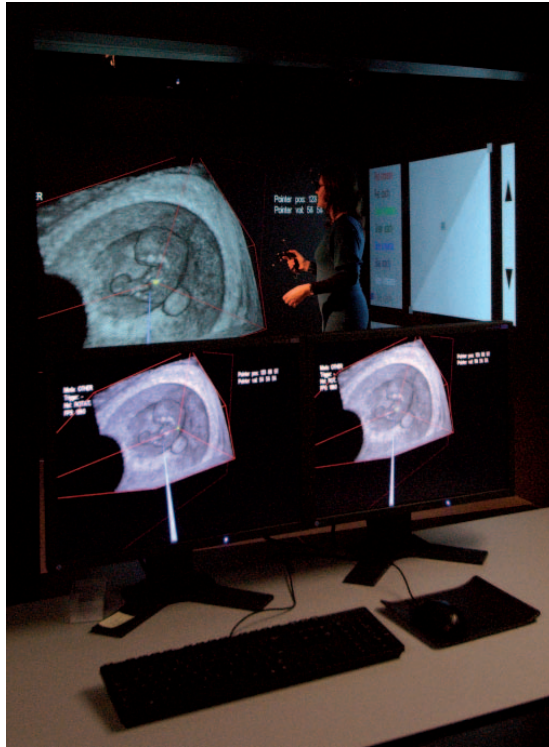


Figure 4. Picture of an observer (MR) in the Barco I-Space. An embryo of eight weeks' GA is projected on the walls.

with volumetric datasets, like 3D ultrasound, CT and MRI⁸. The joystick emits a virtual pointer and is used to enlarge and rotate the hologram, and cut it with a clipping plane in any arbitrary direction. V-Scope also allows the user to change the grey scale, color and opacity of the data. In addition to the clipping plane a virtual eraser can brush away parts to get the best view of the object of interest. Finally, V-Scope also implements several tools to perform optimal biometric and volumetric measurements.

It is possible to change the scale, orientation, grey scale, color and opacity of the data. The clipping plane and brush function enable the user to 'cut' away or brush away parts to get the best view of the object of interest. In addition to these tools, it is possible to perform optimal biometric and volumetric measurements.

Biometry

An integrated 'tracing tool' allows 3D length measurements by placing two or more measuring points (or 'calipers'). Standard biometric measurements like the crown-rump length (CRL) (movie 1), biparietal diameter (BPD), occipito-frontal diameter (OFD) and abdominal diameter (AD) can be performed by placing two calipers⁹.

Movie 1. This movie presents a CRL measurement performed at 10 weeks gestational age. The virtual pointer is used to perform the length measurement in the I-Space VR system.

This technique is also valuable for non-standard biometric measurements like the width of the hip, knee, elbow, shoulder and the length of the ear and foot⁹. The length of the umbilical cord and vitelline duct are measured by placing multiple calipers along the length of the structure (figure 5). The diameter and thickness of the cerebellum are measured using the same principle. Depth perception and 3D interaction enables measuring of new non-standard biometric parameters and verification of accurate placement of the calipers for precise and reliable measurements¹⁰. As a result the use of VR may improve prenatal care.

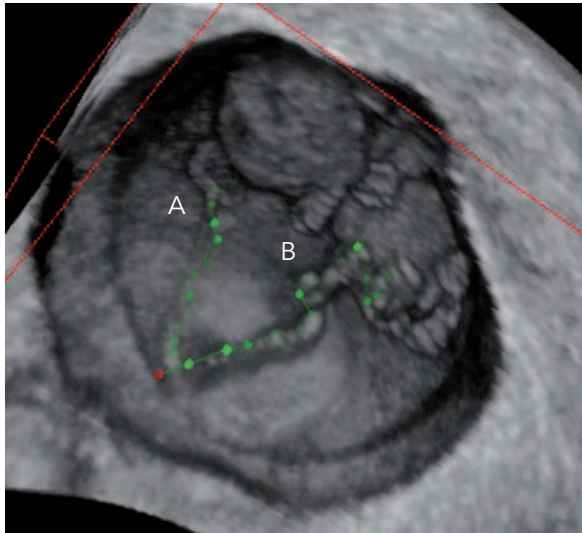


Figure 5. A screen shot of an I-Space hologram of nine weeks' GA. The length of the vitelline duct (A) and umbilical cord (B) is traced.

Volumetry

A volume is defined as the amount of space that is present within an object or solid shape. The use of 3D ultrasound datasets enables volumetric measurements of structures during the first trimester of pregnancy. These measurements can be used as parameters for fetal growth. One way to obtain these measurements is to count the number of voxels in (side) a structure. A voxel, short for Volumetric Picture Element, is the 3D equivalent of the better known 2D pixel, and represents a value on a regular grid in three dimensional space (Source: Wikipedia).

As human beings are three dimensional, only a 3D dataset can fully capture all parameters of growth and development. 2D measurements (like the CRL) are just derived parameters.

V-Scope allows the user to perform volume measurements using a semi-automated segmentation algorithm. This algorithm is based on a region-growing approach in combination with a neighborhood variation threshold, as originally proposed for MRI data by Myers and Brinkley¹¹. The algorithm has been modified to handle the speckles in ultrasound data by simplifying some of the parameters of the original algorithm and (optionally) smoothing the grey level data. The user selects an upper and lower grey level threshold and an upper threshold for the variance of the voxel's neighborhood. After placing a seed point the algorithm will segment (grow) the region by adding connected voxels that fall within the thresholds. Using this function, the volumes of hyperechoic and hypoechoic structures, like the gestational sac, brain ventricles and embryonic body, can be measured. Prior to a volume measurement, connections to other structures with the same gray value range have to be brushed away to avoid segmentation of other parts than the structure of interest. If a structure consists of both hyperechoic and hypoechoic parts, like the embryonic body, the segmentation must be performed in two steps. V-Scope can automatically add the segments and calculate the total volume.

If the segmentation is not perfect, the user can place additional seed points, manually grow or shrink the segmented region or use the brush function to add or delete voxels from the segmented structure.

Staging

The Carnegie Staging system has been used almost a century to describe human embryonic development¹²⁻¹³. The different stages are based on internal and external morphological and histological criteria, and do not include the gestational age and length of the embryo. Ultrasound can be used to study the embryogenesis *in vivo* (movie 2), but until now only possibilities of staging embryos based on some external morphological criteria have been evaluated¹⁴.

Movie 2. This 2D movie presents 3D ultrasound datasets of different embryos at different gestational ages as rendered by the V-Scope VR application. The observer (MR) uses different functions to get the best impression of the developing embryo.

Abnormal growth and development

The measurement of the crown-rump length (CRL) is the cornerstone in first trimester obstetric care and was described first by Robinson^{2, 15-17}. If the CRL does not match the gestational age based on the last menstrual period, the duration of pregnancy may be different as result of a late ovulation or late

implantation. A discordant CRL measurement may also be an indication of early growth retardation¹⁸, a pregnancy which is going to end as a miscarriage¹⁹ or a chromosomal abnormality²⁰⁻²¹. Recently, studies have shown that the maternal age, ethnic background of the mother and fetal sex also affect the CRL²²⁻²³. Additionally, variation in first trimester growth of the developing embryo can be caused by environmental factors such as nutrition (folate intake) and other life-style factors such as smoking²⁴. It is therefore important to perform the CRL measurement correctly and in case of abnormalities consider all possible explanations. This will aid in the detection of growth problems early in pregnancy. This thesis describes the possibility of first trimester prediction of intra uterine growth restriction in the second and third trimester using the CRL and embryonic volume.

The V-Scope application is also being used to evaluate the clinical value of VR for early detection and description of embryonic and fetal congenital malformations. In different case studies the additional value of this approach is described²⁵⁻²⁷. Included in this thesis are three cases of conjoined twins. Depth perception allows optimal visualization of complex embryonic structures like the limbs and central nervous system. We plan to further study the possibilities of detecting embryonic defects early in pregnancy, especially in high risk patients due to their genetic and/or medical background, using this new technique.

In conclusion, VR opens new ways of studying embryonic and early fetal growth and development *in vivo*. Secondly, biometry, volumetry and morphology can be studied optimally using VR. Applying these techniques may contribute to prenatal diagnostics being brought forward from the second and third trimester to the first trimester of pregnancy, entering a new area of embryonic medicine.

REFERENCES

1. Fauchon DE, Benzie RJ, Wye DA, Cairns DR. What information on fetal anatomy can be provided by a single first-trimester transabdominal three-dimensional sweep? *Ultrasound Obstet Gynecol.* 2008;31:266-70.
2. Robinson HP, Fleming JE. A critical evaluation of sonar "crown-rump length" measurements. *BJOG.* 1975;82:702-10.
3. Blaas HG, Eik-Nes SH. Sonoembryology and early prenatal diagnosis of neural anomalies. *Prenat Diagn.* 2009;29:312-25.
4. Grisolia G, Milano K, Pilu G, Banzi C, David C, Gabrielli S, Rizzo N, Morandi R, Bovicelli L. Biometry of early pregnancy with transvaginal sonography. *Ultrasound Obstet Gynecol.* 1993;3:403-11.
5. Pistorius L, Stoutenbeek P, Visser GH. First trimester neurosonoembryology with automated follicle tracking: preliminary findings. *J Matern Fetal Neonatal Med.* 2009;22:949-51.
6. Timor-Tritsch IE, Monteagudo A, Santos R. Three-dimensional inversion rendering in the first- and early second-trimester fetal brain: its use in holoprosencephaly. *Ultrasound Obstet Gynecol.* 2008;32:744-50.
7. Blaas HG, Eik-Nes SH, Berg S, Torp H. In-vivo three-dimensional ultrasound reconstructions of embryos and early fetuses. *Lancet.* 1998;352:1182-6.
8. Koning AH, Rousian M, Verwoerd-Dikkeboom CM, Goedknecht L, Steegers EA, van der Spek PJ. V-scope: design and implementation of an immersive and desktop virtual reality volume visualization system. *Stud Health Technol Inform.* 2009;142:136-8.
9. Verwoerd-Dikkeboom CM, Koning AH, Hop WC, van der Spek PJ, Exalto N, Steegers EA. Innovative virtual reality measurements for embryonic growth

- and development. *Hum Reprod.* 2010;25:1404-10.
10. Verwoerd-Dikkeboom CM, Koning AH, Hop WC, Rousian M, Van Der Spek PJ, Exalto N, Steegers EA. Reliability of three-dimensional sonographic measurements in early pregnancy using virtual reality. *Ultrasound Obstet Gynecol.* 2008;32:910-6.
 11. Myers LM, Brinkley JF. Visualization of Brain Surface Features Using Registered Partially Segmented MRI Scans. SPIE Medical Imaging. 1995:43-52.
 12. O'Rahilly R, Muller F. Developmental stages in human embryos. Washington: Carnegie Institution of Washington Publication 1987.
 13. O'Rahilly R, Muller F. Developmental stages in human embryos: revised and new measurements. *Cells Tissues Organs.* 2010;192:73-84.
 14. Verwoerd-Dikkeboom CM, Koning AH, van der Spek PJ, Exalto N, Steegers EA. Embryonic staging using a 3D virtual reality system. *Hum Reprod.* 2008;23:1479-84.
 15. Bottomley C, Van Belle V, Mukri F, Kirk E, Van Huffel S, Timmerman D, Bourne T. The optimal timing of an ultrasound scan to assess the location and viability of an early pregnancy. *Hum Reprod.* 2009;24:1811-7.
 16. Robinson HP. Sonar measurement of fetal crown-rump length as means of assessing maturity in first trimester of pregnancy. *BMJ.* 1973;4:28-31.
 17. Bottomley C, Bourne T. Dating and growth in the first trimester. *Best Pract Res Clin Obstet Gynaecol.* 2009;23:439-52.
 18. Bukowski R, Smith GC, Malone FD, Ball RH, Nyberg DA, Comstock CH, Hankins GD, Berkowitz RL, Gross SJ, Dugoff L, Craigo SD, Timor-Tritsch IE, Carr SR, Wolfe HM, D'Alton ME. Fetal growth in early pregnancy and risk of delivering low birth weight infant: prospective cohort study. *BMJ.* 2007;334:836.
 19. Mantoni M, Pedersen JF. Fetal growth delay in threatened abortion: an ultrasound study. *BJOG.* 1982;89:525-7.
 20. Bahado-Singh RO, Lynch L, Deren O, Morrotti R, Copel JA, Mahoney MJ, Williams J, 3rd. First-trimester growth restriction and fetal aneuploidy: the effect of type of aneuploidy and gestational age. *Am J Obstet Gynecol.* 1997;176:976-80.
 21. Schemmer G, Wapner RJ, Johnson A, Schemmer M, Norton HJ, Anderson WE. First-trimester growth patterns of aneuploid fetuses. *Prenat Diagn.* 1997;17:155-9.
 22. Bottomley C, Daemen A, Mukri F, Papa-georghiou AT, Kirk E, Pexsters A, De Moor B, Timmerman D, Bourne T. Assessing first trimester growth: the influence of ethnic background and maternal age. *Hum Reprod.* 2009;24:284-90.
 23. Bukowski R, Smith GC, Malone FD, Ball RH, Nyberg DA, Comstock CH, Hankins GD, Berkowitz RL, Gross SJ, Dugoff L, Craigo SD, Timor-Tritsch IE, Carr SR, Wolfe HM, D'Alton ME, Consortium FR. Human sexual size dimorphism in early pregnancy. *Am J Epidemiol.* 2007;165:1216-8.
 24. Mook-Kanamori DO, Steegers EA, Eilers PH, Raat H, Hofman A, Jaddoe VW. Risk factors and outcomes associated with first-trimester fetal growth restriction. *JAMA.* 2010;303:527-34.
 25. Verwoerd-Dikkeboom CM, Koning AH, Groenenberg IA, Smit BJ, Brezinka C, Van Der Spek PJ, Steegers EA. Using virtual reality for evaluation of fetal ambiguous genitalia. *Ultrasound Obstet Gynecol.* 2008;32:510-4.
 26. Verwoerd-Dikkeboom CM, van Heesch PN, Koning AH, Galjaard RJ, Exalto N, Steegers EA. Embryonic delay in growth and development related to confined placental trisomy 16 mosaicism, diagnosed by I-Space Virtual Reality. *Fertil Steril.* 2008;90:2017.e19-22.
 27. Groenenberg IA, Koning AH, Galjaard RJ, Steegers EA, Brezinka C, van der Spek PJ. A virtual reality rendition of a fetal meningomyelocele at 32 weeks of gestation. *Ultrasound Obstet Gynecol.* 2005;26:799-801.

PART 1

PART 2

PART 3

REPRODUCIBILITY OF
IN VIVO AND *IN VITRO*
VOLUME MEASUREMENTS



CHAPTER 2.1

EARLY PREGNANCY VOLUME
MEASUREMENTS: VALIDATION
OF ULTRASOUND TECHNIQUES
AND NEW PERSPECTIVES

ABSTRACT

Objective To investigate accuracy and reliability of four different ultrasound related volume-measuring methods.

Design Observational study.

Setting Both *in vitro* and *in vivo*.

Population or Sample Ten phantoms for *in vitro* measurements and 28 pregnancies with gestational ages ranging from six to 11 weeks for *in vivo* measurements were included.

Methods Three-dimensional (3D) ultrasound images of phantoms (with known variable contents) and yolk sacs were used to calculate volumes using four different methods; Virtual Organ Computed-Aided Analysis (VOCAL), Inversion mode, Sono Automatic Volume Calculation (SonoAVC) and V-Scope. V-Scope is a newly developed 3D volume visualisation application using a Barco I-Space Virtual Reality system. Intra- and interobserver agreement was established by calculating intraclass correlation coefficients (ICC).

Main Outcome Measures Evaluation of accuracy and reliability by comparing the different techniques with true volumes (*in vitro*) and with each other (*in vitro* and *in vivo*).

Results In the *in vitro* study volume measurements by VOCAL, Inversion mode and V-Scope proved to be accurate. SonoAVC measurements resulted in a substantial systematic underestimation. Correlation coefficients of measured versus true volumes were excellent in all four techniques. For all techniques an intra- and interobserver agreement of at least 0.91 was found. Yolk sac measurements by the different techniques proved to be highly correlated (ICCs > 0.91).

Conclusions We demonstrated that VOCAL, Inversion mode and V-Scope can all be used to measure volumes of hypoechoic structures. The newly introduced V-Scope application proved to be accurate and reliable.

Keywords VOCAL; Inversion mode; SonoAVC; V-Scope; Virtual Reality; yolk sac volumes

Melek Rousian, Christine M. Verwoerd-Dikkeboom, Anton H.J. Koning, Wim C. Hop, Peter J. van der Spek, Niek Exalto, Eric A.P. Steegers

BJOG. 2009;116:278-285

INTRODUCTION

Until recently mathematical formulae were used to estimate volumes using two dimensional (2D) ultrasound images. For instance the prolate ellipsoid or trapezoid formula, is used for measuring ovarian volumes¹ and the ellipsoid formula for foetal bladder volume calculations². In such volume calculations, a certain regularity of shape of the structure is assumed and correction for surface irregularities is not possible.

The introduction of three dimensional (3D) ultrasound allows visualisation of planes that cannot be obtained using 2D ultrasound. In this way volumetric measurements without geometric assumptions as well as corrections or assessments of surface irregularities are obtainable.

Computer software programs have been developed for volume measurements, either incorporated into the ultrasound equipment or for off-line evaluation on personal computers. Conventional volume measurements involve the delineation of the object of interest in one plane of the multiplanar display. Several *in vitro*³ and *in vivo*⁴ studies for validation of volume measurements demonstrated this to be an accurate and reliable technique. The operator can conduct as many serial slices as needed so that less regularly shaped or larger objects can also be measured^{5, 6, 7}.

The introduction of the Virtual Organ Computer-Aided AnaLysis (VOCAL™) imaging program makes it possible to measure volumes by rotation around a central axis. Raine-Fenning et al⁸ demonstrated that this rotational technique is better than the conventional measuring method. After several *in vitro*⁸ and *in vivo*^{9, 10, 11} experiments the VOCAL imaging application is now considered to be the 'gold standard' for volume measurements in ultrasound imaging.

In this paper we evaluate three other volume-measuring techniques that use grey level information instead of delineation. Inversion mode is a thresholding algorithm that has been available for several years. It makes visualisation and volume calculation of fluid-filled structures possible in 3D and four dimensional (4D) ultrasound images^{12, 13, 14}.

In 2008 GE Medical Systems recently introduced the Sono Automatic Volume Calculation (SonoAVC) technique on the Voluson E8 ultrasound system. This new algorithm allows semi-automatic measurements of volumes, mean diameters and absolute dimensions of hypoechoic regions in a 3D ultrasound dataset^{11, 15}.

The latest technique uses a Virtual Reality (VR) system to benefit from all three dimensions offered by 3D ultrasound datasets. In this study we will use the V-Scope application in a Barco I-Space, a system that uses stereo projection on three screens and the floor to immerse viewers in a 3D world. This application has already been successfully applied to 3D prenatal ultrasonography¹⁶⁻²⁰. A region growing segmentation algorithm has been implemented in this program that calculates the volume of selected structures of interest semi-automatically.

The aim of this study is to investigate the accuracy and reliability of currently available volume measuring methods and of the two newly introduced techniques, SonoAVC and V-scope, both *in vitro* and *in vivo* settings. Robust establishment of accuracy and reliability is needed as a validation before these techniques can be applied in daily clinical practice.

METHODS

Our study was performed using a 3.7-9.3 MHz transvaginal probe of the GE Voluson 730 Expert system (GE, Zipf, Austria) for the *in vivo* part and a 1.9-7.8 MHz abdominal probe of the GE Voluson E8 (GE, Zipf, Austria), which recently became available at our department, for the *in vitro* part. Four dimensional view (version 5.0 and 7.0, GE Kretz, Zipf, Austria) software was used to explore and visualise the data sets and to measure volumes using VOCAL, inversion mode and SonoAVC. The fourth, innovative, application used in our study, V-scope, is not available on ultrasound machines or personal computers. Since 2004, the department of Bioinformatics of the Erasmus MC in The Netherlands operates a BARCO I-Space. The I-Space is a so-called 4-walled CAVE-like²¹ (Cave Automatic Virtual Environment) VR system, allowing depth perception and interaction with the rendered objects in an intuitive manner. We use an in-house developed volume rendering application¹⁷ (CAVORE, which in 2008 was renamed to V-Scope).

VOCAL

VOCAL is a volume-measuring algorithm based on 2D segmentations around a central rotational axis. The user can specify the number of rotational steps. Kusanovic et al¹² described this volume measuring method in detail. The user is able to define the rotation step and the mode of interest. The software calculates the volumes of the structures automatically, which are expressed in cubic centimetres. A 'manual mode' can be chosen, allowing drawing around the object of interest with the use of a computer mouse in the A, B or C plane. Measurements can then be performed in various degrees of rotational steps.

Inversion mode

This segmentation algorithm uses grey scale voxels (3D pixels or volume elements) in the 3D dataset for volumetric measurements²². Only hypoechoic regions can be estimated with the inversion mode, because it uses a single upper threshold after inverting the grey value. Kusanovic et al¹² already provided a detailed description and manual of this system. As inversion mode is a global operator, working on the entire dataset, it is necessary to erase incorrectly segmented areas, before calculating the segmented volume. Inversion mode can also be used in combination with VOCAL, where the contour serves as a delineation of the 'volume of interest'.

SonoAVC

SonoAVC is a new algorithm that identifies and quantifies hypoechoic regions within a 3D dataset and provides automatic estimation of their absolute dimensions (x, y, z diameters), mean diameter and volume¹⁵. It was originally developed for measurements of follicle volumes, and therefore can produce multiple volumes as a result of the segmentation. SonoAVC works only within a specified region of interest (ROI), and only inner volumes can be estimated.

Similar to inversion mode, SonoAVC calculates volumes by counting all volume elements (voxels) within hypoechoic regions and converting them to a standard unit (cm³).

Post-processing is available for correction by allowing the user to add or delete incorrectly segmented areas. If there are aberrances in the ROI, the 'growth' or 'separation' function can also be used¹⁵.

V-Scope

The V-Scope application is used to create a 'hologram' of the ultrasound image that can be manipulated by means of a virtual pointer, controlled by a wireless joystick. Three dimensional ultrasound datasets can be transferred to the BARCO I-Space, after transformation to Cartesian (rectangular) volumes. For use in the V-Scope application, we have implemented a flexible and robust segmentation algorithm that does not depend on 2D interaction, like the VOCAL algorithm. The algorithm is based on a region-growing approach in combination with a neighborhood variation threshold, as proposed for magnetic resonance imaging data by Myers and Brinkley²³. The algorithm has been modified to accommodate the 'noisy nature' of ultrasound data: in addition to simplifying some of the parameters of the original algorithm, the grey level and variation thresholds are applied to a 'blurred version' of the original data, to average out most of the noise²⁴.

The user selects an upper and lower grey level threshold, and an upper threshold for the SD based on the characteristics of the target area. A seed point in the area and the algorithm will segment out (grow) the region starting from the seed point. SD threshold will stop the region growing when it reaches a tissue interface.

When evaluating the yolk sac, the tissue interface (the 'skin' of the yolk sac) is recorded much wider than it really is. To correct this the user can manually grow (or shrink) the segmented region. In addition, should the region have grown outside the actual object (for instance as a result of noise or drop outs) or part of the object have been skipped (due to artefacts), a spherical, freehand 'paint brush' can be used to add voxels to or delete voxels from the segmented object.

In vitro study

For the *in vitro* part of our study, we placed a water-filled object in an ultrasound test reservoir. This reservoir contained a tissue-mimicking fluid medium, created by a suspension of graphite particles in sterile water and glycerine. We used simple structured objects; water balloons filled with different volumes of sterile

water. A total of ten balloons were filled with 1.0, 1.3, 1.5, 1.8, 2.0, 2.2, 2.3, 2.5, 2.8 and 3.0 millilitre of volume respectively. One observer acquired all of the different ultrasound data sets of the objects using the Voluson E8 (figure 1). Dynamic range was set at 12, harmonics was set on low and 3D volumes were acquired at maximum quality. All images were stored for off-line evaluation. Another observer evaluated the quality and completeness of the data sets, and for each balloon, the best image was selected.

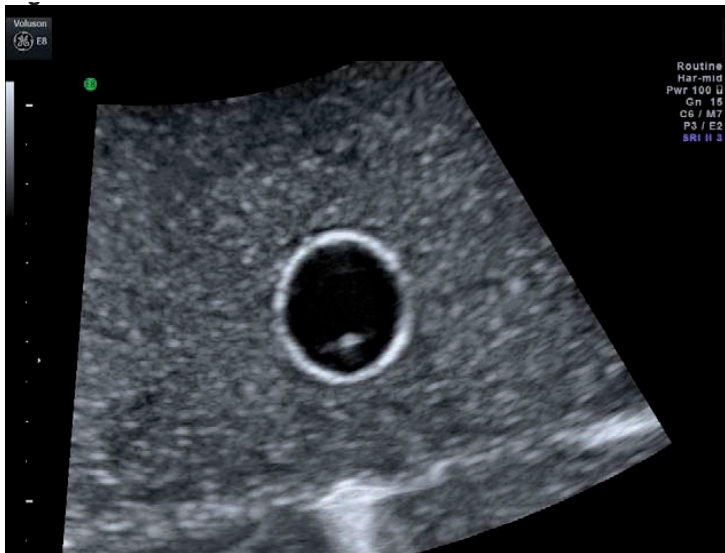


Figure 1. Image of a water balloon on the ultrasound machine (Voluson E8).

Volumes of the balloons were measured with all four techniques (figure 2). For VOCAL, we used rotational angles of 15° and 30° . The inversion mode technique was applied without the VOCAL option. In the SonoAVC application, the 'growth' function was set to maximum and the 'separation' function to minimum.

All volume measurements were repeated three times; mean values were used for comparison of the techniques. The observer was blinded for the true volume of the balloons. All measurements were performed twice by one observer (M.R.) and repeated independently by another (C.M.V-D). The second series of measurements by M.R. were performed at least two weeks later than the first series to prevent recollection bias. The observers were blinded to each other's results.

The duration of time required to obtain all measurements was registered by observer one, to evaluate applicability in daily clinical practice. Timing was started when the data were loaded and ended when the final estimated volume was shown.

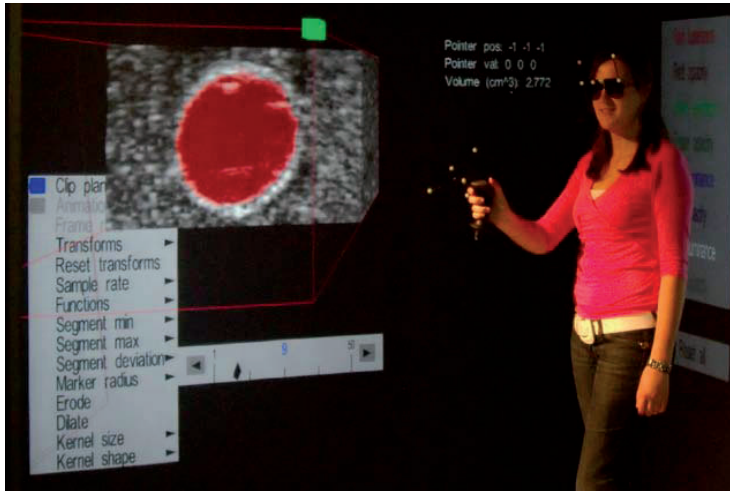


Figure 2. I-Space image of a water balloon. The red color marks the segmented volume. The true volume of the water balloon was 2.8 milliliters.

In vivo study

To evaluate the use of the four different techniques in daily clinical practice, 24 pregnancies were examined at a median gestational age of 9 weeks (range 6–11 weeks) to visualise the yolk sac in 3D. These data sets were obtained in another study to evaluate embryonic growth and development by Verwoerd et al²⁰. We used the yolk sac as our object of interest, since it is an easy to identify, well-defined fluid-filled structure. All measurements using the four different techniques were performed off-line (figure 3) as described in the *in vitro* part and repeated three times; mean values of these three assessments were used for comparison. The duration of time required to obtain measurements was monitored as described in the *in vitro* section.

Statistical analysis

Data analysis was performed using SPSS (SPSS Release 12.0.1 for Windows, SPSS Inc, Chicago, IL, USA).

In the *in vitro* part of the study, the accuracy and reliability were investigated. To assess the accuracy of the different techniques, differences between measured volumes and true volumes were calculated and compared with the paired t-test. A P value of 0.05 (two sided) was considered the limit of significance. In addition, Pearson correlation coefficients were calculated of measured against true volumes.

Reliability is the extent to which we can assume that a measurement will yield the same result if repeated a second time. To assess this, intraclass correlation coefficients (ICC) were used. In addition, we tested both intraobserver and interobserver reliability for all four measuring methods. For good agreement, ICC has to be 0.90 or higher.

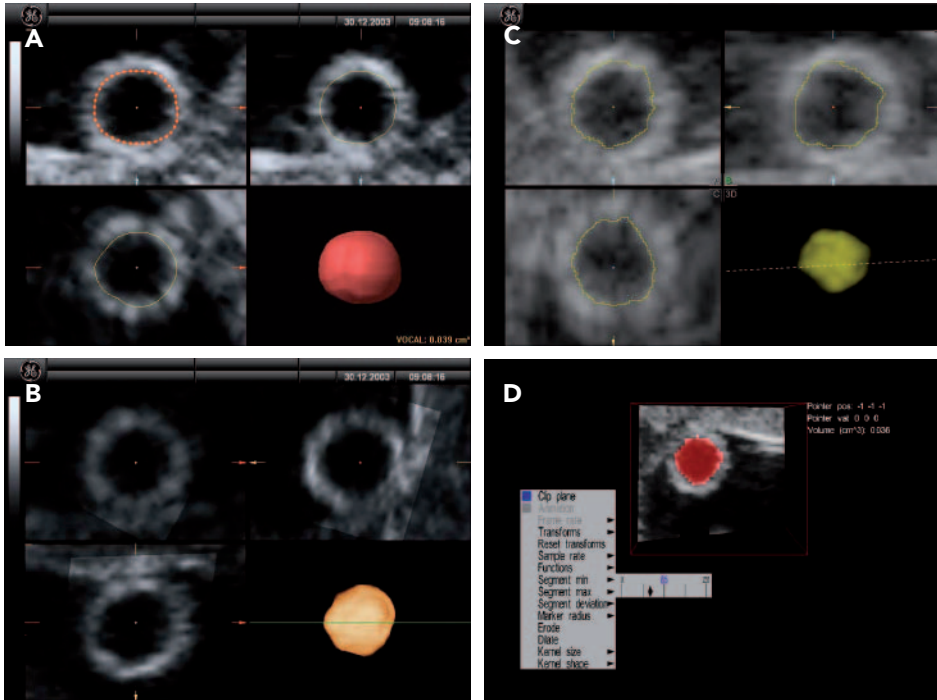


Figure 3. Images of yolk sac (66 days of gestational age) volume measurements obtained by four different techniques. **(A)** VOCAL. The balloon is traced in the A plane, and the estimated volume is 0.039 cm³. **(B)** Inversion mode. The estimated volume is 0.04 cm³. **(C)** SonoAVC. The 3D image shows an estimated volume of 0.04 cm³. **(D)** V-Scope. The segmented volume is marked with a color. The volume of the yolk sac is 0.036 cm³.

In the *in vivo* part of the study ICCs were calculated for all four measuring methods as described for the *in vitro* part. We further calculated the mean difference and limits of agreement (mean difference \pm 1.96SD) as described by Bland and Altman²⁵ to show the agreement between measurements when different methods are used. The mean time needed to perform volume measurements, the associated SDs and the time ranges were calculated for the *in vitro* and *in vivo* part.

RESULTS

In vitro study

Of the original ten water-filled balloons, in seven balloons, image quality was good enough to perform volume measurements with all four different techniques. These seven balloons contained 1.3, 2.0, 2.2, 2.3, 2.5, 2.8 and 3.0 ml of sterile water respectively.

Table I shows the mean differences between the measured volumes and the real volumes, with the corresponding significance. For VOCAL, inversion mode and V-Scope, there are no significant differences. SonoAVC, however, demonstrates a systematic underestimation (mean difference of -0.63 for both observers) of the measured volume compared with the true volume (both $P < 0.001$). All measured volumes correlate well with the true volume (all correlation coefficients > 0.91 , both for observer one and observer two).

Table II shows the agreement between measurements performed by the same observer (intraobserver variability) and the agreement between two different observers (interobserver variability). ICCs were all greater than 0.99 , representing excellent agreement in all women.

Table I. Evaluation of accuracy of the *in vitro* study using the different techniques of volume estimation.

Observer	Technique	Mean difference (cm ³)	Standard deviation of differences (cm ³)	95% CI of the difference (cm ³)	P-value
Observer 1	VOCAL 30°	0.019	0.063	-0.039 to 0.780	0.449
	VOCAL 15°	0.020	0.055	-0.031 to 0.071	0.371
	Inversion	0.011	0.063	-0.047 to 0.069	0.662
	SonoAVC	-0.632	0.240	-0.854 to -0.410	< 0.001
	V-Scope	0.011	0.035	-0.022 to 0.043	0.449
Observer 2	VOCAL 30°	0.023	0.112	-0.081 to 0.127	0.605
	VOCAL 15°	0.015	0.105	-0.082 to 0.113	0.716
	Inversion	-0.007	0.080	-0.081 to 0.067	0.822
	SonoAVC	-0.626	0.243	-0.851 to -0.402	< 0.001
	V-Scope	-0.010	0.006	-0.025 to 0.004	0.135

The mean difference between measured volumes minus the real volumes of the balloons with the associated standard deviation and 95% confidence interval (CI) are displayed. The results of both observers are displayed.

Table II. Intraobserver (ICC-A) and interobserver (ICC-B) correlation coefficients of the *in vitro* study.

Technique	ICC-A	95% CI ICC-A	ICC-B	95% CI ICC-B
VOCAL 30°	0.998	0.990 to > 0.999	0.995	0.971 to 0.999
VOCAL 15°	0.999	0.996 to > 0.999	0.993	0.962 to 0.999
Inversion	0.998	0.988 to > 0.999	0.995	0.973 to 0.999
SonoAVC	0.999	0.994 to > 0.999	0.996	0.980 to 0.999
V-Scope	0.998	0.992 to > 0.999	0.997	0.982 to 0.999

In vivo study

Yolk sac volumes could be measured with VOCAL, inversion mode and V-Scope in all 24 ultrasound scans. With SonoAVC, we were not able to measure the volume of four yolk sacs. All techniques were compared to each other and ICCs were calculated. Results of these comparisons are reported in Table III. In all women, the ICC is at least 0.91, suggesting good reliability. The best ICC with narrowest CI is demonstrated between V-Scope and VOCAL. The mean difference and 95% limits of agreement are displayed in Table III.

Results of the time required for each separate volume calculation are shown in Table IV. In the *in vitro* study, VOCAL is fastest and V-Scope slowest when compared to the other techniques. All the comparisons result in statistically significant differences ($P < 0.001$). However, in the *in vivo* study, V-Scope is faster than the other techniques (for all comparisons: $P < 0.004$) and has the smallest time range. VOCAL 15° takes the most time (for all comparisons: $P < 0.001$).

DISCUSSION

In this study, we tested the accuracy and reliability of four different 3D ultrasound volume-measuring methods in both an *in vitro* and an *in vivo* setting. Clinical use of volume measurements using 3D ultrasound is likely to become increasingly

Table III. Evaluation of reliability of the yolk sac volume measurements.

Technique	N	Mean difference* (cm ³)	95% CI of mean difference (cm ³)	Limits of agreement** (cm ³)	ICC	95% CI of ICC
VOCAL 30° vs VOCAL 15°	24	-0.001	-0.003 to 0.003	-0.004 to 0.002	0.996	0.990 to 0.998
VOCAL 30° vs Inversion	24	-0.004	-0.013 to 0.001	-0.010 to 0.003	0.963	0.715 to 0.989
VOCAL 30° vs SonoAVC	20	0.002	-0.008 to 0.012	-0.007 to 0.012	0.958	0.884 to 0.984
VOCAL 30° vs V-Scope	24	-0.000	-0.004 to 0.004	-0.005 to 0.004	0.992	0.981 to 0.996
Inversion vs SonoAVC	20	0.006	-0.003 to 0.020	-0.004 to 0.016	0.909	0.340 to 0.975
Inversion vs V-Scope	24	0.003	-0.004 to 0.016	-0.006 to 0.012	0.943	0.777 to 0.981
SonoAVC vs V-Scope	20	-0.002	-0.012 to 0.006	-0.012 to 0.007	0.956	0.879 to 0.983

N is the number of yolk sacs that could be compared.

* Mean difference is calculated as technique 1 minus technique 2.

** Limits of agreement are calculated as mean difference $\pm 1.96SD$.

Table IV. Time required to perform one volume measurement using the different techniques.

Study	Technique	Mean time \pm SD (seconds)	Range (seconds)
<i>In vitro</i> part	VOCAL 30°	66 \pm 9	51 to 86
	VOCAL 15°	110 \pm 12	89 to 129
	Inversion mode	78 \pm 17	50 to 118
	SonoAVC	99 \pm 25	40 to 142
	V-Scope	123 \pm 78	40 to 281
<i>In vivo</i> part	VOCAL 30°	96 \pm 29	56 to 160
	VOCAL 15°	159 \pm 24	89 to 208
	Inversion mode	112 \pm 28	65 to 197
	SonoAVC	81 \pm 23	41 to 134
	V-Scope	61 \pm 22	29 to 117

important in the study of human reproduction and embryogenesis. In recent years, new techniques have been developed for estimating volumes in 3D. This is the first study comparing four of these techniques; VOCAL, inversion mode, SonoAVC and V-Scope.

We have limited our research to measurements of hypochoic structures, since only these structures can be measured by all four techniques. However, hyperechoic structures, such as the fetal body and placenta, can also be measured using VOCAL and V-Scope.

VOCAL is considered to be an important development in volume measurements in 3D ultrasound images. The *in vitro* study by Raine-Fenning et al.⁸ demonstrated that VOCAL is more reliable and accurate in calculating volumes than conventional methods. Using an angle of 30° for performing the volume measurements showed good accuracy, especially when regularly shaped structures were measured. In our study, we used both the 30° and 15° rotational angles, to verify that their conclusion also applies to very small structures. We did not find significant differences between the two volume angles.

Although VOCAL is generally recognized as the gold standard for performing volumetric measurements, it does have some limitations.

The *in vitro* study performed by Raine-Fenning et al.⁸ showed that VOCAL has a tendency to overestimate true volumes. In our study, we do not find a tendency of overestimation, neither *in vitro* nor *in vivo*. Another limitation is the time required for measuring the volume of interest. Different studies illustrate that the time needed to perform the volumetric measurements can range between 1 and 10 minutes^{8, 11, 12, 26}. The greater the angle is, the shorter the measuring time. In our study mean time for VOCAL measurements was shorter than usually reported in the literature. This can probably be explained by the fact that we used only

regularly shaped structures. This also means that, using the VOCAL approach, possible inaccuracies when measuring very irregularly shaped volumes cannot be excluded. Finally, it can be difficult to determine the boundaries of some structures because of shadows, other structures²⁶ or dispersion of the boundaries in women with limited image quality.

Inversion mode was mainly developed to generate information about the anatomical and pathological characteristics of fluid-filled structures; for instance, the visualisation of abnormal systemic venous connections¹⁴. In addition to visualisation, volume measurements can be performed¹³ with a high degree of reliability, when compared with other techniques like VOCAL¹². Kusanovic et al¹² concluded that inversion mode had larger volume measurements than VOCAL, which they contributed to the fact that relatively high threshold levels were chosen⁸. A limitation of their study was that accuracy could not be evaluated, since the true volumes were not known. They also concluded that inversion mode is a slightly faster technique than VOCAL. We found this to be true only for the rotational angle of 15°. We show with the *in vitro* part of our study that the accuracy and reliability of volume measurements performed with the inversion mode are very high. Like VOCAL, image quality is very important when using inversion mode. Adjustments in contrast, threshold and transparency may improve image quality. In our study, the combination of the 'surface smooth' and 'gradient light' filters produced the best 3D images, although visualisation problems still persisted. Especially, dispersion of the borders from the structures of interest was found to affect the outcome of the volume estimation.

In 2008, SonoAVC has become available as a semi-automatic volume measuring application, which has the potential to remove observer bias and to reduce the time needed for measurements¹⁵. Studies have shown that SonoAVC is able to provide highly accurate automatic follicular volume measurements in a short time, especially when image quality is high^{15, 27}. Again image quality greatly influences the ability to measure volumes. If noise speckles are present in the data set, SonoAVC will measure the volume of interest without these speckles (including an area surrounding each speckle), producing a substantial underestimation. In some women the post-processing tools in SonoAVC can be used to improve the value of the measurement, but this is at the cost of extending the time required for measuring the volumes.

In the *in vitro* part of our study, we found that SonoAVC gives a substantial systematic underestimation of the phantoms. All speckles visible within the phantom images were not included into the volume calculation, and this led to an underestimation of the true volumes. This underestimation persisted even after the use of post-processing tools. For the *in vivo* study, in 4 of the 24 yolk sacs, SonoAVC could not be applied due to image quality problems. The remaining 20 yolk sac volumes were in concordance with the other measuring techniques. We therefore conclude that SonoAVC is a reliable measuring method, but very dependent on image quality and with a tendency to underestimate true volume.

Since post-processing tools had to be used in all women, we do not consider this technique to be 'automatic' in a true sense.

The I-Space uses stereo projection, which makes it possible to visualise a 'real' 3D ultrasound image. Studies using this VR technology have demonstrated that it provides additional insights¹⁶⁻²⁰, especially where structures that need depth for accurate interpretation of size and position are concerned. Verwoerd et al²⁰ already demonstrated the reliability of this system in measuring standard human embryonic biometry. The volume-measuring tool of V-Scope is a new development. Our study reveals that accuracy and reliability are very good. In the *in vitro* part of this study, V-Scope measurements took the longest time. This can be attributed to the low image quality of two of the balloons. In these two objects, ultrasound fall-out created an apparent gap in the shell of the balloons, and therefore, voxels outside of the balloons were also included. Erasing these voxels is a time-consuming process. Disregarding these balloons brings the time required in line with the other methods.

The basis of every measuring method, accuracy, was tested in the *in vitro* part of this study. VOCAL and V-Scope turns out to have the best correlation coefficients when measured volumes are compared with the true volumes. Both applications measure the volumes without a statistically significant difference. SonoAVC gives a substantial systematic underestimation of the volumes. Inter- and intraobserver variability reveals very good results (ICC > 0.90) for all four techniques. The *in vivo* part of this study demonstrates that for yolk sac volumes, all four techniques are capable of making precise measurements. Feasibility, an important aspect for implementation in daily clinical practice, is good in general for all four systems. In the *in vitro* setting VOCAL 30° and in the *in vivo* study V-Scope are the fastest techniques, but time alone is not the most important factor. Image quality greatly influences the time needed to measure a volume, and may be related to several factors such as maternal obesity and oligohydramnios. Especially for the (semi-) automatic volume - measuring methods (SonoAVC and V-scope), good image quality reduces measuring time. In women with poor image quality, SonoAVC is very labour-intensive, mainly as a result of the post-processing required. Although V-Scope is currently only available in the Erasmus MC I-Space, it is being adapted to run on a desktop system using a 3D auto-stereoscopic computer monitor. The advantage of this type of display is that it can be used without any viewing aids, i.e. without 3D polarizing glasses. These low-cost VR displays may well become available embedded in daily clinical practice in the near future.

As V-Scope performs at least as good as the established VOCAL technique, it can be used in research on human embryogenesis. Measurements can be made of any volume such as the entire embryo, the amniotic sac or the embryonic brain. After obtaining reference values of early pregnancy volumes, associations can be studied with clinical outcomes such as miscarriage, congenital abnormalities and intra-uterine growth restriction. This technique, tentatively called Virtual Embryoscopy, may help to improve our knowledge on embryonic growth and development.

REFERENCES

1. Pavlik EJ, DePriest PD, Gallion HH, Ueland FR, Reedy MB, Kryscio RJ, van Nagell JR. Ovarian volume related to age. *Gynecol Oncol.* 2000;77:410-2.
2. Fagerquist M, Fagerquist U, Oden A, Blomberg SG. Fetal urine production and accuracy when estimating fetal urinary bladder volume. *Ultrasound Obstet Gynecol.* 2001;17:132-9.
3. Berg S, Torp H, Blaas HG. Accuracy of in-vitro volume estimation of small structures using three-dimensional ultrasound. *Ultrasound Med Biol.* 2000;26:425-32.
4. Nosir YF, Fioretti PM, Vletter WB, Boersma E, Salustri A, Postma JT, Reijs AE, Ten Cate FJ, Roelandt JR. Accurate measurement of left ventricular ejection fraction by three-dimensional echocardiography. A comparison with radionuclide angiography. *Circulation.* 1996;94:460-6.
5. Aviram R, Shpan DK, Markovitch O, Fishman A, Tepper R. Three-dimensional first trimester fetal volumetry: comparison with crown rump length. *Early Hum Dev.* 2004;80:1-5.
6. Falcon O, Peralta CF, Cavoretto P, Faiola S, Nicolaidis KH. Fetal trunk and head volume measured by three-dimensional ultrasound at 11 + 0 to 13 + 6 weeks of gestation in chromosomally normal pregnancies. *Ultrasound Obstet Gynecol.* 2005;26:263-6.
7. Hoesli IM, Surbek DV, Tercanli S, Holzgreve W. Three dimensional volume measurement of the cervix during pregnancy compared to conventional 2D-sonography. *Int J Gynaecol Obstet.* 1999;64:115-9.
8. Raine-Fenning NJ, Clewes JS, Kendall NR, Bunkheila AK, Campbell BK, Johnson IR. The interobserver reliability and validity of volume calculation from three-dimensional ultrasound datasets in the in vitro setting. *Ultrasound Obstet Gynecol.* 2003;21:283-91.
9. Moeglín D, Talmant C, Duyme M, Lopez AC. Fetal lung volumetry using two- and three-dimensional ultrasound. *Ultrasound Obstet Gynecol.* 2005;25:119-27.
10. Peixoto-Filho FM, Sa RA, Lopes LM, Velarde LG, Marchiori E, Ville Y. Three-dimensional ultrasound fetal urinary bladder volume measurement: reliability of rotational (VOCAL) technique using different steps of rotation. *Arch Gynecol Obstet.* 2007;276:345-9.
11. Raine-Fenning NJ, Campbell BK, Clewes JS, Johnson IR. The interobserver reliability of ovarian volume measurement is improved with three-dimensional ultrasound, but dependent upon technique. *Ultrasound Med Biol.* 2003;29:1685-90.
12. Kusanovic JP, Nien JK, Goncalves LF, Espinoza J, Lee W, Balasubramaniam M, Soto E, Erez O, Romero R. The use of inversion mode and 3D manual segmentation in volume measurement of fetal fluid-filled structures: comparison with Virtual Organ Computer-aided AnaLysis (VOCAL®). *Ultrasound Obstet Gynecol.* 2008;31:177-86.
13. Messing B, Cohen SM, Valsky DV, Rosenak D, Hochner-Celnikier D, Savchev S, Yagel S. Fetal cardiac ventricle volumetry in the second half of gestation assessed by 4D ultrasound using STIC combined with inversion mode. *Ultrasound Obstet Gynecol.* 2007;30:142-51.
14. Espinoza J, Goncalves LF, Lee W, Mazor M, Romero R. A novel method to improve prenatal diagnosis of abnormal systemic venous connections using three- and four-dimensional ultrasonography and 'inversion mode'. *Ultrasound Obstet Gynecol.* 2005;25:428-34.
15. Raine-Fenning N, Jayaprakasan K, Clewes J. Automated follicle tracking facilitates standardization and may improve work flow. *Ultrasound Obstet Gynecol.* 2007;30:1015-8.
16. Groenenberg IA, Koning AH, Galjaard RJ, Steegers EA, Brezinka C, van der Spek PJ. A virtual reality rendition of a fetal meningomyelocele at 32 weeks of gestation. *Ultrasound Obstet Gynecol.* 2005;26:799-801.
17. Verwoerd-Dikkeboom CM, Koning AHJ, van der Spek PJ, Exalto N, Steegers EAP. Embryonic staging using a 3D Virtual Reality System. *Hum Reprod.* 2008;23:1479-84.
18. Verwoerd-Dikkeboom CM, van Heesch PNACM, Koning AHJ, Galjaard RJH, Exalto N, Steegers EAP. Embryonic delay in growth and development related to confined placental trisomy 16 mosaicism, diagnosed by Virtual Reality. *Fertil Steril.* 2008;90:2017.e19-22.
19. Verwoerd-Dikkeboom CM, Koning AHJ, Groenenberg IAL, Smit BJ, Brezinka C, Van der Spek PJ, Steegers EA. Using Virtual Reality for Evaluation of Fetal

- Ambiguous Genitalia. *Ultrasound Obstet Gynecol.* 2008;32:510-4.
20. Verwoerd-Dikkeboom CM, Koning AHJ, Hop W, Rousian M, van der Spek PJ, Exalto N, Steegers EA. Reliability of early pregnancy measurements in 3D using Virtual Reality. *Ultrasound Obstet Gynecol.* 2008;32:910-6.
 21. Cruz-Neira C SD, DeFanti T. Surround-screen projection-based virtual reality: the design and implementation of the CAVE (tm). *Proceedings of the 20th annual conference on computer graphics and interactive techniques.* 1993;135-42.
 22. Lee W, Goncalves LF, Espinoza J, Romero R. Inversion mode: a new volume analysis tool for 3-dimensional ultrasonography. *J Ultrasound Med.* 2005;24:201-7.
 23. Myers LM, Brinkley JF. Visualization of Brain Surface Features Using Registered Partially Segmented MRI Scans. In: *Image Display: SPIE Medical Imaging.* 1995: 43-52.
 24. Shapiro LG, Stockman GL. *Computer Vision: Prentice Hall;* 2001.
 25. Bland JM, Altman DG. Statistical methods for assessing agreement between two methods of clinical measurement. *Lancet.* 1986;1:307-10.
 26. Yaman C, Jesacher K, Polz W. Accuracy of three-dimensional transvaginal ultrasound in uterus volume measurements; comparison with two-dimensional ultrasound. *Ultrasound Med Biol.* 2003;29:1681-4.
 27. Raine-Fenning N, Jayaprakasan K, Clewes J, Joergner I, Bonaki SD, Chamberlain S, Devlin L, Priddle H, Johnson I. SonoAVC: a novel method of automatic volume calculation. *Ultrasound Obstet Gynecol.* 2008;31:691-6.

PART 2

PART 3

PART 4

AUTOMATED EMBRYONIC
VOLUME MEASUREMENTS
TO IMPROVE OUR
KNOWLEDGE ABOUT
IN VIVO EMBRYOGENESIS



CHAPTER 3.1

AN INNOVATIVE VIRTUAL REALITY
TECHNIQUE FOR AUTOMATED
HUMAN EMBRYONIC VOLUME
MEASUREMENTS

ABSTRACT

Background The recent introduction of virtual reality (VR) enables us to use all three dimensions in a three-dimensional (3D) image. The aim of this prospective study was to evaluate an innovative VR technique for automated 3D volume measurements of the human embryo and yolk sac in first trimester pregnancies.

Methods We analyzed 180 3D first trimester ultrasound scans of 42 pregnancies. Scans were transferred to an I-Space VR system and visualized as 3D 'holograms' with the V-Scope volume rendering software. A semi-automatic segmentation algorithm was used to calculate the volumes.

The logarithmically transformed outcomes were analyzed using repeated measurements ANOVA. Interobserver and intraobserver agreement was established by calculating intraclass correlation coefficients (ICCs).

Results 88 embryonic volumes (EVs) and 118 yolk sac volumes (YSV) were selected and measured between 5⁺⁵ and 12⁺⁶ weeks of gestational age (GA). EV ranged from 14 mm³ to 29 877 mm³ and YSV ranged from 33 mm³ to 424 mm³. ANOVA calculations showed that when the crown-rump length doubles, the mean EV increases 6.5 fold and when the GA doubles, the mean EV increases 500 fold ($p < 0.001$). Furthermore, it was found that a doubling in GA results in a 3.8 fold increase of the YSV and when the CRL doubles, the YSV increases 1.5 fold ($p < 0.001$). Interobserver and intraobserver agreement were both excellent with ICCs of 0.99.

Conclusions We measured the human EV and YSV in early pregnancy using a VR system. This innovative technique allows us to obtain unique information about the size of the embryo using all dimensions which may be used to differentiate between normal and abnormal human development.

Keywords Embryonic volume; fetal volume; virtual reality; 3D ultrasound; first trimester

Melek Rousian, Anton H.J. Koning, Robbert H.J. van Oppenraaij, Wim C. Hop, Christine M. Verwoerd-Dikkeboom, Peter J. van der Spek, Niek Exalto, Eric A.P. Steegers

Hum Reprod. 2010;25:2210-2216

INTRODUCTION

First trimester ultrasound is widely used for early pregnancy localization and assessment of viability. The crown-rump length (CRL) measurement is used for an accurate determination of gestational age (GA)¹. From recent studies on first trimester dating and growth, however, it is now known that a smaller than expected CRL may also be related to impaired embryonic growth². The latter is not only associated with first trimester miscarriage³ and aneuploidy⁴⁻⁵, but also with fetal growth restriction in the second and third trimester of pregnancy^{2, 6-7}. As a consequence there is a growing interest in tools for more precise measurement of embryonic growth.

A better assessment of embryonic growth by embryonic volume measurements in comparison to CRL measurements has been suggested in several studies⁸⁻¹⁰. Because of the irregular shape of the embryo, however, it is difficult to acquire accurate embryonic volume (EV) measurements. The first successful attempt was published by Blaas et al.¹¹. The authors used vaginal three-dimensional (3D) ultrasound data and segmented the objects by manually drawing contours in several parallel two-dimensional (2D) slices. Polyhedrons were created, using specialized software, to define the surface and volume of these objects. This group reported that a significant proportion of the EV is represented by the limbs¹². Others used the Virtual Organ Computer Added anaLysis (VOCAL™) method, which makes it possible to accomplish rotational volume measurements. These volume estimations are performed by drawing contours around the embryo in various rotational steps, without including the limbs, resulting in a fetal trunk and head volume only^{9-10, 13}.

In a virtual reality (VR) system, such as the I-Space, high resolution 3D ultrasound datasets can be visualized as holograms with optimal depth perception. We use the V-Scope volume rendering application to benefit from all three dimensions in the immersive I-Space (Barco, Belgium) VR system (figure 1). The combination of V-Scope and the I-Space has already been successfully applied to 3D prenatal ultrasonography¹⁴⁻¹⁸. Even the classical staging system of embryonic development, the Carnegie stages, could be determined by inspecting the embryo from different angles¹⁷.

Recently a region growing segmentation algorithm, which calculates the volume of selected structures of interest semi-automatically, has been implemented in V-Scope. The algorithm was validated by Rousian et al.¹⁵ both *in vitro* and *in vivo*, using balloons and yolk sacs. The next step is to test the V-Scope technique for complex structures like the embryo, including the limbs. Although the measurements were performed in the embryonic as well as in the early fetal period, in this manuscript we use the term embryo throughout.

The aim of this study was to evaluate the use of an automated VR application for volume measurements of first trimester human embryos, including the limbs. We also measured the human yolk sac volumes and studied the interobserver and intraobserver variability of the EV measurements.



Figure 1. Image of the I-Space VR system. The datasets are projected on the floor and three walls by eight different projectors. An embryo of 10 weeks and 4 days gestational age is projected on the walls.

PATIENTS AND METHODS

Patient selection

A group of 50 volunteering pregnant women, without any predisposing condition or medication use that could interfere with normal embryonic growth, was included in a longitudinal first trimester 3D ultrasound study¹⁶⁻¹⁷. Written informed consent was obtained, and the regional committee for medical ethics approved the study. We performed 3D ultrasound scans in the 25 spontaneous and 25 IVF/ICSI pregnancies, which were made serially from about 6-8 weeks to 12 weeks of gestation. GA was calculated using the first day of the last menstrual period, and in cases of an unknown last menstrual period or a discrepancy of more than a week, GA was determined by the CRL measurements performed in the first trimester. For the IVF/ICSI pregnancies the GA was based on the date of oocyte retrieval. During the ultrasound examinations, three patients were found to have twin pregnancies and two patients were diagnosed with non-viable pregnancy. These patients were excluded during the examination period. One patient was diagnosed with a placental confined trisomy 16 mosaicism¹⁸ and two patients developed severe placental insufficiency during the second half of pregnancy. We also excluded these ultrasound examinations. Data from 42 women, consisting of 21 spontaneous and 21 IVF/ICSI pregnancies, remained in our study cohort. In this group a total of 180 3D ultrasound scans were performed, with a mean of 4.3 ultrasound scans per patient (standard deviation (SD): 1.7 scans).

Not all 180 images could be visualized optimally in the I-Space and since this is the first study describing embryonic and yolk sac growth by using a VR application, we included the images with the best image quality only. So images were excluded because the embryonic features could not be recognized due to poor image quality or because they were lacking parts of the embryo or the yolk sac. Finally, 88 images of the embryo of 40 women and 118 images of the yolk sac of 41 women remained for further study.

Ultrasound measurements

Our study was performed using a 3.7-9.3 MHz transvaginal probe of the GE Voluson 730 Expert system (GE, Zipf, Austria). The 3D ultrasound scans were acquired by examiner CMV. Later, the scans were stored as Cartesian volumes using specialized 3D software (4D View, version 5.0, GE Medical Systems) and visualized using the I-Space, a so-called four-walled CAVE™-like¹⁹ (Cave Automatic Virtual Environment) VR system.

I-Space measurements

The V-Scope²⁰ application is used to create an interactive hologram of the ultrasound image that can be manipulated by means of a virtual pointer, controlled by a wireless joystick. To perform volume measurements, this application includes a flexible and robust segmentation algorithm that is based on a region-growing

approach in combination with a neighbourhood variation threshold, as originally proposed for magnetic resonance imaging data by Myers and Brinkley²¹. The algorithm has been modified to handle the speckles in ultrasound data by simplifying some of the parameters of the original algorithm and smoothing the grey level data using a Gaussian blur. The user selects an upper and lower grey level threshold and an upper threshold for the SD of the voxels neighbourhood. A seed point is placed and the algorithm will segment (grow) the region starting from the seed point. The SD threshold will stop the region growing when it reaches a tissue interface.

Prior to the volume measurement the embryonic insertion of the umbilical cord and the vitelline duct insertion at the yolk sac have to be 'brushed' away with the eraser to avoid segmentation of other parts than the whole-body or yolk sac. To measure the volume of the embryo first the hyperechoic structures have to be segmented (movie 3), followed by the hypoechoic structures (the brain ventricles). For the yolk sac volume (YSV) measurement, first the hypoechoic interior and then the hyperechoic shell has to be segmented. V-Scope can automatically add the segments and calculate the total volume.

Movie 3. In this movie an embryo is shown of 10 weeks gestational age. First, the surrounding structures are 'brushed' away, and next to this the embryonic volume is segmented automatically (red). This movie gives an impression of the I-Space, but we have to be aware that we are looking at a 3D hologram on a 2D screen.

If the volume measurement is incomplete, the user can manually grow (or shrink) the segmented region and a spherical, free hand 'paint brush' can be used to add voxels to or delete voxels from the segmented structure when necessary. All EVs (figure 2 and 3) and YSVs were measured three times and the mean of these three assessments was used in the analysis. The EV measurements were performed by one examiner (M.R.) and in a randomly chosen subset of 20 embryos these measurements were repeated independently, at a different time, by another examiner (R.v.O). Both examiners were blinded for each other's volume measurements. M.R. was an experienced examiner and R.v.O. was a non-experienced examiner. But the level of experience is less important when there is a large contribution of automatic procedures, which is the case in volume measurements performed by using the V-Scope application. The duration of the off-line V-Scope embryonic volume measurement ranged between five and ten minutes. In a previous study by Rousian et al.¹⁵ the duration of the yolk sac volume measurement with V-Scope had a mean of 61 seconds.

V-Scope CRL measurements, already validated by Verwoerd et al.¹⁶, were performed three times by examiner MR and the mean values of these were used for analysis.

EVs of IVF/ICSI and spontaneous pregnancies were analyzed separately and tested for differences.

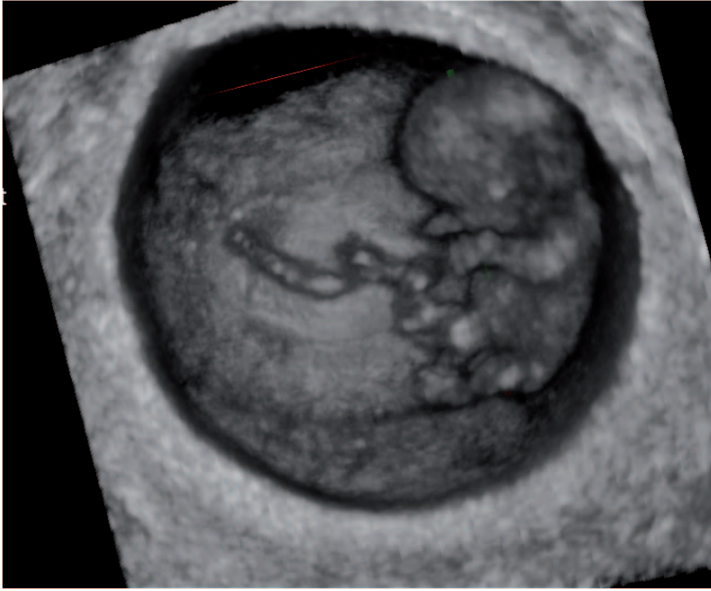


Figure 2. Image of an embryo at 9 weeks and 5 days gestational age in the I-Space VR system. This 2D picture does not fully reflect the 3D image of the I-Space.

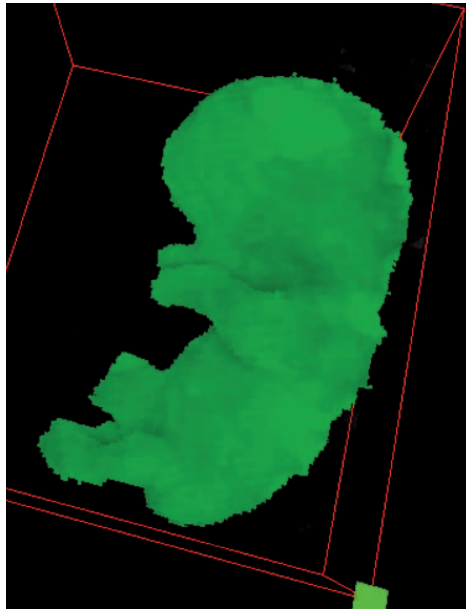


Figure 3. Image of the same embryo as seen in figure 2; now the volume of the embryo has been calculated to be approximately $3\,060\text{ mm}^3$ (green).

Statistical analysis

Data analysis was performed using SPSS (SPSS release 15.0 for Windows) and SAS PROC MIXED (release 8.02; SAS Institute Inc, Cary, NC, USA). To analyse the longitudinal measurements we used repeated measurements ANOVA (random coefficient models). To analyse the EV and YSV versus the CRL, we used the equation: $\text{Log}_{10}(\text{EV or YSV}) = a + b \times \text{log}_{10}(\text{CRL})$. The same model equation was used for the analysis of GA by replacing CRL with GA.

Intraclass correlation coefficient (ICC) was used to quantify the interobserver and intraobserver reliability of the volume measurements. For a good agreement, the ICC has to be 0.90 or higher.

RESULTS

The 88 EV measurements ranged from 14 mm³ to 29 877 mm³ (median: 2214 mm³) and are presented in figure 4 and grouped together per completed gestational week in table I. The GA ranged from 42 to 90 days (mean: 66 days; SD: 11 days). The CRL ranged from 3.0 to 68.0 mm (median: 25.7 mm).

In our study the mean EV measurements can be presented by the following equations:

$$\begin{aligned}\text{Log}_{10}(\text{EV (cm}^3)) &= -3.56 + 2.72 \times \text{log}_{10}(\text{CRL(mm)}) \\ \text{Log}_{10}(\text{EV (cm}^3)) &= -16.50 + 9.03 \times \text{log}_{10}(\text{GA(days)})\end{aligned}$$

From these equations can be calculated that when the CRL doubles, the mean EV increases 6.5 fold (95% confidence interval (CI): 6.2 - 7.0; $p < 0.001$). For each doubling of GA, the mean EV increases approximately 500 fold (95% CI: 403 - 680; $p < 0.001$).

These two equations did not statistically significantly differ between IVF/ICSI and spontaneous pregnancies (both $p > 0.5$ for the slopes; both $p > 0.5$ for the intercepts).

Of the 42 included women the GA at delivery ranged from 35⁺⁰ to 42⁺⁰ weeks (mean: 39⁺² weeks; SD: 10 days). Birth weight ranged from 2 175 gram to 4 750 gram (mean: 3 346 gram; SD: 588 gram). Postnatally all 22 girls and 20 boys were healthy.

The YSV measurements are shown in table II.

The resulting mean YSV can be represented by the following equations:

$$\begin{aligned}\text{Log}_{10}(\text{YSV (cm}^3)) &= -1.75 + 0.57 \times \text{log}_{10}(\text{CRL(mm)}) \\ \text{Log}_{10}(\text{YSV (cm}^3)) &= -4.44 + 1.92 \times \text{log}_{10}(\text{GA(days)})\end{aligned}$$

In figure 5 the YSVs are plotted against the CRL and GA. The YSV increases on average 3.8 fold (95% CI: 2.8 - 5.1; $p < 0.001$) for each doubling of gestational days. When the CRL doubles, the YSV increases 1.5 fold (95% CI: 1.4 - 1.6; $p < 0.001$).

3.1

HUMAN EMBRYONIC VOLUME MEASUREMENTS

Interobserver variability was calculated by comparing 20 EV measurements of examiner MR with the measurements of examiner RvO, which resulted in an ICC of 0.999 (95% CI: 0.997 – 0.999), representing excellent agreement. The intraobserver variability was calculated by comparing the EV measurements of MR, which resulted in an ICC of 0.999 (95% CI: 0.998 - 0.999).

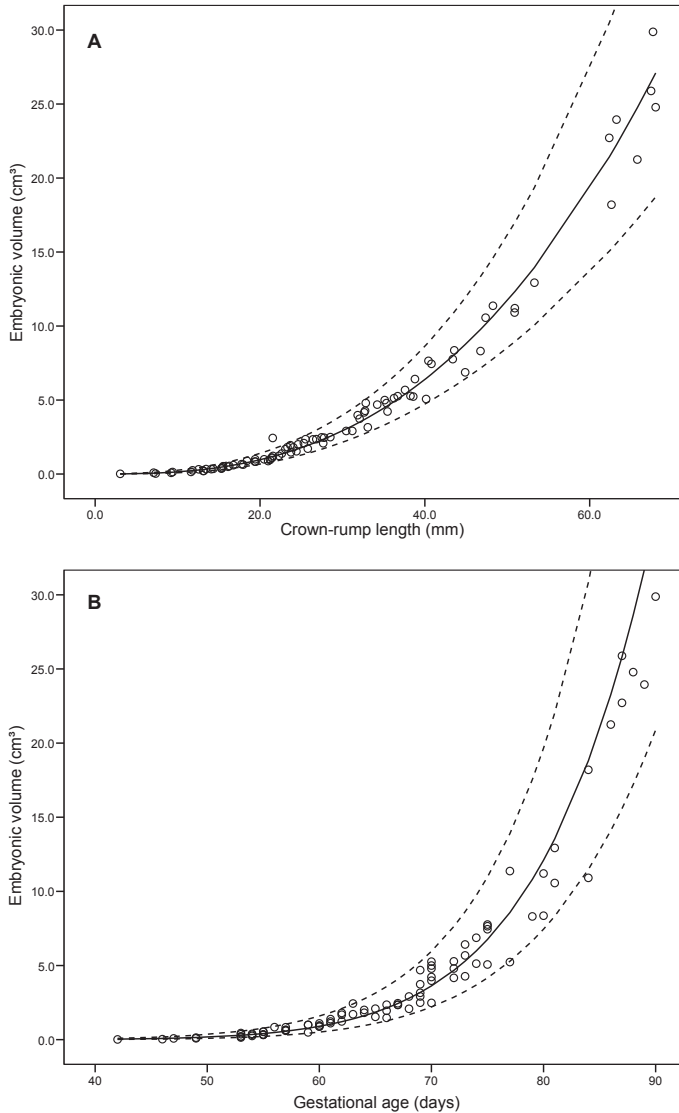


Figure 4. **A.** Measured whole-body volume related to crown-rump length. **B.** Measured whole-body volume related to gestational age. In both graphs the mean value and 95% reference interval are indicated by the solid and dotted lines, respectively.

Table I. Mean embryonic volume and crown-rump length estimations with the corresponding standard deviation (SD), number (N) per complete gestational week and / or range.

Gestational age (weeks)	N	Mean embryonic volume (mm ³)	SD (mm ³)	Range (mm ³)	Mean CRL (mm)	SD (mm)
6	3	42	34	14 – 80	6.5	3.2
7	15	310	137	90 – 543	13.2	2.5
8	18	1 017	352	489 – 1 800	20.3	2.2
9	19	2 447	785	1 469 – 4 691	27.2	3.6
10	18	5 348	1 412	2 478 – 7 761	36.7	4.4
11	7	9 709	2 579	5 232 – 12 927	47.0	4.8
12	8	22 195	5 693	10 911 – 29 877	63.5	5.6

Table II. Mean yolk sac volume and crown-rump length estimations with the corresponding standard deviation (SD), number (N) per complete gestational week and / or range.

Gestational age (weeks)	N	Mean yolk sac volume (mm ³)	SD (mm ³)	Range (mm ³)	Mean CRL (mm)	SD (mm)
6 and <6	8	48	13	33 – 72	7.0	2.3
7	22	79	23	40 – 139	13.3	2.0
8	28	100	39	49 – 245	19.9	2.6
9	25	122	42	63 – 206	26.1	2.8
10	22	147	37	99 – 228	37.0	4.5
11	10	180	104	75 – 424	48.3	5.8
12	3	116	43	76 – 160	61.8	6.0

DISCUSSION

In this prospective study based on longitudinally collected ultrasound data we show, for the first time, that first trimester human embryonic whole-body volumes and YSVs can be measured using an instant and automated VR system.

The development of 3D ultrasound at the end of the 1980s was a step forward for volume based growth and weight estimations. Since then several studies have been published on reliability and accuracy of 3D volume measurement^{11,15,22-24}. Subsequently, specialized software used by Blaas et al.^{11-12, 22}, the multiplanar method²³ and VOCAL software^{8-10, 13, 23, 25-26} have been used for the estimation of EVs and YSVs. In all studies the examiner had to place contours around the structure of interest on a 2D screen, which is subject to individual variation. Blaas

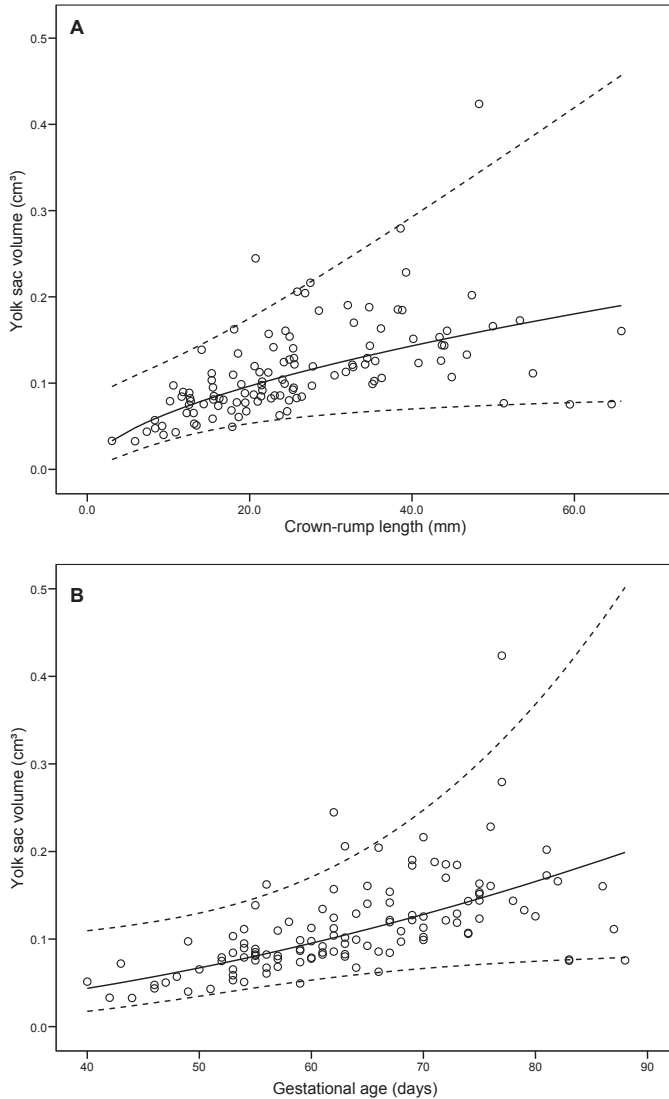


Figure 5. **A.** Measured yolk sac volume related to crown-rump length. **B.** Measured yolk sac volume related to gestational age. In both graphs the mean value and 95% reference interval are indicated by the solid and dotted lines, respectively.

et al.^{11,22} showed that the examiner usually draws the segmentation line slightly away from the real surface, resulting in larger volumes with outer surfaces and smaller volumes in case of cavities with inner surfaces. The I-Space offers depth perception and subsequently the dataset can be examined in all dimensions and from all different sides. This makes it easy for an examiner to measure volumes, and to prevent incomplete segmentations. The V-Scope software enables to

measure volumes in real 3D semi-automatically, and proves to be less sensitive to individual variation¹⁵, because there is no need to draw contours around the structure of interest.

Another advantage of the I-Space is that this algorithm allows to compute the whole-body volume, including the limbs, while with VOCAL only a head and trunk volume can be measured, resulting in a substantial underestimation^{9-10,13}. Blaas et al.¹² showed that the volume of the limbs, as a percentage of the total EV, increases from 5% at 7 weeks' GA to 10% at the end of the first trimester.

Each volume measurement took 5 to ten minutes starting from the moment a data set was loaded, including all post-processing time. The more experienced one gets, the faster it goes, which makes it also useful in a clinical setting. Compared to the other techniques the VR volume measurement is less time consuming, due to its segmentation algorithm¹⁵. Clinical applicability will be tested in the near future. Our main goal in this translational research was to provide new insights in embryonic growth and development and the feasibility of automated analysis. Furthermore the interobserver and intraobserver agreement for YSV¹⁵ and EV measurements appeared to be very good.

We measured the embryonic body volume in 49% of the datasets. In this translational research setting we only included these datasets with a very high image quality, as our main goal was to provide new insights in embryonic growth and development using automated analysis. New studies will be conducted with regards to applications in a clinical setting.

In comparison to the cross-sectional embryonic volume data of Blaas et al.¹² we found on average 23% higher volumes above a CRL of 30 mm and comparable volumes below a CRL of 30 mm. The relatively small number of women studied, however, is a limitation of both studies.

It has been suggested that reduced embryonic growth might be better assessed by embryonic volume than by CRL measurement⁸⁻¹⁰, because the increment of EV between the 7th and 12th gestational week is much larger than the respective increment of the CRL, as was also demonstrated in our study. Between 11⁺⁰ and 13⁺⁶ weeks of gestation the fetal head and trunk volume has also been shown, when compared to chromosomally normal fetuses, to be about 10-15% lower in trisomy 21 and monosomy X fetuses and about 45% lower in trisomy 18 and triploidy fetuses⁹⁻¹⁰. A generalized disturbance in growth of these embryos was illustrated by the fact that the volumes were smaller, even after correction for CRL.

As we know that there is a relation between abnormal first trimester growth and adverse obstetric outcomes from CRL studies^{3, 6-7}, it can be expected that EV measurements may be even more accurate in prediction models. EV measurements may therefore be implemented in routine clinical practice in the nearby future. However, more research is needed to validate the assumption that abnormal volume measurements can be successfully used to predict a miscarriage or low birth weight.

The yolk sac, being an embryonic structure with biosynthetic, haemopoietic and absorptive functions, plays a critical role in embryonic development. From the first sonographic analysis of the human yolk sac in 1979²⁷ researchers tried to find a relation between the yolk sac appearance and size, and pregnancy outcome. Kupesic et al.²⁸ were the first to study yolk sac volumes by using the planimetric 3D ultrasound method. In recent publications VOCAL was used for YSV measurements²⁵⁻²⁶. The volumes correlated with GA even more than the diameter of the yolk sac²⁵⁻²⁶. Associations between an abnormal YSV and pregnancy outcome were noted in some^{26, 29}, but not in all studies³⁰.

In the I-Space these volumes can be measured automatically in one minute¹⁵. These very high reproducible and accurate measurements can therefore be performed for research and may also be implemented in a clinical setting to study the predictive value of the YSV for an abnormal pregnancy outcome.

In conclusion, we have demonstrated that an innovative VR system can be used for automated first trimester measurement of human EV and YSV. This 3D VR approach allows us to obtain unique information about the size of the embryo using all dimensions, which opens a new area to study embryonic growth and development. This innovative technique may improve the differentiation between normal and abnormal human development in early pregnancies.

REFERENCES

1. Robinson HP, Fleming JE. A critical evaluation of sonar "crown-rump length" measurements. *BJOG*. 1975;82:702-10.
2. Bottomley C, Bourne T. Dating and growth in the first trimester. *Best Practice Res Clin Obstet Gynaecol*. 2009;23:439-52.
3. Mukri F, Bourne T, Bottomley C, Schoeb C, Kirk E, Papageorgiou AT. Evidence of early first-trimester growth restriction in pregnancies that subsequently end in miscarriage. *BJOG*. 2008;115:1273-8.
4. Goldstein SR, Kerenyi T, Scher J, Papp C. Correlation between karyotype and ultrasound findings in patients with failed early pregnancy. *Ultrasound Obstet Gynecol*. 1996;8:314-7.
5. Schemmer G, Wapner RJ, Johnson A, Schemmer M, Norton HJ, Anderson WE. First-trimester growth patterns of aneuploid fetuses. *Prenat Diagn*. 1997;17:155-9.
6. Bukowski R, Smith GC, Malone FD, Ball RH, Nyberg DA, Comstock CH, Hankins GD, Berkowitz RL, Gross SJ, Dugoff L, Craigo SD, Timor-Tritsch IE, Carr SR, Wolfe HM, D'Alton ME. Fetal growth in early pregnancy and risk of delivering low birth weight infant: prospective cohort study. *BMJ*. 2007;334:6.
7. Smith GC, Smith MF, McNay MB, Fleming JE. First-trimester growth and the risk of low birth weight. *NEJM*. 1998;339:1817-22.
8. Aviram R, Shpan DK, Markovitch O, Fishman A, Tepper R. Three-dimensional first trimester fetal volumetry: comparison with crown rump length. *Early Hum Dev*. 2004;80:1-5.
9. Falcon O, Peralta CF, Cavoretto P, Auer M, Nicolaides KH. Fetal trunk and head volume in chromosomally abnormal fetuses at 11+0 to 13+6 weeks of gestation. *Ultrasound Obstet Gynecol*. 2005;26:517-20.
10. Falcon O, Peralta CF, Cavoretto P, Faiola S, Nicolaides KH. Fetal trunk and head volume measured by three-dimensional ultrasound at 11 + 0 to 13 + 6 weeks of gestation in chromosomally normal pregnancies. *Ultrasound Obstet Gynecol*. 2005;26:263-6.
11. Blaas HG, Eik-Nes SH, Berg S, Torp H. In-vivo three-dimensional ultrasound

- reconstructions of embryos and early fetuses. *Lancet*. 1998;352:1182-6.
12. Blaas HG, Taipale P, Torp H, Eik-Nes SH. Three-dimensional ultrasound volume calculations of human embryos and young fetuses: a study on the volumetry of compound structures and its reproducibility. *Ultrasound Obstet Gynecol*. 2006;27:640-6.
 13. Martins WP, Ferriani RA, Nastri CO, Filho FM. First trimester fetal volume and crown-rump length: comparison between singletons and twins conceived by in vitro fertilization. *Ultrasound Med Biol*. 2008;34:1360-4.
 14. Groenenberg IA, Koning AH, Galjaard RJ, Steegers EA, Brezinka C, van der Spek PJ. A virtual reality rendition of a fetal meningomyelocele at 32 weeks of gestation. *Ultrasound Obstet Gynecol*. 2005;26:799-01.
 15. Rousian M, Verwoerd-Dikkeboom CM, Koning AH, Hop WC, van der Spek PJ, Exalto N, Steegers EA. Early pregnancy volume measurements: validation of ultrasound techniques and new perspectives. *BJOG*. 2009;116:278-85.
 16. Verwoerd-Dikkeboom CM, Koning AH, Hop WC, Rousian M, Van Der Spek PJ, Exalto N, Steegers EA. Reliability of three-dimensional sonographic measurements in early pregnancy using virtual reality. *Ultrasound Obstet Gynecol*. 2008;32:910-6.
 17. Verwoerd-Dikkeboom CM, Koning AH, van der Spek PJ, Exalto N, Steegers EA. Embryonic staging using a 3D virtual reality system. *Hum Reprod*. 2008;23:1479-84.
 18. Verwoerd-Dikkeboom CM, van Heesch PN, Koning AH, Galjaard RJ, Exalto N, Steegers EA. Embryonic delay in growth and development related to confined placental trisomy 16 mosaicism, diagnosed by I-Space Virtual Reality. *Fertil Steril*. 2008;90:2017.e19--22.
 19. Cruz-Neira C SD, DeFanti T. Surround-screen projection-based virtual reality: the design and implementation of the CAVE (tm). Proceedings of the 20th annual conference on computer graphics and interactive techniques. 1993:135-42.
 20. Koning AH, Rousian M, Verwoerd-Dikkeboom CM, Goedknegt L, Steegers EA, van der Spek PJ. V-scope: design and implementation of an immersive and desktop virtual reality volume visualization system. *Stud Health Technol Inform*. 2009;142:136-8.
 21. Myers LM, Brinkley JF. Visualization of Brain Surface Features Using Registered Partially Segmented MRI Scans. *Image Display; SPIE Medical Imaging*. 1995:43-52.
 22. Berg S, Torp H, Blaas HG. Accuracy of in-vitro volume estimation of small structures using three-dimensional ultrasound. *Ultrasound Med Biol*. 2000;26:425-32.
 23. Cheong KB, Leung KY, Chan HY, Lee YP, Yang F, Tang MH. Comparison of inter- and intraobserver agreement between three types of fetal volume measurement technique (XI VOCAL, VOCAL and multiplanar). *Ultrasound Obstet Gynecol*. 2009;33:287-94.
 24. Raine-Fenning NJ, Clewes JS, Kendall NR, Bunkheila AK, Campbell BK, Johnson IR. The interobserver reliability and validity of volume calculation from three-dimensional ultrasound datasets in the in vitro setting. *Ultrasound Obstet Gynecol*. 2003;21:283-91.
 25. Rolo LC, Nardoza LM, Araujo Junior E, Nowak PM, Moron AF. Yolk sac volume assessed by three-dimensional ultrasonography using the VOCAL method. *Acta Obstet Gynecol Scand*. 2008;87:499-502.
 26. Figueras F, Torrents M, Munoz A, Comas C, Antolin E, Echevarria M, Carrera JM. Three-dimensional yolk and gestational sac volume. A prospective study of prognostic value. *J Reprod Med*. 2003;48:252-56.
 27. Manton M, Pedersen JF. Ultrasound visualization of the human yolk sac. *J Clin Ultrasound*. 1979;7:459-60.
 28. Kupesic S, Kurjak A, Ivancic-Kosuta M. Volume and vascularity of the yolk sac studied by three-dimensional ultrasound and color Doppler. *J Perinat Med*. 1999;27:91-6.
 29. Cho FN, Chen SN, Tai MH, Yang TL. The quality and size of yolk sac in early pregnancy loss. *Aust N Z J Obstet Gynaecol*. 2006;46:413-8.
 30. Babinszki A, Nyari T, Jordan S, Nasser A, Mukherjee T, Copperman AB. Three-dimensional measurement of gestational and yolk sac volumes as predictors of pregnancy outcome in the first trimester. *Am J Perinatol*. 2001;18:203-11.



CHAPTER 3.2

GESTATIONAL SAC FLUID
VOLUME MEASUREMENTS
IN VIRTUAL REALITY

ABSTRACT

Background The aim of this prospective cohort study is to evaluate a virtual reality (VR) application for gestational sac fluid volume (GSFV) measurements in first trimester pregnancies and to study the correlation between different embryonic growth parameters.

Methods We analyzed 180 3D ultrasound scans of 42 healthy women, performed between 5⁺⁵ and 12⁺⁶ weeks gestational age (GA). The 3D datasets were transferred to the I-Space immersive VR system. The V-Scope application is used to create a 'hologram' of the ultrasound image allowing depth perception and interaction with the rendered objects. Volumes can be measured semi-automatically by using a segmentation algorithm. In addition to the GSFV, the total gestational sac volume (GSV) and its diameter (GSD) were measured. The GSV was also calculated using the ellipsoid formula. Previously performed embryonic volume and CRL measurements were included in the study. The outcomes were analyzed using repeated measurement analysis of variance.

Results The GSFV was measured in 78 scans, varying from 434 mm³ to 81491 mm³. The comparison of the GSD formula constructed in our study with a commonly clinically used formula showed an increasing difference with increasing GA. The GSFV/embryonic volume ratio showed a decrease over GA. The GSV calculated by the ellipsoid formula was on average 19.8% greater compared to the GSV measured in VR.

Conclusions New charts for first trimester GSFV were constructed using VR. A positive correlation between GSFV and GA, CRL and the GSD was found. These growth charts could be promising tools for studying normal and abnormal embryonic development.

Keywords Gestational sac volume; gestational sac fluid volume; first trimester; 3D ultrasound; virtual reality

Melek Rousian, Anton H.J. Koning, Wim C. Hop, Peter J. van der Spek, Niek Exalto, Eric A.P. Steegers

Ultrasound Obstet Gynecol. 2011 doi 10.1002/uog.9033

INTRODUCTION

The gestational sac is of great interest, especially in the early pregnancy. This sac consists of two different cavities in the first trimester; namely the amniotic cavity and the exocoelomic cavity¹⁻².

The mean gestational sac diameter (GSD) is used as an important growth parameter in first trimester pregnancies. In the Netherlands and in many other countries, the Grisolia et al.³ chart is used as reference chart for the GSD in relation to the gestational age (GA). Besides the size, also the shape of the gestational sac has been studied in relation to adverse pregnancy outcomes⁴⁻¹¹. Some studies show that there is an association between the size or shape and several abnormal pregnancy outcomes^{5-6,8,10-11}, while others do not^{4,9}.

In addition, the volume of the gestational sac can be used to assess growth with improved accuracy by transvaginal three-dimensional (3D) ultrasound¹². The gestational sac fluid volume (GSFV) represents the gestational sac volume (GSV) minus the volume of the embryonic parts. Until now, the GSV and GSFV were measured in 3D by using three different volume measuring methods^{5, 13-17}.

We introduced a virtual reality (VR) based method to measure volumes of hypoechogenic and hyperechogenic structures¹⁸⁻¹⁹. This method is implemented in V-Scope, an in-house developed volume-rendering application which is used to create a 'hologram' of the 3D ultrasound data that can be controlled by means of a virtual pointer using a wireless joystick. V-Scope runs in the I-Space allowing the use of the third dimension to its fullest, which is not possible when using any of the other available 3D applications. In addition, volume measurements can be performed semi-automatically. The accuracy and reproducibility of the volume measuring method has been proven by previous studies¹⁸⁻¹⁹. Finally, length measurements, like the GSD, can be performed, using a tracing-application²⁰⁻²¹.

The aim of this study is to evaluate the possibility of measuring the GSFV and GSV throughout uncomplicated first trimester pregnancies using the V-Scope application. We also compared the in VR measured GSD with a clinically used chart³.

METHODS

Patients

Between January and July 2006 50 pregnant women were included into a study on first trimester longitudinal 3D ultrasound measurements. These women also contributed to other studies¹⁸⁻²³.

Twenty-five patients conceived spontaneously and the remaining 25 women became pregnant after in-vitro fertilization (IVF) or intra-cytoplasmic sperm injection (ICSI) treatment. The regional committee for medical ethics approved the study. For the spontaneously conceived group the GA was calculated using the first day of the last menstrual period and, in cases with an unknown last

menstrual period or a discrepancy of more than a week, GA was determined by the CRL measurements performed in the first trimester. The GA for the IVF/ICSI pregnancies was based on the date of oocyte retrieval.

The inclusion criteria were women with an ongoing singleton pregnancy, without a structural or chromosomal anomaly detected before or after birth, without an intra-uterine fetal death or severe growth retardation. In total, 8 women were excluded because they did not meet the inclusion criteria for the following reasons: a non-viable pregnancy (n=2), twin pregnancy (n=3), placental confined trisomy 16 (n=1)²³, severe growth retardation (n=1) and intra-uterine fetal death (n=1)²⁰⁻²¹. All 42 remaining pregnancies resulted in the birth of a healthy child.

Ultrasound

All women were scanned weekly between 5⁺⁵ and 12⁺⁶ weeks' gestation by using the transvaginal probe (3.7-9.3 MHz) of the GE Voluson 730 Expert system (GE, Zipf, Austria). In total 180 3D datasets of the previously studied 42 women were re-examined. The collected datasets had been examined in other studies to evaluate embryonic growth and development¹⁸⁻²³ and the focus at the time of collecting these 3D datasets had not been on the gestational sac. Off-line evaluation using specialised 3D software (4D view, version 5.0, GE Medical Systems) showed that in 78 3D datasets the entire gestational sac had been recorded. These 3D datasets were saved as Cartesian volumes and transferred to the BARCO I-Space for the current study.

Measurements

The I-Space is a so-called 4-walled CAVETM-like²⁴⁻²⁵ (Cave Automatic Virtual Environment) VR system (figure 1), allowing depth perception and 3D interaction with the rendered datasets. The V-Scope application is used to create a 'hologram' of the 3D ultrasound data that can be controlled by means of a virtual pointer, which is controlled by a wireless joystick.

The available volume measuring algorithm is based on a region-growing approach with variance threshold as originally proposed for magnetic resonance imaging data^{19,26-27}. Differences in intensity allow the measurement of various structures. In the present study, the gestational sac images only consist of hypoechoic parts and the intensity difference between the sac and the uterus wall is very large. This makes it very easy to segment out the GSFV. A volume measurement is performed in a couple of seconds. Post-processing tools allow the user to correct for incomplete segmentations. Even if post-processing is needed, the total measurement of the GSFV takes less than one minute. The embryo consists of hypoechoic and hyperechoic parts and therefore the volume of this structure has to be segmented in steps¹⁸. If the structure of interest has a connection with structures one does not want to include in the segmentation, this connection has to be erased. The embryonic volume measurements included, have also contributed to another study¹⁸. Any measurement of the GSFV includes the combined volumes of the exocoelomic cavity and the amniotic fluid, but not

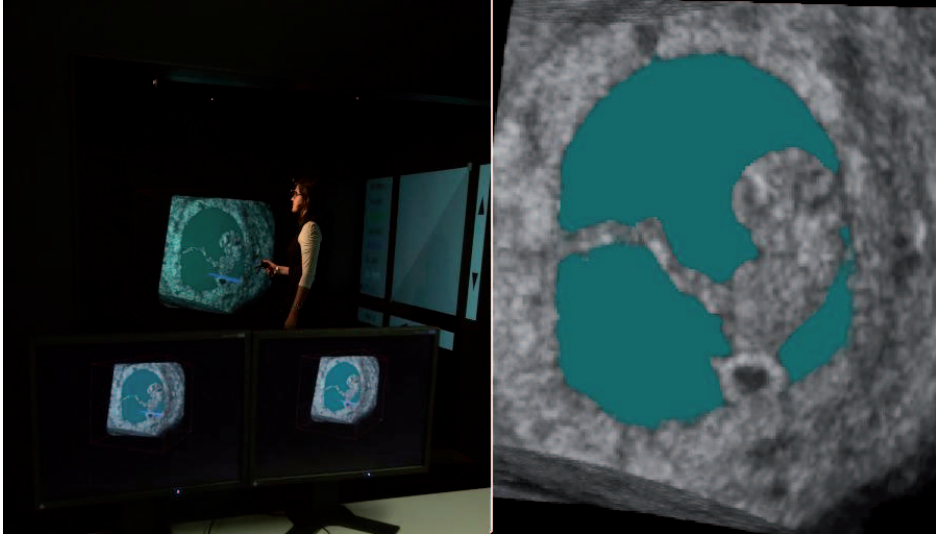


Figure 1. Left: Image of an observer in the I-Space. An embryo of 8 weeks and 5 days gestational age is projected on the wall. **Right:** The segmented gestational sac fluid volume is displayed in blue and has a value of 14 593 mm³.

the embryo, the yolk sac or umbilical cord. In figure 1 we can see a 2D picture of an I-Space hologram where the GSFV is shown in blue. The GSV was calculated by adding the embryonic volume to the GSFV. All measurements were performed three times, and mean values of these three assessments were used in the analysis.

The GSV was also calculated using the following ellipsoid formula:

$$\text{Volume} = 1/6 \pi \times \text{length} \times \text{width} \times \text{height}$$

A distance measuring tool allows the observer to measure distances by placing callipers with the joystick. This tool has already been validated and described in detail by Verwoerd et al.²⁰. With this tool we measured the CRL and the GSD in all scans where this was possible. Some of the CRL measurements were already performed in other studies^{18,20-21}. The three perpendicular diameters of the gestational sac were measured, one of which was the maximal diameter. The GSD was calculated by averaging these three perpendicular diameters. All measurements were performed three times; mean values of these three assessments were used in the analysis.

Statistical analysis

Data analysis was performed using SPSS (SPSS Release 15.0 for Windows, SPSS Inc, Chicago, IL, USA) and SAS PROC MIXED (release 9.2; SAS Institute Inc, Cary, NC, USA). Repeated measurement ANOVA (random coefficient model) was used for the assessment of the longitudinal measurements in our study. Because

logarithmic transformation of both axes resulted in an approximate linear relationship, the following equation was used to analyse the GSFV versus the CRL data: $\text{Log}_{10}(\text{GSFV}) = a + b \times \text{log}_{10}(\text{CRL})$. This model equation was also used for the analysis of GA and the GSD by replacing CRL with GA or GSD. Finally, we used the following equation for the analysis of the GSD = $a + b \times \text{GA}$. The ratio of the GSFV divided by the embryonic volume was also calculated.

The GSV calculated using the ellipsoid formula was compared to the GSV measured in VR. A p-value of 0.05 (two sided) was considered the limit of significance.

Finally, the GSD measurements performed in VR were compared to the Grisolia et al.³ GSD chart, which has the following formula for mean values: $\text{GSD} = -26.7091 + 8.0396 \times \text{gestational weeks} - 0.1342 \times (\text{gestational weeks})^2$.

RESULTS

In 29 out of the 42 pregnant women, GSFV measurements could be performed. We measured the GSFV in 78 different ultrasound scans, varying from 434 mm³ and 81491 mm³ (median: 11500 mm³). The GA varied from 40 to 90 days (mean: 62 days). In these 78 scans the CRL was measurable in 75 scans (96%), varying from 5.0 to 63.5 mm (median: 21.4 mm). The mean diameter of the gestational sac varied from 10.7 mm to 65.4 mm (mean: 33.6 mm), and could be measured in all 78 scans. The median number of datasets per patient in which it was possible to perform GSFV measurements was 3.0 (range: 1 to 6 scans).

The associations between the GSFV and CRL and GA are displayed in figure 2. Figures 2A and B show that the approximate individual linear relationships on the logarithmic scales used are apparent.

In figure 3, the raw longitudinal association is depicted between the GSFV and GSD.

From the equations in table I it follows that the GSFV increases on average by a factor of 50.8 (95% confidence interval (CI): 37.8 – 68.3; $p < 0.001$) when the GA doubles. When the CRL doubles, the GSFV increases 3.0 fold (95% CI: 2.8 – 3.3; $p < 0.001$). Finally, when the GSD doubles, the GSFV increases 7.1 fold (95% CI: 6.5 - 7.6; $p < 0.001$).

The GSFV/embryonic volume ratio versus GA showed a decrease ($p < 0.001$) from 63.1 at 40 days GA to 2.3 at 90 days GA.

The difference between the GSV measured with the ellipsoid formula and the GSFV measured with V-Scope increased systematically from 5.1% at 40 days GA to 78.1% at 90 days GA, and the difference increased significantly ($p < 0.001$) by 1.5% per gestational day. The embryonic volume was measured in 61 datasets and is added to the previously established GSFV; which results in the total GSV. The embryonic body volume ranged from 21 to 23010 mm³ (median: 959 mm³). The mean difference between the GSV measured with the ellipsoid formula and the total GSV measured with V-Scope was 19.8% (95% CI: 15.1 – 24.6; $p < 0.001$). This difference was constant over time.

3.2

GESTATIONAL SAC VOLUMES

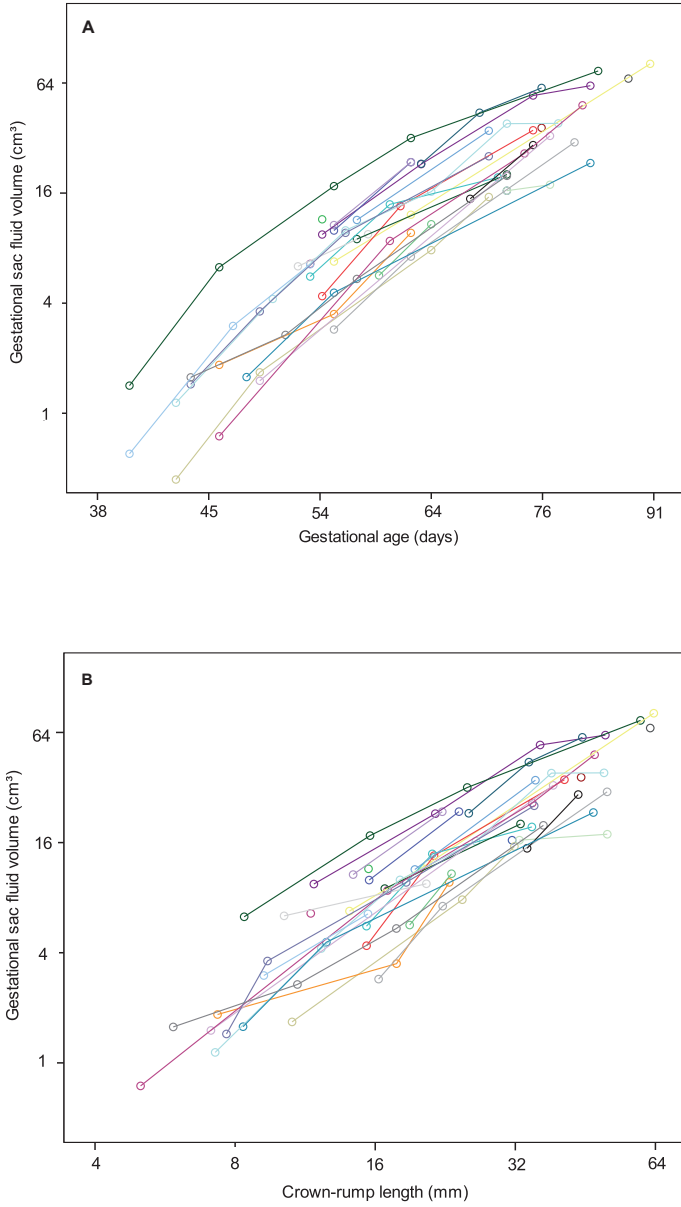


Figure 2. A. The raw longitudinal representation of the measured gestational sac fluid volume against the gestational age. The separate lines indicate different subjects. Both axes are represented on a logarithmic scale. **B.** The raw longitudinal presentation of the measured gestational sac fluid volume against the crown-rump length. The separate lines indicate different subjects. Again, the axes represented are on a logarithmic scale.

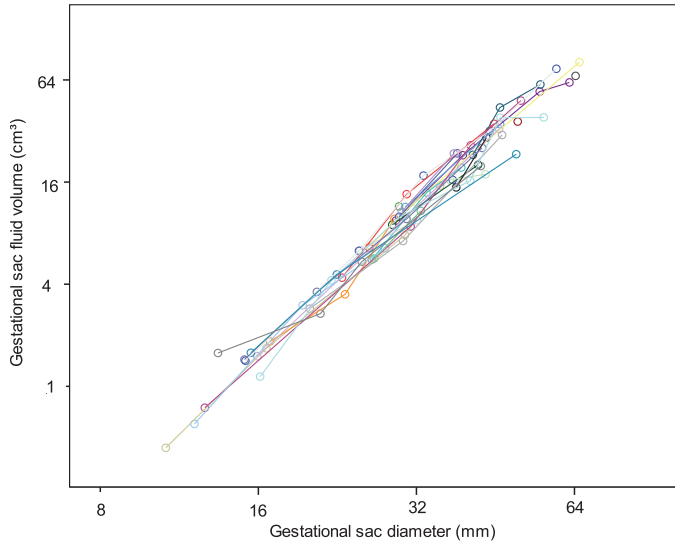


Figure 3. The raw longitudinal representation of the measured gestational sac fluid volume against the gestational sac diameter. The separate lines indicate different subjects. Logarithmic scaling of both axes is performed.

Figure 4 shows the GSD measurements versus GA. The curve of means according to Grisolia et al.³ and our fitted curve of means (fitted equation is shown in table I) are also indicated. The mean difference between our measurements and the Grisolia curve increases by 1.7 mm per gestational week ($p < 0.001$). There is no difference between the two curves at 8+5 weeks' of gestation. At six weeks GA, the difference between our mean line and the mean line of Grisolia et al.³ equals -4.6 mm. At week 12, this difference equals +5.4 mm.

DISCUSSION

This study shows that the GSFV can be measured in longitudinally obtained 3D ultrasound datasets, rapidly and automated with a VR application. We established charts for the GSFV between 6 and 13 weeks GA, and found correlations with GA and CRL. Secondly, the clinically used chart on GSD constructed by Grisolia et al.³ appears to differ significantly from the one obtained in our study.

The reference chart for GSD measurements of Grisolia et al.³, is being used in daily clinical practice at our medical centre in the Netherlands. They studied the first trimester GSD in a prospective cross-sectional study including 248 women³. The comparison of the GSD measured in VR and the GSD measured by Grisolia et al.³ showed that there is an increasing difference between our findings and their findings. Until the ninth week of pregnancy, their measurements seem larger

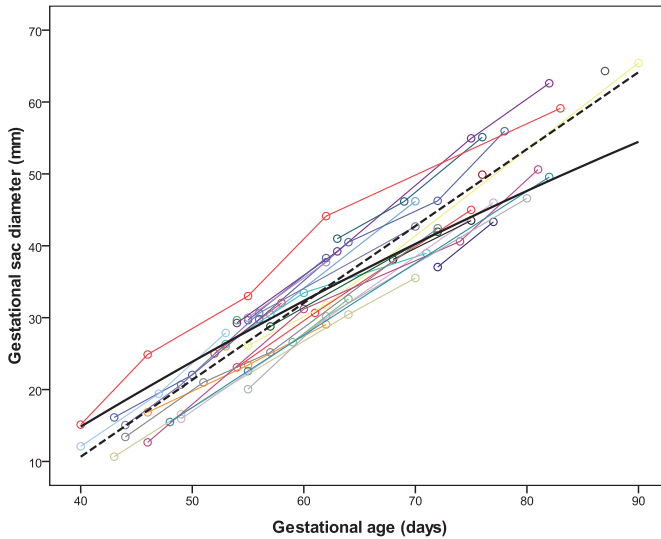


Figure 4. The raw longitudinal representation of the measured gestational sac diameter against the gestational age. The separate lines indicate different subjects. The mean curve determined by Grisolia et al.³ is indicated by the black solid line. The mean line calculated in our study is indicated by the black dotted line.

Table I. The calculated formulae for different growth parameters.

Parameters	Formula
GSFV versus CRL	$\text{Log}_{10}(\text{GSFV (cm}^3)) = -1.07 + 1.60 \times \text{log}_{10}(\text{CRL(mm)})$
GSFV versus GA	$\text{Log}_{10}(\text{GSFV (cm}^3)) = -9.09 + 5.67 \times \text{log}_{10}(\text{GA(days)})$
GSFV versus GSD	$\text{Log}_{10}(\text{GSFV (cm}^3)) = -3.19 + 2.82 \times \text{log}_{10}(\text{GSD(mm)})$
GSD versus GA	$\text{GSD (mm)} = -32.15 + 1.07 \times (\text{GA(days)})$

and after the ninth week they seem smaller compared to our measurements. The advantage of using VR is the fact that one can check the measurements, because it is possible to control whether the callipers are placed in a proper position by rotating the dataset. This is impossible with the regularly used 2D ultrasound equipment. Which chart represents first trimester gestational sac growth best, however, needs to be studied in a larger group of women.

There exist only a few longitudinal (2D) ultrasound studies on first trimester GSD growth²⁸⁻²⁹. Rossavik et al.²⁹ carried out a pioneering longitudinal study on the measurements of the GSD in patients conceiving spontaneously or due to IVF treatment (including also twins and triplets), which is a different study group when compared to the present study. The relationship between the GSD and GA is

linear in their study. Blaas et al.²⁸ showed also a linear relationship when the GSD was compared to GA in 29 patients (145 GSD measurements).

More than 30 years ago, Robinson³⁰ measured the GSV, including the embryonic structures, and the GSFV using the planimetric method in 2D ultrasound datasets. The GSFV was obtained by subtracting the embryonic volume from the GSV, which was derived from the data of Streeter³¹ in 1921. His results showed that the GSFV increased from 1 mL at 6 weeks to 28 mL at 10 weeks and to 80 mL at 13 weeks GA. In our study we showed these volumes to be 1 mL at 6 weeks and 24 mL at 10 weeks GA. This shows us that the findings of Robinson in 1975 correspond well with our findings, using a VR application.

In more recent days, it became possible to measure the GSV and GSFV in 3D. For this purpose three different volume measuring applications have been used, being the VOCAL method, multiplanar method and SonoAVC^{5,13-17}. Using the VOCAL method, a high correlation was found between the GSV and GA as well as CRL^{13,15-16,32}. The GSV found in these studies was slightly larger than the GSV in our study. This can be explained by the fact that we only added the embryonic volume to the GSFV and not the volume of the umbilical cord, yolk sac and amniotic membrane, while in the GSV measurement performed with VOCAL the umbilical cord, yolk sac and amniotic membrane are also included. In our study a difference of almost 20% was found between the measured GSV and the calculated GSV, using the ellipsoid formula, confirming previous findings of Lee et al.¹³

We were able to add the embryonic volume to the GSFV in 61 datasets. In two datasets, the embryo was not clearly present yet, and in the remaining 15 datasets the position of the embryo did not allow for proper differentiation between the embryo and the placenta. Due to this, the eraser function could not be used accurately. The measurement of the GSFV was not influenced and could be appropriately performed.

An important point is the fact that by using the VOCAL and multiplanar method, the observer has to draw the contours around the object of interest in various 2D slices of the 3D dataset, interpolating the space between the contours and estimating the total volume, which makes these techniques labour intensive and sensitive to individual variation. The third 3D technique, SonoAVC can be used to measure the GSFV semi-automatically, but in the only available study the GSFV was measured between 11 and 13 weeks GA¹⁷.

Volume measurements of structures like the GSFV and embryonic volume are performed semi-automatically with V-Scope. Any need for post-processing influences measurement time and subjectivity. Nevertheless, in previous studies V-Scope measurements proved to be less sensitive to individual variation than others¹⁹. The semi-automatic segmentation algorithm makes V-Scope also less labour intensive, especially for the measurement of simple volumes, such as the GSFV. A volume measurement with V-Scope takes only a couple seconds. This is very fast compared to the other techniques, which makes V-Scope very useful for testing in a clinical setting.

The relationship between the GSFV and the GSD is approximately linear on logarithmic scales, with little inter-individual differences. The corresponding graph (figure 3) also indicated remarkably similar growth during the first trimester.

Using a VR application for measurements like these described in this study are new and the VR technique is not yet widely used. The department of Bioinformatics of the Erasmus MC is working on a desktop version of the I-Space. The V-Scope application can be run on a desktop, which uses a low-cost 3D screen and a similar tracking system as used in the I-Space. This makes VR widely available in the nearby future for a fraction of the cost.

Until now, different studies showed that the GSV has some predictive value for adverse pregnancy outcomes^{7,11}. Falcon et al.⁵ assessed the GSV with the VOCAL approach and showed that fetuses with trisomy 18, 21 or Turner syndrome had a normal sized gestational sac, while fetuses with triploidy and trisomy 13 had a significant smaller GSV when related to GA.

In conclusion, we constructed new charts for growth in the first trimester using VR. These newly constructed first trimester growth charts are a valuable starting point for future research and might be of clinical use for differentiation between normal and abnormal first trimester pregnancies.

REFERENCES

1. Carlson B. Human embryology and developmental biology: Elsevier Mosby 2004.
2. Jauniaux E, Johns J, Burton GJ. The role of ultrasound imaging in diagnosing and investigating early pregnancy failure. *Ultrasound Obstet Gynecol.* 2005;25:613-24.
3. Grisolia G, Milano K, Pilu G, Banzi C, David C, Gabrielli S, Rizzo N, Morandi R, Bovicelli L. Biometry of early pregnancy with transvaginal sonography. *Ultrasound Obstet Gynecol.* 1993;3:403-11.
4. Acharya G, Morgan H. Does gestational sac volume predict the outcome of missed miscarriage managed expectantly? *J Clin Ultrasound.* 2002;30:526-31.
5. Falcon O, Wegrzyn P, Faro C, Peralta CF, Nicolaides KH. Gestational sac volume measured by three-dimensional ultrasound at 11 to 13 + 6 weeks of gestation: relation to chromosomal defects. *Ultrasound Obstet Gynecol.* 2005;25:546-50.
6. Oh JS, Wright G, Coulam CB. Gestational sac diameter in very early pregnancy as a predictor of fetal outcome. *Ultrasound Obstet Gynecol.* 2002;20:267-9.
7. Figueras F, Torrents M, Munoz A, Comas C, Antolin E, Echevarria M, Carrera JM. Three-dimensional yolk and gestational sac volume. A prospective study of prognostic value. *J Reprod Med.* 2003;48:252-6.
8. Nyberg DA, Laing FC, Filly RA. Threatened abortion: sonographic distinction of normal and abnormal gestation sacs. *Radiology.* 1986;158:397-400.
9. Goldstein SR, Kerenyi T, Scher J, Papp C. Correlation between karyotype and ultrasound findings in patients with failed early pregnancy. *Ultrasound Obstet Gynecol.* 1996;8:314-7.
10. Rowling SE, Coleman BG, Langer JE, Arger PH, Nisenbaum HL, Horii SC. First-trimester US parameters of failed pregnancy. *Radiology.* 1997;203:211-217.
11. Babinszki A, Nyari T, Jordan S, Nasser A, Mukherjee T, Copperman AB. Three-dimensional measurement of gestational and yolk sac volumes as predictors of pregnancy outcome in the first trimester. *Am J Perinatol.* 2001;18:203-11.
12. Riccabona M, Nelson TR, Pretorius DH. Three-dimensional ultrasound: accuracy of distance and volume measurements. *Ultrasound Obstet Gynecol.* 1996;7:429-34.

13. Lee W, Deter RL, McNie B, Powell M, Balasubramaniam M, Goncalves LF, Espinoza J, Romero R. Quantitative and morphological assessment of early gestational sacs using three-dimensional ultrasonography. *Ultrasound Obstet Gynecol.* 2006;28:255-60.
14. Muller T, Sutterlin M, Pohls U, Dietl J. Transvaginal volumetry of first trimester gestational sac: a comparison of conventional with three-dimensional ultrasound. *J Perinat Med.* 2000;28:214-20.
15. Rolo LC, Nardoza LM, Araujo Junior E, Nowak PM, Moron AF. Gestational sac volume by 3D-sonography at 7-10 weeks of pregnancy using the VOCAL method. *Arch Gynecol Obstet.* 2008;279:821-27.
16. Bagratee JS, Regan L, Khullar V, Connolly C, Moodley J. Reference intervals of gestational sac, yolk sac and embryo volumes using three-dimensional ultrasound. *Ultrasound Obstet Gynecol.* 2009;34:503-9.
17. Borenstein M, Azumendi Perez G, Molina Garcia F, Romero M, Anderica JR. Gestational sac volume: comparison between SonoAVC and VOCAL measurements at 11 + 0 to 13 + 6 weeks of gestation. *Ultrasound Obstet Gynecol.* 2009;34:510-4.
18. Rousian M, Koning AHJ, Van Oppenraaij RHF, Hop WC, Verwoerd-Dikkeboom CM, Van der Spek PJ, Exalto N, Steegers EAP. An innovative virtual reality measurements for embryonic growth and development *Hum Reprod.* 2010;25:2210-6.
19. Rousian M, Verwoerd-Dikkeboom CM, Koning AH, Hop WC, van der Spek PJ, Exalto N, Steegers EA. Early pregnancy volume measurements: validation of ultrasound techniques and new perspectives. *BJOG.* 2009;116:278-85.
20. Verwoerd-Dikkeboom CM, Koning AH, Hop WC, Rousian M, Van Der Spek PJ, Exalto N, Steegers EA. Reliability of three-dimensional sonographic measurements in early pregnancy using virtual reality. *Ultrasound Obstet Gynecol.* 2008;32:910-6.
21. Verwoerd-Dikkeboom CM, Koning AH, Hop WC, van der Spek PJ, Exalto N, Steegers EA. Innovative virtual reality measurements for embryonic growth and development. *Hum Reprod.* 2010;25:1404-10.
22. Verwoerd-Dikkeboom CM, Koning AH, van der Spek PJ, Exalto N, Steegers EA. Embryonic staging using a 3D virtual reality system. *Hum Reprod.* 2008;23:1479-84.
23. Verwoerd-Dikkeboom CM, van Heesch PN, Koning AH, Galjaard RJ, Exalto N, Steegers EA. Embryonic delay in growth and development related to confined placental trisomy 16 mosaicism, diagnosed by I-Space Virtual Reality. *Fertil Steril.* 2008;90:2017.e19-22.
24. Cruz-Neira C SD, DeFanti T. Surround-screen projection-based virtual reality: the design and implementation of the CAVE (tm). *Proceedings of the 20th annual conference on computer graphics and interactive techniques.* 1993:135-42.
25. Kupesic S, Kurjak A, Ivancic-Kosuta M. Volume and vascularity of the yolk sac studied by three-dimensional ultrasound and color Doppler. *J Perinat Med.* 1999;27:91-6.
26. Koning AH, Rousian M, Verwoerd-Dikkeboom CM, Goedknecht L, Steegers EA, van der Spek PJ. V-scope: design and implementation of an immersive and desktop virtual reality volume visualization system. *Stud Health Technol Inform.* 2009;142:136-8.
27. Myers LM, Brinkley JF. Visualization of Brain Surface Features Using Registered Partially Segmented MRI Scans. *Image Display; SPIE Medical Imaging.* 1995: 43-52.
28. Blaas HG, Eik-Nes SH, Bremnes JB. The growth of the human embryo. A longitudinal biometric assessment from 7 to 12 weeks of gestation. *Ultrasound Obstet Gynecol.* 1998;12:346-54.
29. Rossavik IK, Torjusen GO, Gibbons WE. Conceptual age and ultrasound measurements of gestational sac and crown-rump length in in vitro fertilization pregnancies. *Fertil Steril.* 1988;49:1012-7.
30. Robinson HP. "Gestation sac" volumes as determined by sonar in the first trimester of pregnancy. *BJOG.* 1975;82:100-7.
31. Streeter GL. *Contributions to Embryology, Carnegie Institution Publications.* 1921;143:10-1.
32. Odeh M, Hirsh Y, Degani S, Grinin V, Ofir E, Bornstein J. Three-dimensional sonographic volumetry of the gestational sac and the amniotic sac in the first trimester. *J Ultrasound Med.* 2008;27:373-8.

PART 3

PART 4

PART 5

NORMAL GROWTH
DESCRIPTION OF NON-
STANDARD BIOMETRIC
MEASUREMENTS



CHAPTER 4.1

FIRST TRIMESTER UMBILICAL
CORD AND VITELLINE DUCT
MEASUREMENTS USING
VIRTUAL REALITY

ABSTRACT

Background The umbilical cord and vitelline duct are of vital importance to the fetus, but they are rarely the subject of first trimester two-dimensional (2D) ultrasound evaluation due to the complexity of their shape and morphology. Virtual reality (VR) allows efficient visualisation and measurement of complex structures like the umbilical cord and vitelline duct.

Aim To measure normal first trimester human growth of the umbilical cord length (UCL) and vitelline duct length (VDL) using a VR system; and to correlate both measurements with the gestational age (GA) and crown-rump length (CRL) and the VDL with the yolk sac volume (YSV).

Study design Prospective cohort study. Serial three-dimensional (3D) ultrasound measurements were performed from six to 14 weeks GA, resulting in 125 3D volumes. These volumes were analysed using an I-Space VR system.

Subjects Thirty-two healthy pregnant women with an ongoing, normal pregnancy.

Outcome measures The UCL, VDL, YSV and other related structures were measured.

Results The UCL, measurable in 55% of cases, was positively correlated to advancing GA and CRL ($p < 0.001$). The VDL could be measured in 42% of cases and showed a positive relationship with GA and CRL ($p < 0.001$). There was a significant ($p < 0.001$) relationship between YSV and VDL.

Conclusions The present study, facilitated by a VR system, is the first to provide an *in vivo* longitudinal description of normal first trimester growth of the human umbilical cord and vitelline duct. Further studies will reveal whether these parameters can be used in detection of abnormal fetal development.

Keywords Umbilical cord; vitelline duct; virtual reality; three-dimensional ultrasound; first trimester

Melek Rousian, Christine M. Verwoerd-Dikkeboom, Anton H.J. Koning, Wim C. Hop, Peter J. van der Spek, Eric A.P. Steegers, Niek Exalto

Early Hum Dev. 2010;87:77-82

INTRODUCTION

First-trimester ultrasound evaluation is predominantly used for the establishment of normal intrauterine fetal development and verification of gestational age (GA). Several biometric measurements are used, crown-rump length (CRL) being the most important.

However, structures such as the umbilical cord and vitelline duct are rarely the subject of first trimester ultrasound evaluation, although their function is of vital importance for embryogenesis. This can be explained by the fact that these structures are difficult to evaluate from two-dimensional (2D) media (such as a regular computer screen) due to their complex shape and morphology.

The Erasmus MC in Rotterdam operates a Barco I-Space, an innovative virtual reality (VR) system. This system allows depth perception and the V-Scope volume rendering application is used to create holograms from three-dimensional (3D) datasets. We have already demonstrated its use in the assignment of Carnegie Stages during fetal life¹, its use in the demonstration of fetal developmental delay² and in complex anatomical fetal malformations³⁻⁴. Furthermore, it is shown that the length and volume measurement tools of V-Scope are reliable and accurate⁵⁻⁷.

Depth perception enables the measurement of structures that have not been measured routinely before, mainly due to technical limitations. This enables us to efficiently measure the umbilical cord length (UCL) and vitelline duct length (VDL) in the early fetal life. The umbilical cord and vitelline duct are of vital importance to the developing fetus. Abnormalities in the umbilical cord may affect the fetus adversely, and some are associated with fetal malformations and chromosomal anomalies⁸⁻¹⁰. Therefore early detection seems clinically useful¹¹, which has also been described in classical studies about pathology of miscarriages¹²⁻¹³. Knowledge of the development of these structures in the first trimester may eventually also serve as a background for early detection of abnormal fetal development.

The aim of this study is to measure the UCL, VDL and other related structures in relation to GA and the CRL in normal and uncomplicated first trimester pregnancies. The relation between the VDL and yolk sac volume (YSV) is also studied.

MATERIAL AND METHODS

Patient selection

Over a time period of seven months a total of 47 female volunteers were included for longitudinal 3D ultrasound evaluation of early pregnancy^{1, 14-15}. The regional medical ethics review board approved this study and written consent was obtained. Two patients conceived with intra-uterine insemination (IUI) and 22 with *in vitro* fertilization (IVF) / intra-cytoplasmic sperm injection (ICSI) treatment. The other 23 patients all conceived spontaneously. Ultrasound scans were performed, when possible weekly, from about six weeks GA till the 14th week of pregnancy.

Gestational age for IVF/ICSI/IUI pregnancies was based on the date of oocyte retrieval or IUI. Gestational age for the patients who conceived spontaneously was based on the first day of the last menstrual period, verified by ultrasound measurements.

In order to provide charts for normal uncomplicated singleton pregnancies we had to exclude 15 patients. Two of these patients were diagnosed with non-viable pregnancies at their first examination, three carried twin pregnancies, one patient was diagnosed with placental confined trisomy 16 mosaicism, complicated by severe intra-uterine growth restriction², two patients developed severe placental malfunction. Finally, four patients who conceived spontaneously were excluded because of a discrepancy of more than seven days between the GA based on last menstrual period and the CRL measurement.

A total of 11 ultrasound volumes were excluded because fetal features could not be recognized due to poor image quality of the data.

Thirty-two patients with normal uncomplicated singleton pregnancies remained for further analyses, resulting in a total of 125 usable 3D volumes.

Materials

Three-dimensional ultrasound scanning was performed using a GE Voluson 730 Expert system (GE, Zipf, Austria). The ultrasound examinations were performed transvaginally using a standard 3.7-9.3 MHz probe. Three-dimensional sweeps were made at a moment when the fetus did not move. These 3D datasets were then saved as cartesian (rectangular) volumes and transferred to the BARCO I-Space at the department of Bioinformatics. This 4-walled CAVE-like VR system uses passive stereo to immerse viewers in a virtual world¹⁶. The images are projected on three walls and the floor of a small room and viewed through polarizing glasses in order to perceive depth. A "hologram" of the 3D dataset is created by the V-Scope volume rendering application^{5, 17}. A virtual pointer, controlled by a wireless joystick, is used for manipulation of the 3D dataset. The computer provides a correct perspective and motion parallax through wireless tracking of the viewer's head. In the I-Space, volumes are resized, turned and clipped to provide an unobstructed view of the fetus and optimal image quality is obtained by adjusting grey levels and opacity.

Measurements

All measurements were performed by CVD and repeated three times and the mean value of the three assessments was calculated. Crown-rump length was measured by placing the callipers from crown to caudal rump in a straight line.

The measuring tools of V-Scope include a tracing function. We could therefore measure the total UCL, even when it was looped. The total length was measured tracing it from the abdominal insertion of the cord to the amniotic membrane. We followed the midline of the umbilical cord whenever looping was present. We also measured the distance between the amniotic membrane and the placental insertion of the umbilical cord. We called this the AP (amniotic-placental) distance.

4.1

The mean diameter of the umbilical cord was measured in two places, at amniotic level as well as at the insertion into the abdomen. When a physiological herniation was present, the diameter was measured directly distal from the herniation.

VDL was measured from the outside border of the yolk sac towards the point where the vitelline duct joins the umbilical cord at amniotic level. The mean diameter of the vitelline duct was measured in two places at yolk sac side and umbilical cord side. Figure 1 shows a fetus at 10⁺⁵ weeks GA visualised in the I-Space, with measurements of both UCL and VDL.

The YSV was measured semi-automatically with a region growing segmentation algorithm which uses grey-scale differences to perform volume measurements. This measurement was already described in detail by Rousian et al.⁵ and was also used in another study¹⁴.

Statistical analysis of the maternal characteristics was performed using SPSS (Release 15.0, SPSS Inc, USA). The Mann-Whitney test was used to calculate the p-value and a value below 0.05 was considered as statistically significant.

To analyse the longitudinal measurements we used repeated measurements ANOVA (random coefficient models) in SAS PROC MIXED (release 9.2, SAS

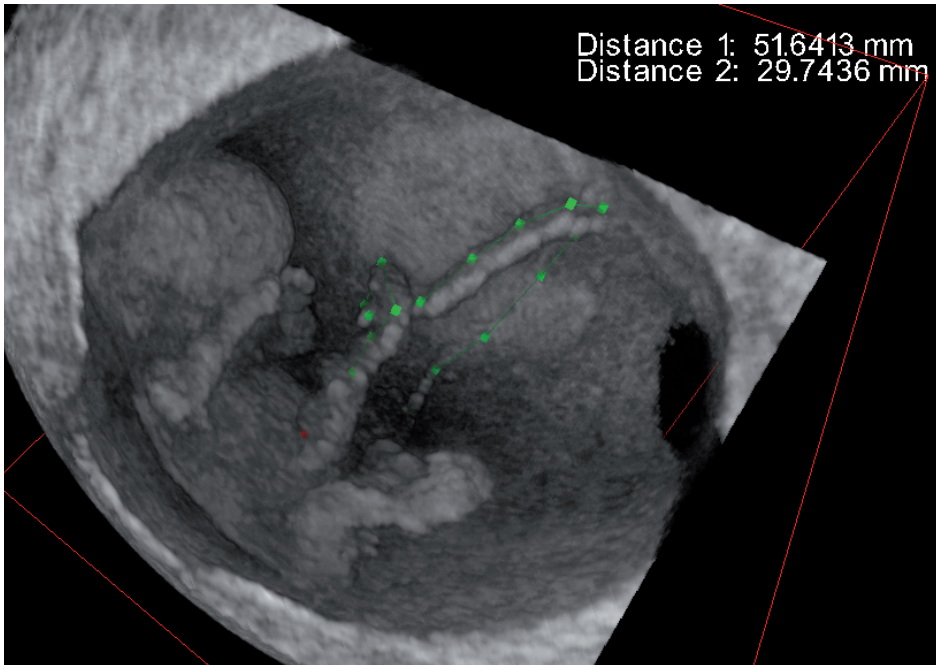


Figure 1. A picture of a fetus at 10⁺⁵ weeks GA in the I-Space. Both UCL (distance 1) and VDL (distance 2) are measured. It should be noted that this 2D picture cannot fully reflect the 3D image of the I-Space.

Institute Inc, USA). Different models describing the relationships between the growth parameters and GA or CRL were needed. These included linear, quadratic or log-transformed models for one or both axes to get approximate normal distributions. P = 0.05 (two sided) was considered the limit of significance.

RESULTS

All pregnancies selected for this study resulted in the birth of a healthy child. There were no significant differences in general characteristics (maternal age, GA at birth, mean birth weight, maternal body mass index) between the group with assisted fertility treatment and the group who conceived spontaneously (table I).

The GA ranged from 42 to 97 days (median: 70 days). The CRL measurements could be performed in 124 (99.2%) of the cases and ranged from 3.04 to 91.11 mm (median: 32.48 mm).

Table II shows how often the other parameters could be measured, the minimum and maximum GAs at which the parameters were measured and the range of the parameters.

The UCL could be measured in 55% of the cases. Scatterplots of UCL versus GA and CRL show that log-transformations of all parameters result in approximate linear relationships ($p < 0.001$). Figure 2 demonstrates the relationship between UCL and GA and CRL. Most problems in measuring the total length were encountered in the advanced GAs (>75 days), as can be seen in figure 2A from the limited amount of data. In advanced GAs the cord often contained too many loops to allow precise measurements.

Table I. The mean and range of the patient characteristics of the total group and separated by mode of conception.

Patient characteristics	Total group (N=32)	Conception mode		P-value
		Spontaneous (N=16)	IVF/ICSI (N=16)	
Maternal age (years)	33 (21 – 43)	32 (21 – 40)	33 (24 – 43)	0.651
Body mass index (kg/length ²)	24.2 (19.0 – 34.9)	24.6 (19.7 – 34.9)	24.1 (19.0 – 34.3)	0.516
Number of weekly examinations	3.9 (1 – 7)	3.6 (1 – 6)	4.2 (1 – 7)	0.577
Gestational age at birth (weeks+days)	39+2 (35+0 – 42+0)	39+5 (37+3 – 41+4)	39+2 (35+0 – 42+0)	0.836
Birth weight (grams)	3300 (2175 – 4270)	3410 (2690 – 4170)	3191 (2175 – 4370)	0.122

N = total number of patients.

Table II. The total number (N) and percentage (%) of measurements performed in the I-Space.

Variable	N=125 (%)	Gestational age min (days)	Gestational age max (days)	Range (mm)
UCL	69 (55.2)	53	97	4.77 – 107.28
AP Distance	44 (35.2)	53	88	1.10 – 5.02
Mean diameter UC (abdominal site)	105 (84.0)	53	97	1.44 – 5.06
Mean diameter UC (amniotic site)	72 (57.6)	53	97	1.67 – 4.97
VDL	52 (41.6)	46	81	3.06 – 33.14
Mean diameter VD (YS site)	55 (44.0)	46	81	1.00 – 2.24
Mean diameter VD (UC insertion)	36 (28.8)	53	81	0.77 – 2.32

UCL= umbilical cord length
 AP = amnion-placenta
 UC = umbilical cord
 VDL = vitelline duct length
 VD = vitelline duct
 YS = yolk sac

The ability to measure the AP distance depends on image quality and is only performed in 35% of the cases. Log-transformations of the parameters showed that there was no significant relationship between the AP distance and the GA ($p=0.07$) or CRL ($p=0.09$).

Mean diameters of the umbilical cord at the abdominal side could be measured in 84% of the cases and at the amniotic side in 58% of the cases. The mean diameters were positively related with GA and CRL. To describe the relationship with GA, a quadratic component of GA was needed ($p<0.001$). The same applied for CRL ($p<0.001$). There was a statistically significant difference ($p<0.01$) between the diameters at both sides. The diameter at the abdominal cord side was greater compared to the diameter at the amniotic side throughout the study period.

The VDL could be measured in 42% of the cases. A linear model fitted best when the VDL was compared to GA and CRL and a positive linear relationship could be calculated for both parameters ($p<0.001$). Figure 3 demonstrates a positive relationship between the VDL and both the GA and CRL. In advanced GAs the yolk sac and therefore the end of the vitelline duct could no longer be recognized.

Mean diameter of the vitelline duct at the yolk sac side could be measured in 44% of the cases. There was a positive linear relation between the diameter and both the GA and CRL (both $p<0.001$). At the side of the umbilical cord it was only possible to measure the mean diameter in 29% of the cases. There was a linear

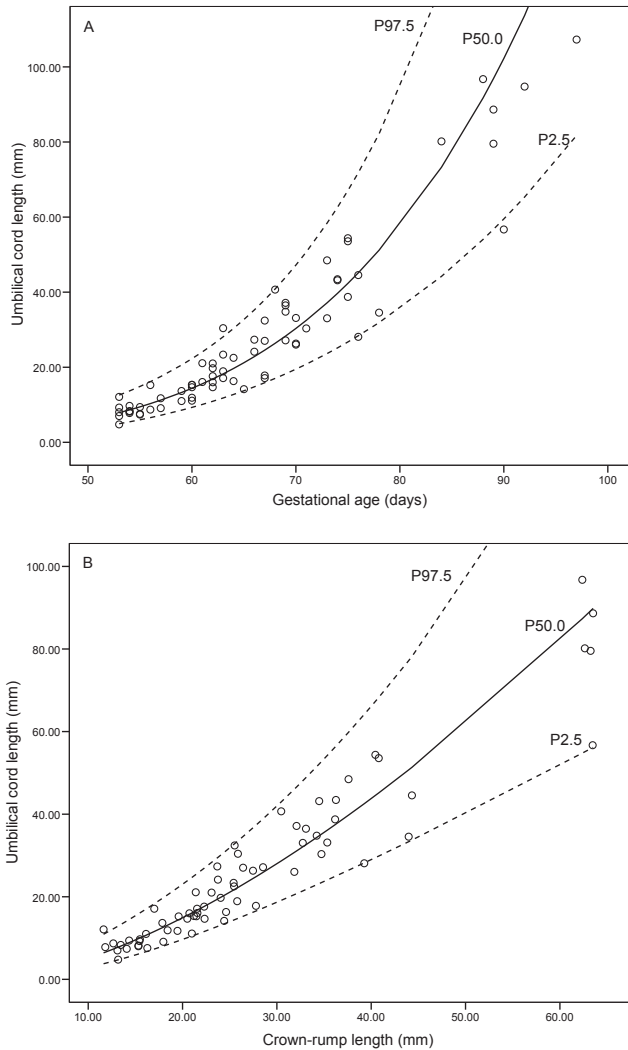


Figure 2. **A.** Relationship between the UCL and the GA. **B.** Relationship between the UCL and the CRL. In both charts the mean value is represented by the solid line and the 95% prediction intervals are presented by the dotted lines.

relationship with GA ($p=0.007$) and with the CRL ($p<0.001$). In two cases it was not possible to measure the VDL, even though the width of the vitelline duct at the yolk sac side could be established.

Table III shows all fitted equations of the relationships described above and the corresponding standard errors.

Finally, there was a significant ($p<0.001$) relation between the logarithmic transformations of the YSV and VDL. We used a total of 56 measurements for this purpose.

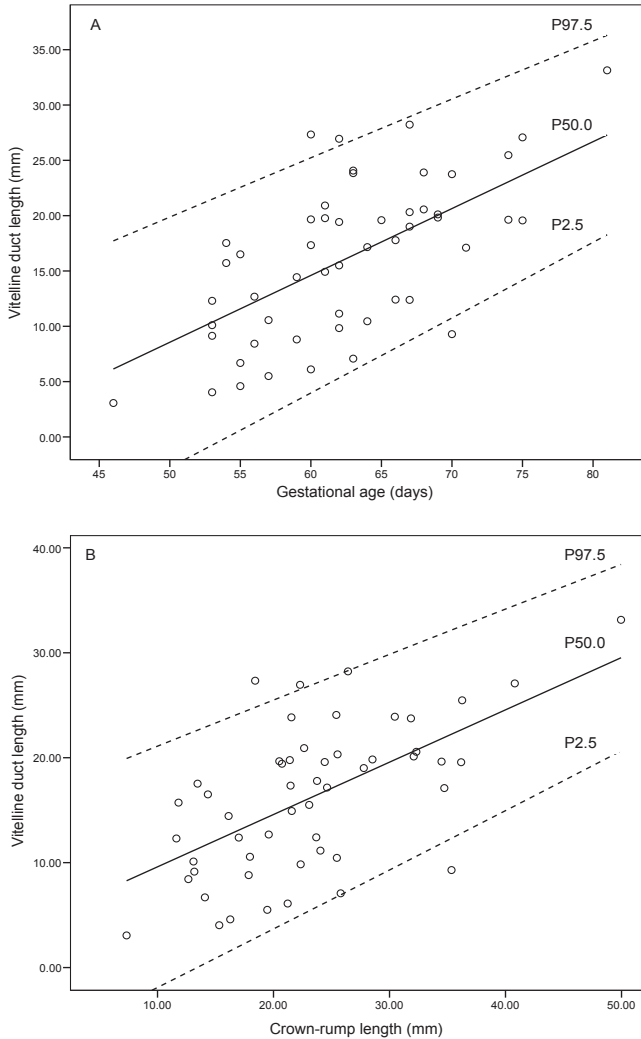


Figure 3. **A.** Relationship between the VDL and the GA. **B.** Relationship between the VDL and the CRL. Again, in both charts the mean value is represented by the solid line and the 95% prediction intervals are presented by the dotted lines.

DISCUSSION

The present study is the first to provide an *in vivo* longitudinal description of normal fetal growth of the human umbilical cord and vitelline duct, facilitated by a VR system.

The UCL is in most studies measured after miscarriage or birth. In our search for relevant studies concerning ultrasonic UCL measurements during the first trimester of pregnancy we found only one study where the umbilical cord was

Table III. Relationships between the measured parameters and the gestational age and CRL and the total number (N) of measurements obtained. Equations represent the P50 relationships. The numbers between the parentheses represent the standard error of the coefficients.

Variable	N=125	Equations (y)
UCL ^a versus GA	69	$-7.4393 + 4.8351 (\pm 0.1835) * {}^{10}\log GA$
UCL ^a versus CRL	69	$-0.8489 + 1.5545 (\pm 0.05979) * {}^{10}\log CRL$
Mean diameter UC (abdominal side) versus GA	105	$-9.2044 + 0.33118 (\pm 0.05280) * GA - 0.00185 (\pm 0.000370) * GA^2$
Mean diameter UC (abdominal side) versus CRL	101	$1.5005 + 0.08341 (\pm 0.01379) * CRL - 0.00068 (\pm 0.000169) * CRL^2$
Mean diameter UC (amniotic side) versus GA	72	$0.2341 + 0.03937 (\pm 0.006982) * GA$
Mean diameter UC (amniotic side) versus CRL	72	$2.1032 + 0.02575 (\pm 0.005161) * GA$
VDL versus GA	52	$-21.6575 + 0.6043 (\pm 0.07558) * GA$
VDL versus CRL	52	$4.6131 + 0.4987 (\pm 0.06450) * CRL$
Mean diameter VD (YS side) versus GA	55	$0.1995 + 0.02061 (\pm 0.004062) * GA$
Mean diameter VD (YS side) versus CRL	55	$1.1194 + 0.01570 (\pm 0.004441) * CRL$
Mean diameter VD (UC insertion) versus GA	36	$-0.6880 + 0.03348 (\pm 0.003221) * GA$
Mean diameter VD (UC insertion) versus CRL	36	$0.7845 + 0.02659 (\pm 0.003473) * CRL$

GA = gestational age

AP = amnion-placenta

UC = umbilical cord

VD = vitelline duct

YS = yolk sac

^a = ¹⁰log transformed value

measured using 2D ultrasound in 53 normal fetus and 15 fetus with an intrauterine demise¹⁸. The authors attempted to visualize the umbilical cord in its entirety and stated that the umbilical cord had to be taut and relatively straight. It was not possible to measure the loops present in the developing umbilical cord. A close linear relationship was found between UCL and GA in the normal group and 60% of fetus with an intrauterine demise had cord lengths more than two standard deviation below the expected value for GA. In our study we noticed that coiling appeared already early in the first trimester. It is impossible to measure the coiling parts of the umbilical cord by tracing in 2D ultrasound datasets. The VR application, however, enabled us to measure the entire umbilical cord, including the coils, because all three dimensions are available during this visualization.

The AP distance was found to vary considerably between cases and there was no relationship with advancing GA and the CRL. It proved to be difficult to obtain this measurement as the quality of the image determined the visibility of the boundaries. We found it striking that in some fetus the AP distance was very small or even not measurable, whereas in other fetus the AP gap was clearly visible and measured 4 or 5 mm in length.

Since the end of the 20th century, most studies on the umbilical cord generally focus on two entities; measurements of the diameter and cross-sectional area of the umbilical cord and coiling of the umbilical cord, mostly expressed by the umbilical coiling index.

In two studies by Ghezzi et al. the umbilical cord diameter correlated positively with the growth of the fetus whereas an umbilical cord diameter above the 95th percentile was a marker for aneuploidy¹⁹⁻²⁰. This can be explained by a difference in the amount of Warton's jelly, which is different in abnormal pregnancies²⁰. The umbilical cord lacks adventitia and Wharton's jelly appears to serve that function²¹. For the quantification of the amount of Wharton's jelly, the diameter of the cross-sectional area of the umbilical cord has been proposed as an appropriate parameter for abnormalities²²⁻²⁵. In our study we found that the diameter of the cord was difficult to measure in most cases, because image resolution was not good enough to distinguish the exact boundaries of the circumference of the cord. We did find, however that the umbilical cord does not have the same diameter at the abdominal side and at the amniotic side. The diameters at both sides were positively related with GA and CRL, which makes these measurements useful parameters during pregnancy.

The spiral coiling of the umbilical cord was already described in 1954 by Edmonds²⁶. Several studies have been performed to evaluate the origin, direction and clinical significance of the umbilical cord coiling²⁷⁻⁴², which is best visualized using Doppler measurements⁴³. In this study we used a first trimester population, and due to questions regarding the safety we did not use Doppler measurements. We were able to distinguish coiling and also the direction of the coiling in only a few cases and therefore no conclusions could be drawn, which is a weakness of the technique.

No previous ultrasound studies about the length or diameter of the vitelline duct were found. Our results demonstrate that the growth patterns of the VDL of the individual cases show more variation than growth patterns of the UCL. Still, there is a clear linear relationship between the VDL and GA and CRL. This is also true for the diameter at both the yolk sac side as at the umbilical cord side. Diameter remains the same both at yolk sac side as at the umbilical cord side during advancing GA. Because the VDL was difficult to measure at advanced GAs, we were unable to identify whether a plateau or decline in growth was present with advancing GA. Our study shows that the vitelline duct keeps growing until week 11 of pregnancy, suggesting functional activity up to that day.

As mentioned before, the VDL is positively correlated with GA and the CRL. The vitelline duct connects the yolk sac with the umbilical cord and the fetus.

We found a relation between the VDL and YSV in our healthy study population, which has never been reported before. The next step will be to study whether this relation is different in abnormal pregnancies.

All of the previous studies used conventional 2D ultrasound. The first study on the use of 3D ultrasound in the visualisation of the umbilical cord during second and third trimester was performed by Hata et al.⁴⁴. They concluded that 3D ultrasound technology has the potential to be a supplement to 2D ultrasound and might be useful in identifying abnormal umbilical cords in utero.

In general, a drawback in this study is that the current generation of ultrasound equipment does not enable reliable recording of datasets allowing VDL and UCL measurements in all cases. However, we expect in the foreseeable future that development of ultrasound equipment will allow us to obtain suitable datasets more frequently.

Present 3D ultrasound systems do not allow the measurement of 3D structures, and therefore UCL and VDL cannot be measured. Virtual reality systems, such as the I-Space, are unique in the ability to view and interact in the third dimension. In the near future a desktop VR system running the same V-Scope application will offer the same benefits at a fraction of the cost. We foresee a future where 3D display technology is as common as 2D displays are today.

In this study we show relationships between the UCL and VDL with GA and CRL, as well as the relationship between the VDL and the YSV. Further studies will reveal whether these parameters can be used in the detection of any anomalies in growth or development of the early fetus.

REFERENCES

1. Verwoerd-Dikkeboom CM, Koning AH, van der Spek PJ, Exalto N, Steegers EA. Embryonic staging using a 3D virtual reality system. *Hum Reprod.* 2008;23:1479-84.
2. Verwoerd-Dikkeboom CM, van Heesch PN, Koning AH, Galjaard RJ, Exalto N, Steegers EA. Embryonic delay in growth and development related to confined placental trisomy 16 mosaicism, diagnosed by I-Space Virtual Reality. *Fertil Steril.* 2008;90:2017.e19-22.
3. Groenberg IA, Koning AH, Galjaard RJ, Steegers EA, Brezinka C, van der Spek PJ. A virtual reality rendition of a fetal meningomyelocele at 32 weeks of gestation. *Ultrasound Obstet Gynecol.* 2005;26:799-801.
4. Verwoerd-Dikkeboom CM, Koning AH, Groenberg IA, Smit BJ, Brezinka C, Van Der Spek PJ, Steegers EA. Using virtual reality for evaluation of fetal ambiguous genitalia. *Ultrasound Obstet Gynecol.* 2008;32:510-4.
5. Rousian M, Verwoerd-Dikkeboom CM, Koning AH, Hop WC, van der Spek PJ, Exalto N, Steegers EA. Early pregnancy volume measurements: validation of ultrasound techniques and new perspectives. *BJOG.* 2009;116:278-85.
6. Verwoerd-Dikkeboom CM, Koning AH, Hop WC, Rousian M, Van Der Spek PJ, Exalto N, Steegers EA. Reliability of three-dimensional sonographic measurements in early pregnancy using virtual reality. *Ultrasound Obstet Gynecol.* 2008;32:910-6.
7. Verwoerd-Dikkeboom CM, Koning AH, Hop WC, van der Spek PJ, Exalto N, Steegers EA. Innovative virtual reality measurements for embryonic growth and development. *Hum Reprod.* 2010;25:1404-10.
8. Nyberg DA, Mahony BS, Luthy D, Kapur R. Single umbilical artery. Prenatal detection of concurrent anomalies. *J Ultrasound Med.* 1991;10:247-53.

9. Saller DN, Jr., Keene CL, Sun CC, Schwartz S. The association of single umbilical artery with cytogenetically abnormal pregnancies. *Am J Obstet Gynecol.* 1990;163:922-5.
10. Sepulveda W, Gutierrez J, Sanchez J, Be C, Schnapp C. Pseudocyst of the umbilical cord: prenatal sonographic appearance and clinical significance. *Obstet Gynecol.* 1999;93:377-81.
11. Deurloo KL, Kist WJ, Vugt JMG. Three dimensional ultrasound: an overview of its clinical use. *Fetal Matern Med Rev.* 2007;18:145-79.
12. Javert CT, Barton B. Congenital and acquired lesions of the umbilical cord and spontaneous abortion. *Am J Obstet Gynecol.* 1952;63:1065-77.
13. Philipp T, Philipp K, Reiner A, Beer F, Kalousek DK. Embryoscopic and cytogenetic analysis of 233 missed abortions: factors involved in the pathogenesis of developmental defects of early failed pregnancies. *Hum Reprod.* 2003;18:1724-32.
14. Rousian M, Koning AH, van Oppenraaij RH, Hop WC, Verwoerd-Dikkeboom CM, van der Spek PJ, Exalto N, Steegers EA. An innovative virtual reality technique for automated human embryonic volume measurements. *Hum Reprod.* 2010;25:2210-6.
15. Verwoerd-Dikkeboom CM, Koning AH, Hop WC, van der Spek PJ, Exalto N, Steegers EA. Innovative virtual reality measurements for embryonic growth and development. *Hum Reprod.* 2010;25:1404-10.
16. Cruz-Neira C, Sandin, D., DeFanti, T., editor. Surround-screen projection-based virtual reality: the design and implementation of the CAVE (tm). Proceedings of the 20th annual conference on computer graphics and interactive techniques; 1993; New York: ACM Press.
17. Koning AHJ, editor. Application of Volume Rendering in the CAVE (tm). Simulation and Visualisation on the Grid, seventh annual Conference; 1999; Paralleldatorcentrum, Stockholm.
18. Hill LM, DiNofrio DM, Guzick D. Sonographic determination of first trimester umbilical cord length. *J Clin Ultrasound.* 1994;22:435-8.
19. Ghezzi F, Raio L, Di Naro E, Franchi M, Bruhwiler H, D'Addario V, Schneider H. First-trimester sonographic umbilical cord diameter and the growth of the human embryo. *Ultrasound Obstet Gynecol.* 2001;18:348-51.
20. Ghezzi F, Raio L, Di Naro E, Franchi M, Buttarelli M, Schneider H. First-trimester umbilical cord diameter: a novel marker of fetal aneuploidy. *Ultrasound Obstet Gynecol.* 2002;19:235-9.
21. Bankowski E, Sobolewski K, Romanowicz L, Chyczewski L, Jaworski S. Collagen and glycosaminoglycans of Wharton's jelly and their alterations in EPH-gestosis. *Eur J Obstet Gynecol Reprod Biol.* 1996;66:109-17.
22. Raio L, Ghezzi F, Cromi A, Cereda E, Passi A. Sonographic morphology and hyaluronan content of umbilical cords of healthy and Down syndrome fetuses in early gestation. *Early Hum Dev.* 2004;77:1-12.
23. Raio L, Ghezzi F, Di Naro E, Franchi M, Bolla D, Schneider H. Altered sonographic umbilical cord morphometry in early-onset preeclampsia. *Obstet Gynecol.* 2002;100:311-6.
24. Raio L, Ghezzi F, Di Naro E, Franchi M, Maymon E, Mueller MD, Bruhwiler H. Prenatal diagnosis of a lean umbilical cord: a simple marker for the fetus at risk of being small for gestational age at birth. *Ultrasound Obstet Gynecol.* 1999;13:176-80.
25. Raio L, Ghezzi F, Di Naro E, Gomez R, Franchi M, Mazor M, Bruhwiler H. Sonographic measurement of the umbilical cord and fetal anthropometric parameters. *Eur J Obstet Gynecol Reprod Biol.* 1999;83:131-5.
26. Edmonds HW. The spiral twist of the normal umbilical cord in twins and in singletons. *Am J Obstet Gynecol.* 1954;67:102-20.
27. Fletcher S. Chirality in the umbilical cord. *BJOG.* 1993;100:234-6.
28. Kalish RB, Hunter T, Sharma G, Baergen RN. Clinical significance of the umbilical cord twist. *Am J Obstet Gynecol.* 2003;189:736-9.
29. Lacro RV, Jones KL, Benirschke K. The umbilical cord twist: origin, direction, and relevance. *Am J Obstet Gynecol.* 1987;157:833-8.
30. de Laat MW, Franx A, Bots ML, Visser GH, Nikkels PG. Umbilical coiling index in normal and complicated pregnancies. *Obstet Gynecol.* 2006;107:1049-55.
31. De Laat MW, Franx A, Nikkels PG, Visser GH. Prenatal ultrasonographic prediction

- of the umbilical coiling index at birth and adverse pregnancy outcome. *Ultrasound Obstet Gynecol.* 2006;28:704-9.
32. de Laat MW, Franx A, van Alderen ED, Nikkels PG, Visser GH. The umbilical coiling index, a review of the literature. *J Matern Fetal Neonatal Med.* 2005;17:93-100.
 33. de Laat MW, Nikkels PG, Franx A, Visser GH. The Roach muscle bundle and umbilical cord coiling. *Early Hum Dev.* 2007;83:571-4.
 34. de Laat MW, van Alderen ED, Franx A, Visser GH, Bots ML, Nikkels PG. The umbilical coiling index in complicated pregnancy. *Eur J Obstet Gynecol Reprod Biol.* 2007;130:66-72.
 35. de Laat MW, van der Meij JJ, Visser GH, Franx A, Nikkels PG. Hypercoiling of the umbilical cord and placental maturation defect: associated pathology? *Pediatr Dev Pathol.* 2007;10:293-9.
 36. Degani S, Leibovich Z, Shapiro I, Gonen R, Ohel G. Early second-trimester low umbilical coiling index predicts small-for-gestational-age fetuses. *J Ultrasound Med.* 2001;20:1183-8.
 37. Predanic M, Perni SC. Absence of a relationship between umbilical cord thickness and coiling patterns. *J Ultrasound Med.* 2005;24:1491-6.
 38. Predanic M, Perni SC, Chasen ST. The umbilical cord thickness measured at 18-23 weeks of gestational age. *J Matern Fetal Neonatal Med.* 2005;17:111-6.
 39. Predanic M, Perni SC, Chasen ST, Baergen RN, Chervenak FA. Ultrasound evaluation of abnormal umbilical cord coiling in second trimester of gestation in association with adverse pregnancy outcome. *Am J Obstet Gynecol.* 2005;193:387-94.
 40. Predanic M, Perni SC, Chasen ST, Baergen RN, Chervenak FA. Assessment of umbilical cord coiling during the routine fetal sonographic anatomic survey in the second trimester. *J Ultrasound Med.* 2005;24:185-91; quiz 92-3.
 41. Qin Y, Lau TK, Rogers MS. Second-trimester ultrasonographic assessment of the umbilical coiling index. *Ultrasound Obstet Gynecol.* 2002;20:458-63.
 42. Strong TH, Jr., Elliott JP, Radin TG. Non-coiled umbilical blood vessels: a new marker for the fetus at risk. *Obstet Gynecol.* 1993;81:409-11.
 43. Predanic M, Perni SC, Chervenak FA. Antenatal umbilical coiling index and Doppler flow characteristics. *Ultrasound Obstet Gynecol.* 2006;28:699-703.
 44. Hata T, Aoki S, Hata K, Miyazaki K. Three-dimensional ultrasonographic assessment of the umbilical cord during the 2nd and 3rd trimesters of pregnancy. *Gynecol Obstet Invest.* 1998;45:159-64.



CHAPTER 4.2

VIRTUAL REALITY FOR EMBRYONIC
MEASUREMENTS REQUIRING
DEPTH PERCEPTION

ABSTRACT

Two real-time three-dimensional images of first-trimester pregnancies visualized using virtual reality (VR) are presented. Inherently three-dimensional structures, like the umbilical cord and limbs, can be efficiently and accurately measured using VR.

Keywords Virtual reality; three-dimensional ultrasound; early pregnancy; first trimester; depth perception

Melek Rousian, Anton H.J. Koning, Peter J. van der Spek,
Eric A.P. Steegers, Niek Exalto

Fertil Steril. 2011;95:773-4

MANUSCRIPT

The I-Space virtual reality (VR) system and the V-Scope software are used to visualize and quantify three-dimensional (3D) ultrasound volumes obtained in the early first-trimester. This system offers depth perception (using stereoscopic projection on multiple screens) and interaction (using a wireless joystick) in the displayed 'hologram'. Three-dimensional structures can now be efficiently visualized and measured. It enables the staging of embryos using the Carnegie criteria¹⁻². Furthermore, structures like the length of the arm³, the legs, the umbilical cord including the coiling parts and the vitelline duct (figures 1 and 2)⁴, can be measured using the tracing tool. Other structures, like the amniotic sac and yolk sac (figures 1 and 2) are also clearly visualized. In addition, it is possible to perform semi-automated volume measurements of for instance the embryonic body, yolk sac and the embryonic brain cavities⁵⁻⁶. In conclusion VR enables the visualization and quantification of morphology, biometry and volumetry using all three dimensions *in vivo*.

4.2

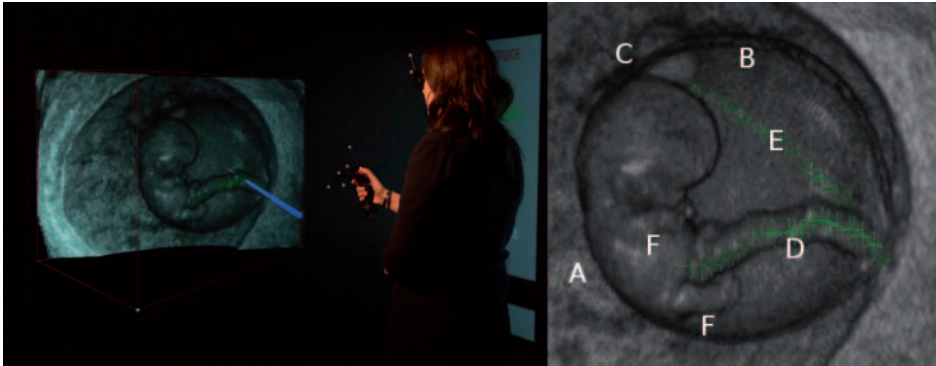


Figure 1. Left image: Embryo of 8+6 weeks' gestational age (GA) visualized in the I-Space VR application. The observer wears stereoscopic glasses and interacts with the displayed 'hologram' by means of a joystick. **Right image:** The embryo (A), amniotic sac (B), yolk sac (C) umbilical cord (D), vitelline duct (E), limbs (F) are clearly visualized. The crown-rump length (CRL) of this embryo is 23.8 mm. The umbilical cord length and vitelline duct length are traced in green. The umbilical cord length is 21.4 mm and the vitelline duct length is 27.1 mm. Note that this two-dimensional picture cannot express the three-dimensionality of the original 'hologram'.

4.2

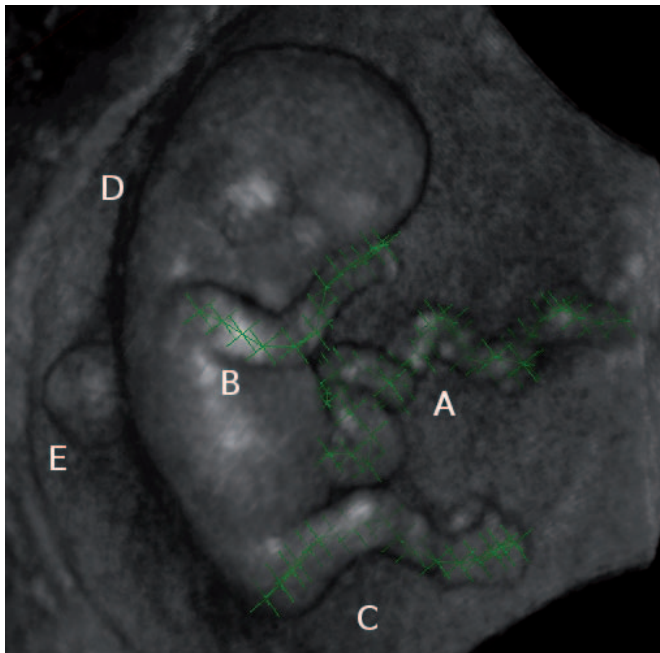


Figure 2. Early fetus of 10+3 weeks' GA and a CRL of 37.5 mm as rendered by V-Scope. The umbilical cord (A) is traced, and the length is 53.2 mm. The length of the arm (B) is 16.8 and the length of the leg (C) is 19.6 mm. The amniotic sac (D) and yolk sac (E) are visualized.

REFERENCES

1. Verwoerd-Dikkeboom CM, Koning AH, van der Spek PJ, Exalto N, Steegers EA. Embryonic staging using a 3D virtual reality system. *Hum Reprod.* 2008;23:1479-84.
2. O'Rahilly R, Müller F. Ventricular system and choroid plexuses of the human brain during the embryonic period proper. *Am J Anat.* 1990;189:285-02.
3. Verwoerd-Dikkeboom CM, Koning AH, Hop WC, van der Spek PJ, Exalto N, Steegers EA. Innovative virtual reality measurements for embryonic growth and development. *Hum Reprod.* 2010;25:1404-10.
4. Rousian M, Verwoerd-Dikkeboom CM, Koning AH, Hop WC, van der Spek PJ, Exalto N, Steegers EA. First trimester umbilical cord and vitelline duct measurements using virtual reality. *Early Hum Dev.* 2010; 87:77-82.
5. Rousian M, Koning AH, van Oppenraaij RH, Hop WC, Verwoerd-Dikkeboom CM, van der Spek PJ, Exalto N, Steegers EA. An innovative virtual reality technique for automated human embryonic volume measurements. *Hum Reprod.* 2010;25:2210-16.
6. Rousian M, Verwoerd-Dikkeboom CM, Koning AH, Hop WC, van der Spek PJ, Exalto N, Steegers EA. Early pregnancy volume measurements: validation of ultrasound techniques and new perspectives. *BJOG.* 2009;116:278-85.

4.2

PART 4

PART 5

PART 6

EMBRYONIC BRAIN
DEVELOPMENT, BIOMETRY
AND VOLUMETRY



CHAPTER 5.1

FIRST TRIMESTER EMBRYONIC BRAIN
DEVELOPMENT AND VOLUMETRY
USING VIRTUAL REALITY

ABSTRACT

Background The aim of this study was to evaluate first trimester brain ventricle development in human pregnancies using an innovative virtual reality (VR) application. We analyzed the relation of the embryonic volume (EV) and brain ventricle fluid volume (BVFV) with gestational age (GA), crown-rump length (CRL) and the Carnegie stage. Finally, the predictive value of CRL and EV measurements on birth weight is studied.

Methods In a prospective cohort study we weekly performed three-dimensional (3D) ultrasound examinations in 112 healthy pregnant women between 6⁺⁰ and 12⁺⁶ weeks GA. This resulted in 696 3D ultrasound scans, which were transferred to the I-Space VR system, and analyzed using V-Scope volume rendering software. V-Scope is used to create a 'hologram' of the ultrasound image and allows depth perception and interaction with the rendered objects. The CRL measurements were performed with a tracing-tool and the volume measurements were automatically performed with a segmentation-algorithm. The embryos were staged according to the internal and external characteristics of the Carnegie staging system. All longitudinal outcomes were analyzed using repeated measurements ANOVA.

Results CRL could be measured in 91% of the datasets, ranging from 2.5 to 79.0 mm. EV could be measured in 66% of the datasets, ranging from 2.4 to 23812.0 mm³ and the BVFV could be measured in 38% of the datasets, ranging from 10.4 to 226.3 mm³. Finally, in 74% of the datasets the embryos were staged according to the Carnegie criteria, starting as early as stage 12. Reference charts of volumes versus GA, CRL and stage were constructed. There was no significant relationship between the CRL and EV and the birth weight.

Conclusions Volumetry and staging of the human embryo by using a VR application makes it possible to obtain unique information about the *in vivo* embryonic normal and abnormal development and size of the ventricles and body.

Keywords First trimester; embryo; brain; brain ventricle fluid volume; virtual reality; Carnegie stage; embryonic volume

Melek Rousian, Wim C. Hop, Anton H.J. Koning, Peter J. van der Spek, Niek Exalto, Eric A.P. Steegers

Submitted

INTRODUCTION

Monitoring brain development during the first trimester of pregnancy is difficult, because of a complex and rapidly changing anatomy. The introduction of transvaginal ultrasonography contributed to some observational studies on brain development in the embryonic period¹⁻³. New insights in primitive brain ventricle appearance along a developmental timeline will enable early detection of cerebral pathology⁴⁻⁵.

The embryonic brain can be visualized by measuring the volume of the brain ventricles^{1,6}. The methods involved, however, have been shown to be very time-consuming and vulnerable to individual variation.

In 2005, the department of Bioinformatics at Erasmus University Medical Center introduced a Barco I-Space Virtual Reality (VR) application. With this system a 3D ultrasound dataset is presented as a free floating 'hologram', which allows the study of the morphology of the embryo in detail⁷. In VR, several biometric measurements can be measured using the length-measuring tool⁸⁻⁹. Volumes can also be measured by a segmentation algorithm¹⁰⁻¹¹, allowing instant and semi-automated volume measurements to be made of different embryonic structures, such as the brain ventricles and total body. Since this tool enables the user to visualize and quantify the brain ventricles, this makes *in vivo* staging of embryos based on their internal and external morphological characteristics possible¹²⁻¹³.

The aim of this study was to evaluate the embryonic development of the brain ventricles and Carnegie stages and to measure the CRL and embryonic volume (EV) in normal first trimester pregnancies using VR. A secondary aim was to study the predictive value of the first trimester CRL and embryonic body volume measurements on the outcome of pregnancy in terms of birth weights.

PATIENTS AND METHODS

Patients

We recruited 141 healthy volunteering pregnant women. These women were recruited via the department of Obstetrics and Gynaecology at the Erasmus University Medical Center. A small proportion (around 20%) of women were recruited from outside the University hospital. All women gave written informed consent and the regional committee for medical ethics approved the study.

After giving birth, data about the outcome of pregnancy were collected. From the 141 women who participated in the study a total of 29 patients were excluded because of possible interference with normal growth and development. Three of them carried a twin or triplet pregnancy, 16 had a first trimester miscarriage, two experienced an intra-uterine fetal death, three carried a child with a structural congenital anomaly and two were diagnosed with a trisomy 21 pregnancy. One patient discontinued the study because of her religious background and two because of being unable to participate in our research on a weekly basis.

The remaining 112 volunteers were scanned weekly from 6 or 7 weeks' until 12 weeks' gestational age (GA). GA was calculated from the first day of the last menstrual period (LMP). In case of an unknown LMP or a discrepancy of a week or more, GA was determined using the CRL measurements performed in the first trimester. The CRL measurements performed in this study are actually the greatest length of the embryo and early fetus. For the IVF/ICSI pregnancies the GA was based on the date of oocyte retrieval.

A total of 696 3D ultrasound scans were performed in these 112 women. When the brain ventricle fluid volumes (BVFV) were measured, a selection was made by excluding images that lacked contrast or parts of the brain cavities of the embryo due to shadowing or an unfavourable position of the embryo. Another reason for excluding images was due to movement artefacts. Before performing EV measurements, scans that lacked contrast or parts of the embryo were excluded.

In six women GA adjustments were made due to a discrepancy of the CRL of seven gestational days or more. These women were excluded when evaluating various parameters in relation to GA.

Ultrasound equipment

The ultrasound examinations were performed using a 4.5 – 11.9 MHz vaginal probe of the GE Voluson E8 (GE, Zipf, Austria) by two different examiners. The scans were evaluated off-line using specialized 3D software (4D View, version 7.0, GE Medical Systems); and the included scans were stored as Cartesian volumes, which were later transferred and visualized using the BARCO I-Space of the Department of Bioinformatics.

Length and volume measurements

The I-Space is a so-called 4-walled CAVE™-like (Cave Automatic Virtual Environment) VR system. A special volume rendering application called V-Scope was written to create an interactive hologram of the ultrasound image¹⁴. This hologram can be manipulated by means of a virtual pointer, which is controlled by a wireless joystick. Two different integrated functions were used in our study: the length-measuring tool and the volume-measuring tool. As described in detail by Verwoerd-Dikkeboom et al.,⁸ a trace application makes it possible to measure the lengths of the structures of interest. This tool was used to measure the CRL of the serially scanned embryos¹⁵. The volume measuring tool is based on a region-growing approach¹¹. The algorithm has been modified to handle the speckles in ultrasound data by simplifying some of the parameters of the original algorithm and smoothing the gray-level data. The user selects an upper and lower gray-level threshold and an upper threshold for the standard deviation of the voxels neighbourhood. A seed point is placed, and the algorithm grows the region starting from the seed point. The standard deviation threshold stops the region growing when it reaches a tissue interface. Post-processing tools are available to correct for incomplete segmentations. The user can manually grow or shrink the segmented region, and a spherical, freehand 'paint brush' can be used to add voxels to, or to

5.1

delete voxels from the segmented structure when necessary. We used this tool to establish the embryonic BVFV (see figure 1) and the embryonic body.

To measure the BVFV, the hypoechoic structures have to be segmented. In order to determine the EV, additionally the hyperechoic structures of the embryo have to be segmented as well¹⁰. Before the EV is measured, the embryonic insertion of the umbilical cord and its connections with the placenta have to be 'brushed' away with the eraser function to avoid segmentation of other parts than the whole-body.

All BVFV and CRL measurements were performed three times and mean values of these three assessments were used for the analysis.

The duration of an off-line V-Scope BVFV measurement was approximately one minute (see movie 4). The duration of an EV measurement ranged between five and ten minutes. Therefore only 1/3rd of all EV measurements were performed three times.

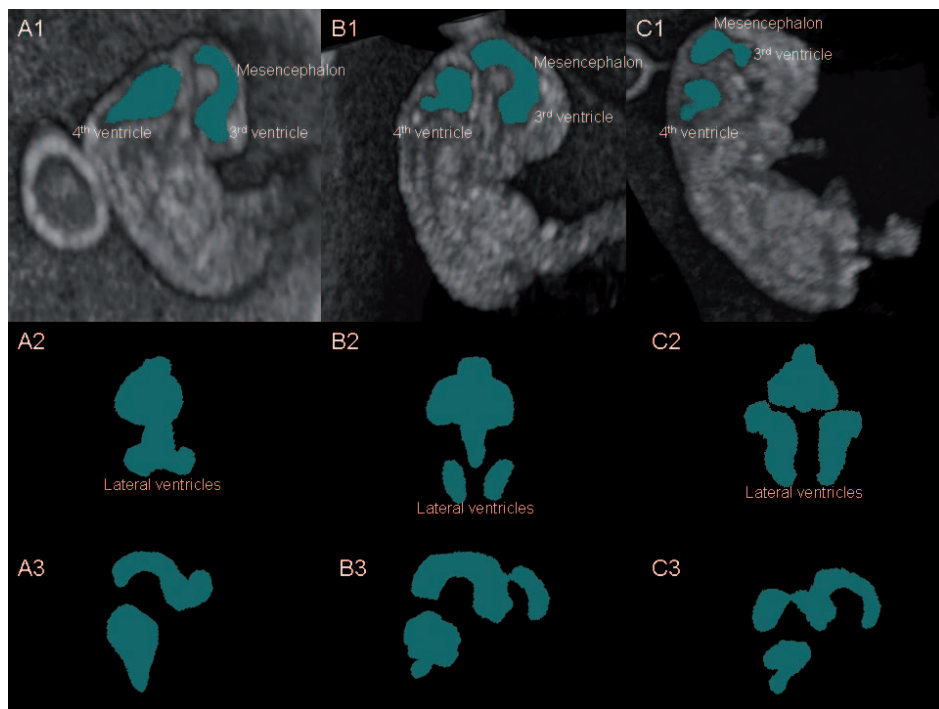


Figure 1. I-Space holograms of three embryos showing development of shape and size of the brain ventricles. **A.** An embryo of 8+2 weeks' GA (CRL of 15 mm and Carnegie stage 18). **B.** An embryo of 8+6 weeks' GA (CRL of 21 mm and Carnegie stage 20). **C.** An embryo of 9+6 weeks' GA (CRL of 28 mm and Carnegie stage 22). **1.** Mid-sagittal plane of the embryo. The BVFV is segmented in magenta. **2.** The axial view of the brain ventricles. **3.** The sagittal view of the brain ventricles. The lateral ventricles, cavity of the mesencephalon, third ventricle (=cavity of diencephalon) and the fourth ventricle (=cavity of the rhombencephalon) are displayed.

Movie 4. This is a 2D movie presenting how exactly a BVFV measurement is performed in a 3D ultrasound dataset of an embryo of nine weeks' GA. The observer uses a wireless joystick with a head tracking system to control the I-Space. The BVFV is indicated by the red colour.

Embryonic staging

The embryos were staged based on their internal and external morphological characteristics using the Carnegie criteria¹²⁻¹³. The Carnegie system is based on 23 stages covering the first eight postfertilizational weeks of development¹³. Embryonic staging was therefore only possible until gestational week 10+1 of pregnancy and took a couple of minutes. Verwoerd-Dikkeboom et al. staged the embryos in VR by using only the limb development criteria. In this study both external and internal morphological criteria were used⁷. As external morphological characteristics especially the Carnegie criteria for the limb development and curvature of the developing embryo were used (see figure 2). For the internal

5.1

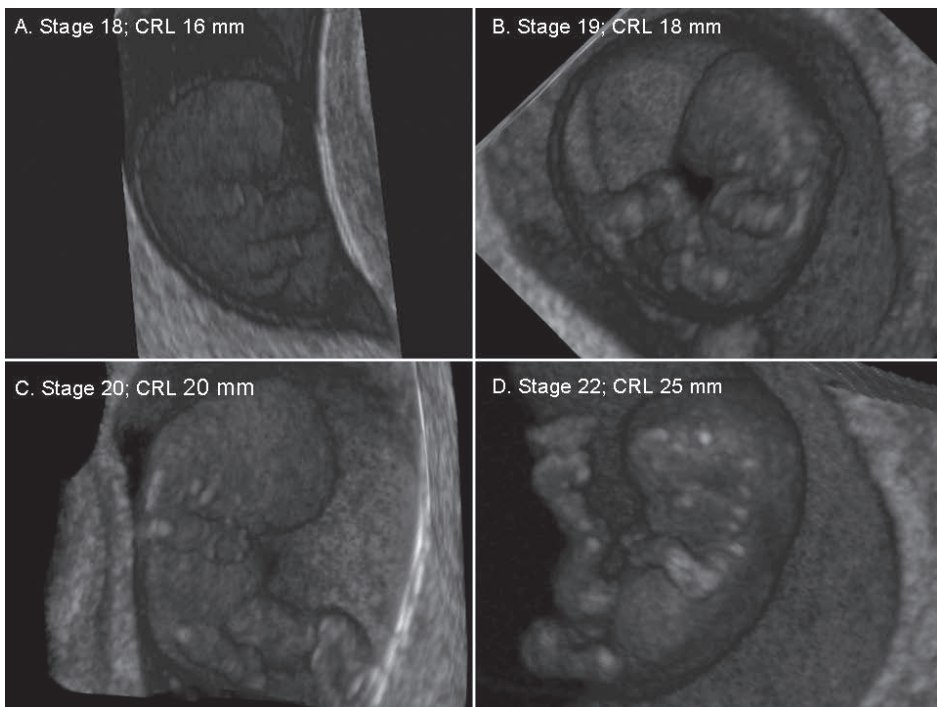


Figure 2. I-Space holograms of four different embryos are displayed. Especially the development of the limbs and the curvature of the embryo are used as external morphological criteria when the embryos were staged. Be aware of the fact that these I-Space holograms are displayed as a 2D image.

morphological development the criteria for the brain ventricle development were mainly used.

Statistical analysis

Data analysis was performed using SPSS (SPSS Release 17.0 for Windows) and SAS PROC MIXED (release 9.2; SAS Institute Inc, Cary, NC, USA). To analyze the longitudinal measurements, we used repeated-measurements ANOVA (random coefficient models).

To analyze the relation between the BVFV with the CRL and GA and the EV with the Carnegie stage we used the equation: $\text{Log}_2(\text{BVFV or EV}) = a + b \times \text{log}_2(\text{CRL or GA or stage})$, because the logarithmic transformation of both axes resulted in an approximate linear relationship. For the relationship between the EV and GA and CRL we used the equation: $\text{Log}_2(\text{EV}) = a + b \times \text{log}_2(\text{CRL or GA}) + c \times \text{log}_2(\text{CRL or GA})^2$. The following equation was used for the analysis of the relation of the BVFV or CRL and the Carnegie stage: $\sqrt{(\text{BVFV or CRL})} = a + b \times \text{stage}$. Finally, a linear relationship fitted best when the GA was related to the Carnegie stage: $\text{GA} = a + b \times \text{stage}$.

In the charts relating the GA and CRL to the Carnegie stage, the range (minimum and maximum values) of the GA and CRL according to O'Rahilly and Muller¹³ were plotted.

In general, when the parameters were related to the GA, the six patients with unreliable GA according to the CRL measurements performed in the first trimester were excluded.

The birth weight standard deviation score (SDS) of the study population was measured using the formulae of a large birth cohort, the Generation R study¹⁶. The calculated SDS are adjusted for gender and for GA at birth. The correlation of the birth weight SDS with the first trimester CRL and EV was measured with linear regression analysis.

Finally, $p = 0.05$ (two sided) was considered the limit of significance.

RESULTS

Data of a total group of 112 women were evaluated. Table I shows the characteristics of these patients and their newborns.

A total of 696 3D ultrasound scans were performed, with a median of 6 scans per patient (range: 4 – 8 scans). The GA had a median of 68 days and ranged between 42 days and 90 days. CRL measurements could be performed in 636 (91.4%) scans (median: 28.1 mm; range: 2.5 – 79.0 mm) and EV measurements in 458 (65.8%) scans (median: 1657.0 mm³; range: 2.4 – 23812.0 mm³). A total of 421 scans were performed between 7+0 and 10+6 weeks GA (median per patient: 4; range: 2 - 5), being the period for the BVFV measurements. BVFV was measured in 161 (38.2%) datasets (median: 45.1 mm³; range: 10.4 – 226.3 mm³). The embryos were staged until 10+1 weeks GA. Between 6+0 and 10+1 weeks

Table I. Characteristics of pregnant women and their newborns. Data shown are median (range) or percentages of patients.

Characteristic	Median (range) or percentage
Mothers (N = 112)	
Maternal age (years)	32.9 (18.9 – 42.7)
Parity	
0	62.5%
1	27.7%
≥ 2	9.8%
Gravidity	2 (1 – 10)
Miscarriages ≥ 2	25.9%
Conception mode	
Spontaneous	70.5%
IVF/ICSI	27.7%
IUI	1.8%
Gestational diabetes	5.4%
Hypertensive disorder	8.9%
Intra-uterine growth retardation	3.6%
Newborns (N = 112)	
Female	52.7%
Birth weight (grams)	3390 (450 – 4700)
Gestational age at delivery (weeks)	39+4 (26+4 – 42+0)

GA 405 scans (median per patient: 4; range: 1 - 5) were performed and staging was possible in 299 (73.8%) scans (median 19; range: 12 – 23). Table II shows the total number of CRL, EV, BVFV and Carnegie staging per gestational week. The total number of datasets used and the total number of measurements performed are also shown.

Figure 3 shows the relation of the EV with GA and CRL. The relation of the brain ventricle volume with GA and CRL is shown in figure 4. The fifth figure illustrates the relation of the EV and brain ventricle volume with the Carnegie stage.

The Carnegie stages are related to the GA and CRL as shown in figure 6. The original data from O’Rahilly and Muller¹³ are also plotted in these graphs (red boxes). A better fit is observed when the Carnegie stage is related to the CRL as compared to GA. The GA has a wider range, but still fits good. Especially in Carnegie stage 22 and 23 embryos the CRL measured in the I-Space is larger in comparison to the CRL measured by O’Rahilly and Muller.

Table III demonstrates the formulae of the relations calculated in this study, with the corresponding variance.

Table II. Numbers and percentages of successful CRL, EV, BVFV and Carnegie stage measurements per gestational week. N is the total number of datasets available per gestational week.

Gestational week	N	CRL	N	EV	N	BVFV	N	Carnegie
6	66	53 (80.3%)	66	37 (56.1%)	-	-	66	38 (57.6%)
7	102	89 (87.3%)	102	77 (75.5%)	102	31 (30.4%)	102	73 (71.6%)
8	103	97 (94.2%)	103	81 (78.6%)	103	54 (52.4%)	103	82 (79.6%)
9	107	103 (96.3%)	107	86 (80.4%)	107	54 (50.5%)	107	86 (80.4%)
10	109	106 (97.2%)	109	75 (68.8%)	109	22 (20.2%)	27	20 (74.1%)
11	108	103 (95.4%)	108	64 (59.3%)	-	-	-	-
12	101	85 (84.2%)	101	38 (37.6%)	-	-	-	-

5.1

The mean birth weight SDS was 0.05 and was normally distributed ($p=0.57$). Separate analysis of CRL and EV data for each week of gestation for their relation with birth weight SDS using regression analysis did not show significant correlations (all $r^2 < 0.033$) for any week between six and 12 weeks' GA. Categorizing birth weight SDS into categories less than -1, -1 to +1 and greater than +1 also did not show differences between these groups for longitudinal profiles of CRL and EV along advancing GA.

DISCUSSION

By measuring the BVFV automatically using transvaginal 3D ultrasound data in a VR application, we were able for the first time to systematically evaluate *in vivo* first trimester brain ventricle development. We secondly measured the CRL and EV, and determined the Carnegie stage on the basis of internal and external morphological criteria.

In various studies Blaas et al. used specialized software to measure the size of the brain ventricles (including the choroid plexuses), outlining them by hand in different 2D slices of the 3D image^{1,6}. In our own study we measured the total fluid volume of the BVFV (excluding the choroid plexus). As the ventricle volume measurements are automated in the I-Space, any visible connection between the ventricles can be used as a medium through which the adjacent ventricle can be measured.

Although post-processing was sometimes necessary to correct for incomplete segmentation of the brain ventricles, this was not necessary in most of the cases of brain ventricle segmentation. BVFV measurement usually takes less than one minute; measuring by manual segmentation is much more time-consuming, and as a previous study on validation of VR volume measurements showed, also less precise¹¹.

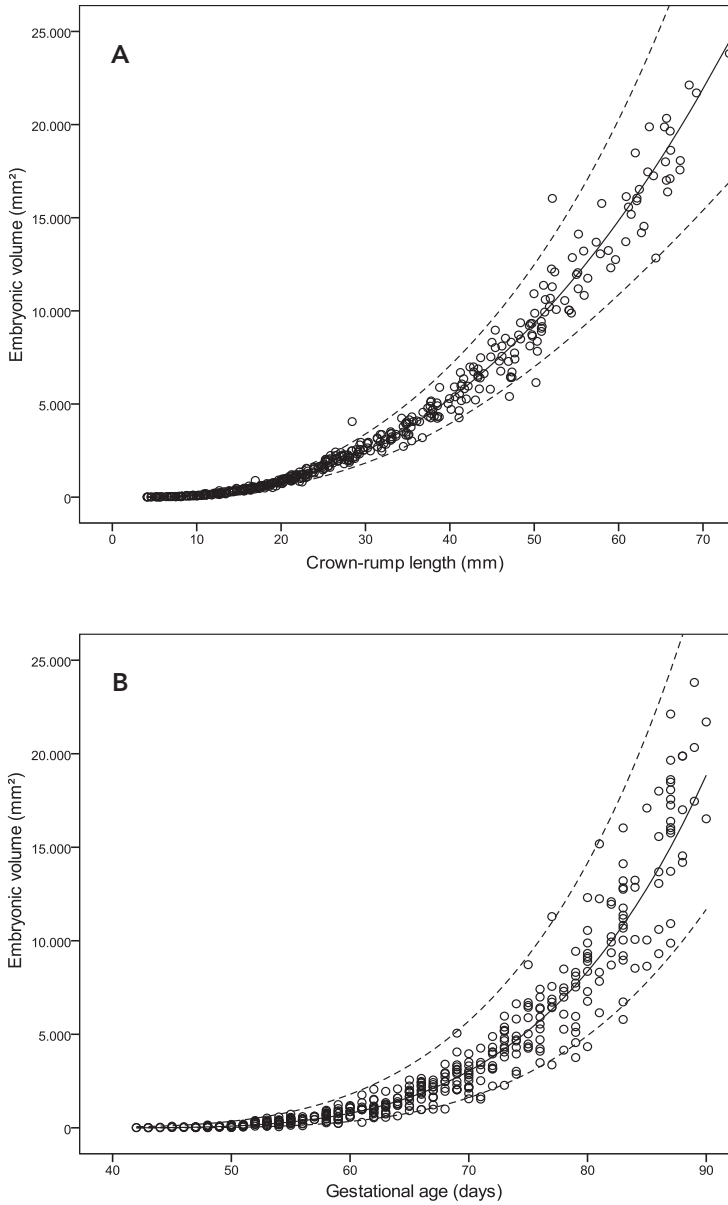


Figure 3. EV related to the CRL (A) and GA (B). The P50 curve is indicated by the solid line and the 95% prediction interval is indicated by the dotted lines.

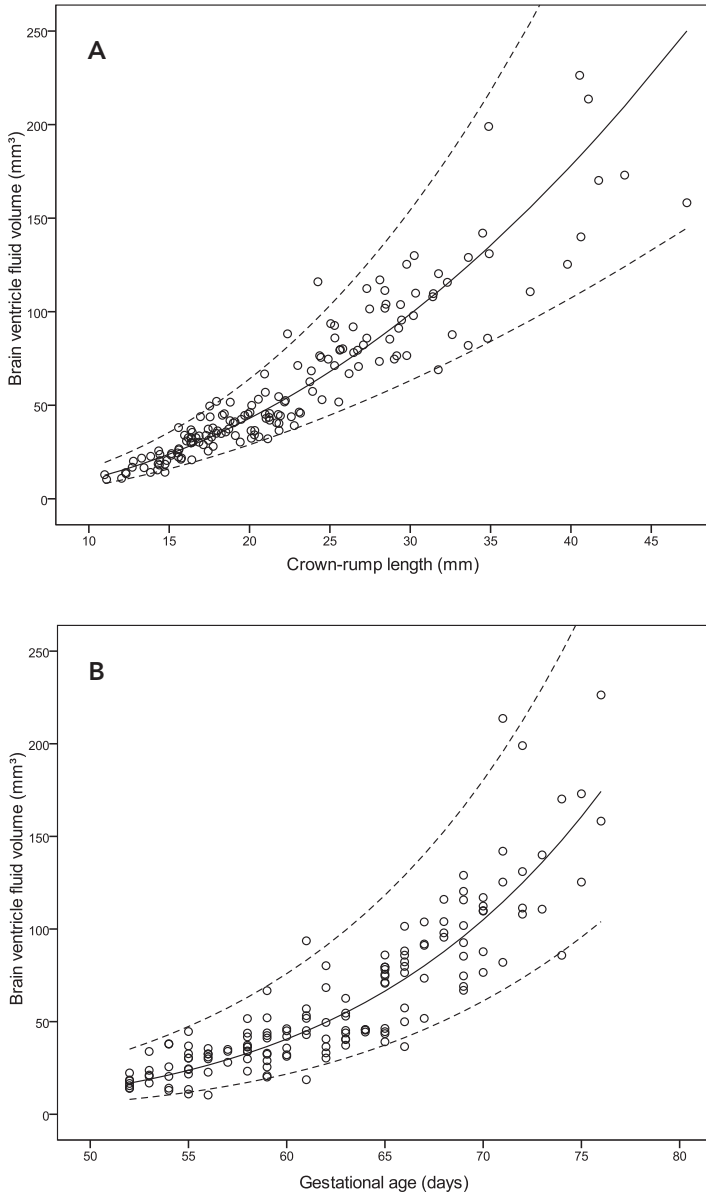


Figure 4. BVFV related to the CRL (A) and GA (B), with the corresponding P50 line (solid line) and 95% prediction interval (dotted lines).

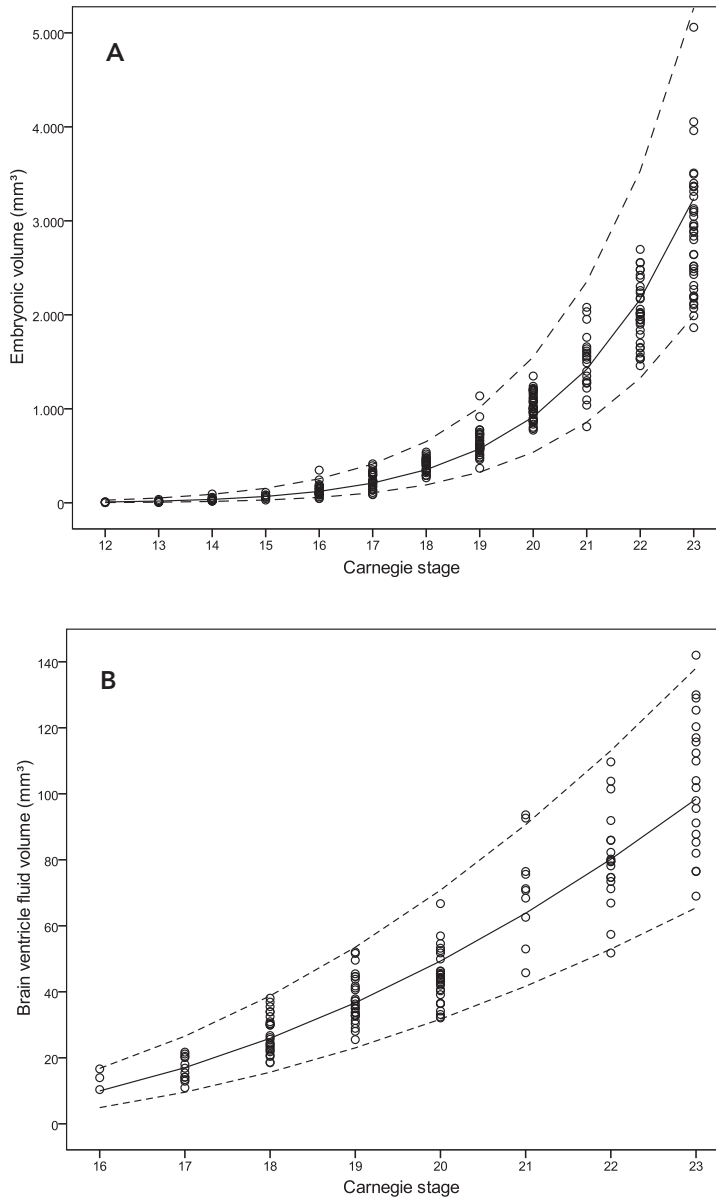


Figure 5. Relationship between the Carnegie stage with the EV (A) and BVFV (B), with the corresponding P50 line (solid line) and 95% prediction intervals (dotted lines).

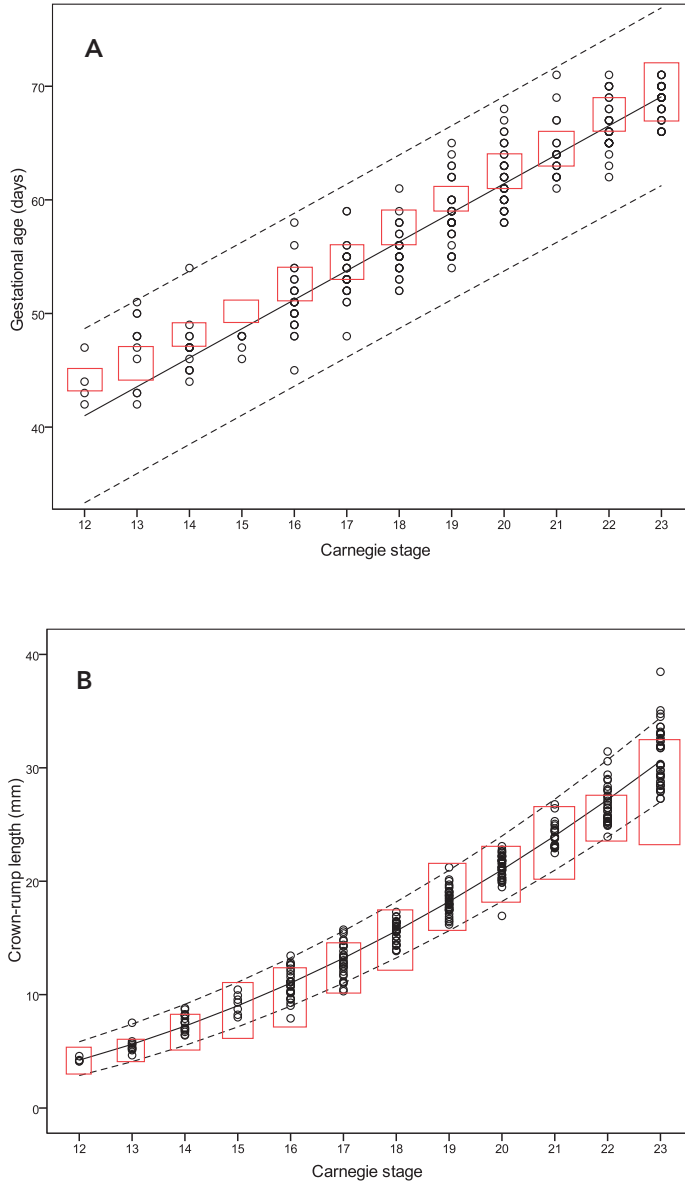


Figure 6. Relationship between the Carnegie stage with the GA (**A**) and CRL (**B**), with the corresponding mean line (solid line) and 95% prediction interval (dotted lines). The minimal and maximal CRL and proposed ages according to O’Rahilly and Muller are indicated by the red boxes.

Table III. Mean and standard deviation (SD) formula for the relation between various parameters. EV and BVFV units are mm³, GA is measured in days and the CRL in mm. N represents the total number of data points on which the formulae are based.

Relationship	N	Line	Formula
BVFV versus GA	158	Mean	$\text{Log}_2(\text{BVFV}) = -31.0782 + 6.1658 \times \text{log}_2(\text{GA})$
		Variance*	$14.95151 - 4.6654 \times \text{log}_2(\text{GA}) + 0.3674 \times \text{log}_2(\text{GA})^2$
BVFV versus CRL	161	Mean	$\text{Log}_2(\text{BVFV}) = -3.4261 + 2.0485 \times \text{log}_2(\text{CRL})$
		Variance	$0.71027 - 0.3044 \times \text{log}_2(\text{CRL}) + 0.03702 \times \text{log}_2(\text{CRL})^2$
EV versus GA	432	Mean	$\text{Log}_2(\text{EV}) = -11.3174 + 1.81004 \times \text{log}_2(\text{GA}-40) + 0.167594 \times \text{log}_2(\text{GA}-40)^2$
		Variance	$15.0974 - 10.1324 \text{log}_2(\text{GA}-40) + 2.7162 \times \text{log}_2(\text{GA}-40)^2 - 0.3400 \times \text{log}_2(\text{GA}-40)^3 + 0.016574 \times \text{log}_2(\text{GA}-40)^4$
EV versus CRL	458	Mean	$\text{Log}_2(\text{EV}) = -8.72 + 1.9812 \times \text{log}_2(\text{CRL}-4) + 0.03279 \times \text{log}_2(\text{CRL}-4)^2$
		Variance	$2.3720 - 2.21634 \times (\text{CRL}-4) + 0.7839 \times (\text{CRL}-4)^2 - 0.12147 \times (\text{CRL}-4)^3 + 0.00695 \times (\text{CRL}-4)^4$
CRL versus Carnegie	299	Mean	$\text{Sqrt}^{**}(\text{CRL}) = -1.7375 + 0.3160 \times \text{stage}$
		Variance	$0.09498 + 2 \times \text{stage} \times -0.00374 + 0.000201 \times \text{stage}^2$
GA versus Carnegie	281	Mean	$10.3612 + 2.5530 \times \text{stage}$
		Variance	$19.0351 - 0.5038 \times \text{stage} + 0.01605 \times \text{stage}^2$
EV versus Carnegie	295	Mean	$\text{Log}_2(\text{EV}) = -39.2655 + 9.0549 \times \text{log}_2(\text{stage})$
		Variance	$13.514 - 5.9324 \times \text{log}_2(\text{stage}) + 0.6573 \times \text{log}_2(\text{stage})^2$
BVFV versus Carnegie	146	Mean	$\text{Sqrt}(\text{BVFV}) = -12.3021 + 0.9662 \times \text{stage}$
		Variance	$1.6102 + 2 \times \text{stage} \times -0.1050 + 0.007735 \times \text{stage}^2$

* The standard deviation (SD) of the individual data point around the fitted curves are obtained by taking the square root of the variance.

** Sqrt denotes the square root transformation.

To date, only Blaas et al. have succeeded in measuring embryonic brain ventricle volumes in a cross-sectional setting by using a specially developed annular array 3D transvaginal probe, in which they manually drew the contours of the ventricles in several parallel two-dimensional (2D) slices of the 3D image^{1, 6}. This was very time-consuming and vulnerable to individual variation. Two other 3D ultrasound visualization methods have been used to visualize the human embryonic brain ventricles semi-automatically^{5, 17}. These cross-sectional case studies followed the embryonic brain development in only a few patients. Although enhanced imaging

of the human embryonic brain ventricles was possible in these studies, volume measurements were not due to the small size of the ventricles.

Enlarged brain cavities are important diagnostic markers for the detection of central nervous system disorders in very early pregnancy^{4-5, 18-20}. The reference charts constructed in this study provide quantitative and accurate information, and may help to differentiate between early normal and abnormal brain development.

In contrast with 3D ultrasound, where the 3D image is evaluated on 2D media (screen or on paper), the I-Space allows us to use the third dimension of the 3D ultrasound image to its fullest, and to obtain a real impression of the developing embryo. As this is essential for *in vivo* staging according to the classical Carnegie stage system, it provides us with unique information about the state of development – which, together with age and size of the embryo, is an independent parameter¹²⁻¹³. The stages were related to CRL, BVFV and EV; resulting in smaller prediction intervals in comparison to GA alone. However, it is important to remember that this staging system is based not only on morphological characteristics, but also on histological ones, which cannot be determined in the I-Space¹³. Secondly, we should remember that *in vitro* verification was not possible in this study.

Low birth weight babies are at increased risk of perinatal and infant morbidity and mortality, and of cardiovascular and metabolic diseases in later life^{16, 21-23}. While some studies have correlated late first trimester CRL growth with a low birth weight²⁴⁻²⁶, another study has not²⁷. The CRL and EV between six and 12 weeks GA measured in our study was not associated with birth weight SDS. The SDS formulae used in this study, are based on women living in Rotterdam, which, given the normally distributed birth weight SDS, fits well with our population. There may be a power problem due to the limited number of measurements included. Almost 30 percent of women had a certain GA due to assisted reproductive therapy. An explanation may be that in the remaining patients a relatively wide range (+/- 7 gestational days) of variance in the CRL was accepted when dating based on their last menstrual period.

In case of the brain ventricle segmentation, a clear delineation between fluid and the tissue interface is needed to measure the BVFV. Unfortunately embryonic and fetal position, movements and acoustic shadows may affect the rendering and negatively influence the measurement abilities. VR BVFV measurements are affected by these factors in approximately 50% of the cases in gestational weeks eight and nine, which indicates that these two gestational weeks have the highest quality images collected using a transvaginal probe. The EV is a greater structure, which is less affected by small movements or acoustic artefacts.

We are aware of the fact that other hospitals have had limited access to VR equipment until now. A desktop version running the same software as in the I-Space is now under development. This low-cost VR desktop system will become

available in the near future and will enable other hospitals to use 3D images to its fullest in the same manner as in our study.

In conclusion, the I-Space VR application enables us to measure EV and BVFV automatically, and to follow their embryonic development in the first trimester by visualizing all three dimensions. This makes it possible to base *in vivo* staging of the embryos on internal and external morphological characteristics.

The next step will be to study abnormal development of the embryo and early fetus in VR systematically. This will provide us with new insights into normal development *in vivo*, and makes early diagnosis of abnormal embryogenesis possible.

REFERENCES

1. Blaas HG, Eik-Nes SH, Kiserud T, Berg S, Angelsen B, Olstad B. Three-dimensional imaging of the brain cavities in human embryos. *Ultrasound Obstet Gynecol.* 1995;5:228-32.
2. Blaas HG, Eik-Nes SH, Kiserud T, Hellevik LR. Early development of the forebrain and midbrain: a longitudinal ultrasound study from 7 to 12 weeks of gestation. *Ultrasound Obstet Gynecol.* 1994;4:183-92.
3. Blaas HG, Eik-Nes SH, Kiserud T, Hellevik LR. Early development of the hindbrain: a longitudinal ultrasound study from 7 to 12 weeks of gestation. *Ultrasound Obstet Gynecol.* 1995;5:151-60.
4. Blaas HG, Eik-Nes SH, Vainio T, Isaksen CV. Alobar holoprosencephaly at 9 weeks gestational age visualized by two- and three-dimensional ultrasound. *Ultrasound Obstet Gynecol.* 2000;15:62-5.
5. Timor-Tritsch IE, Monteagudo A, Santos R. Three-dimensional inversion rendering in the first- and early second-trimester fetal brain: its use in holoprosencephaly. *Ultrasound Obstet Gynecol.* 2008;32:744-50.
6. Blaas HG, Eik-Nes SH, Berg S, Torp H. In-vivo three-dimensional ultrasound reconstructions of embryos and early fetuses. *Lancet.* 1998;352:1182-6.
7. Verwoerd-Dikkeboom CM, Koning AH, van der Spek PJ, Exalto N, Steegers EA. Embryonic staging using a 3D virtual reality system. *Hum Reprod.* 2008;23:1479-84.
8. Verwoerd-Dikkeboom CM, Koning AH, Hop WC, Rousian M, Van Der Spek PJ, Exalto N, Steegers EA. Reliability of three-dimensional sonographic measurements in early pregnancy using virtual reality. *Ultrasound Obstet Gynecol.* 2008;32:910-6.
9. Verwoerd-Dikkeboom CM, Koning AH, Hop WC, van der Spek PJ, Exalto N, Steegers EA. Innovative virtual reality measurements for embryonic growth and development. *Hum Reprod.* 2010;25:1404-10.
10. Rousian M, Koning AH, van Oppenraaij RH, Hop WC, Verwoerd-Dikkeboom CM, van der Spek PJ, Exalto N, Steegers EA. An innovative virtual reality technique for automated human embryonic volume measurements. *Hum Reprod.* 2010;25:2210-6.
11. Rousian M, Verwoerd-Dikkeboom CM, Koning AH, Hop WC, van der Spek PJ, Exalto N, Steegers EA. Early pregnancy volume measurements: validation of ultrasound techniques and new perspectives. *BJOG.* 2009;116:278-85.
12. O'Rahilly R, Muller F. Developmental stages in human embryos. Washington: Carnegie Institution of Washington Publication 1987.
13. O'Rahilly R, Muller F. Developmental stages in human embryos: revised and new measurements. *Cells Tissues Organs.* 2010;192:73-84.
14. Koning AH, Rousian M, Verwoerd-Dikkeboom CM, Goedknegt L, Steegers EA, van der Spek PJ. V-scope: design and implementation of an immersive and desktop virtual reality volume visualization system. *Stud Health Technol Inform.* 2009;142:136-8.
15. O'Rahilly R, Muller F. Prenatal ages and stages-measures and errors. *Teratology.* 2000;61:382-4.

16. Mook-Kanamori DO, Steegers EA, Eilers PH, Raat H, Hofman A, Jaddoe VW. Risk factors and outcomes associated with first-trimester fetal growth restriction. *JAMA*. 2010;303:527-34.
17. Pistorius L, Stoutenbeek P, Visser GH. First trimester neurosonoembryology with automated follicle tracking: Preliminary findings. *J Matern Fetal Neonatal Med*. 2009;1-3.
18. Becker R, Mende B, Stiemer B, Entezami M. Sonographic markers of exencephaly at 9 + 3 weeks of gestation. *Ultrasound Obstet Gynecol*. 2000;16:582-4.
19. Machado RA, Brizot ML, Carvalho MH, Waissman AL, Bunduki V, Zugaib M. Sonographic markers of exencephaly below 10 weeks' gestation. *Prenat Diagn*. 2005;25:31-3.
20. Matsunaga E, Shiota K. Holoprosencephaly in human embryos: epidemiologic studies of 150 cases. *Teratology*. 1977;16:261-72.
21. Kramer MS. Determinants of low birth weight: methodological assessment and meta-analysis. *Bull World Health Organ*. 1987;65:663-737.
22. Barker DJ. The fetal and infant origins of adult disease. *BMJ*. 1990;301:1111.
23. Gluckman PD, Hanson MA, Cooper C, Thornburg KL. Effect of in utero and early-life conditions on adult health and disease. *NEJM*. 2008;359:61-73.
24. Leung TY, Sahota DS, Chan LW, Law LW, Fung TY, Leung TN, Lau TK. Prediction of birth weight by fetal crown-rump length and maternal serum levels of pregnancy-associated plasma protein-A in the first trimester. *Ultrasound Obstet Gynecol*. 2008;31:10-4.
25. Bukowski R, Smith GC, Malone FD, Ball RH, Nyberg DA, Comstock CH, Hankins GD, Berkowitz RL, Gross SJ, Dugoff L, Craigo SD, Timor-Tritsch IE, Carr SR, Wolfe HM, D'Alton ME, Consortium FR. Fetal growth in early pregnancy and risk of delivering low birth weight infant: prospective cohort study. *BMJ*. 2007;334:836.
26. Smith GC, Smith MF, McNay MB, Fleming JE. First-trimester growth and the risk of low birth weight. *NEJM*. 1998;339:1817-22.
27. Habayeb O, Daemen A, Timmerman D, De Moor B, Hackett GA, Bourne T, Lees CC. The relationship between first trimester fetal growth, pregnancy-associated plasma protein A levels and birth-weight. *Prenat Diagn*. 2010;30:873-8.



CHAPTER 5.2

HUMAN EMBRYONIC GROWTH
AND DEVELOPMENT OF THE
CEREBELLUM USING THREE-
DIMENSIONAL ULTRASOUND AND
VIRTUAL REALITY

ABSTRACT

Background To evaluate first trimester cerebellar growth and development using two different measuring techniques: three-dimensional (3D) and virtual reality (VR) ultrasound visualization. The cerebellum measurements were related to gestational age (GA) and crown-rump length (CRL). Finally, the reproducibility of both methods was tested.

Methods We collected 630 first trimester, serially obtained, 3D ultrasound scans of 112 uncomplicated pregnancies in a prospective cohort study. Only scans with high quality images of the fossa posterior were selected for analysis. Measurements were performed off-line in the coronal plane, using 3D and VR software. VR enables the observer to use all available dimensions in a dataset by visualizing the rendered volume as a 'hologram'. Total cerebellar diameter, left and right hemispherical diameter and left and right hemispherical thickness were measured. All measurements were performed three times and means were used in repeated measurements analysis. The reproducibility was established in a subset of 35 datasets.

Results A total of 177 (28%) 3D datasets between 7⁺⁰ and 12⁺⁶ weeks GA could be used for cerebellum measurements. The median GA was 10+0 weeks and the median CRL was 31.4 mm (range: 5.2 – 79.0 mm). The total cerebellar diameter measured using VR had a median of 5.5 mm (range: 2.2 – 13.9 mm) and was measurable from seven gestational weeks onwards. The ICC values for both methods were at least 0.98 for all cerebellar parameters. Reference charts were constructed according to GA and CRL.

Conclusions Reference charts for normal embryonic cerebellar growth were constructed. Both methods proved to be reproducible.

Keywords 3D ultrasound; brain; first trimester; cerebellum; virtual reality; 4D view

Melek Rousian, Irene A.L. Groenenberg, Wim C. Hop, Anton H.J. Koning, Peter J. van der Spek, Niek Exalto, Eric A.P. Steegers

Submitted

INTRODUCTION

During the last decennium, the ultrasound equipment has improved, enabling more detailed two-dimensional (2D) and three-dimensional (3D) examinations by using high resolution transvaginal probes, which can be performed even in the embryonic period. During this period major changes occur in the central nervous system.¹⁻³ Malformations of the central nervous system have been detected as early as nine weeks' gestational age.⁴⁻⁶

The cerebellum is formed in the early embryonic period and at Carnegie stage 14 the cerebellar plates can be identified anatomically.⁷ The group of Blaas et al. was the first to describe the ultrasonographic development of the cerebellum as early as eight weeks' GA.⁽⁸⁾ Their study showed that it is possible to study the embryonic cerebellum development *in vivo* in great detail.

Particularly transvaginal 3D ultrasound enables a detailed visualization and description of the embryonic development.⁹ It has the potential to evaluate first trimester embryonic anatomy using a single 3D ultrasound dataset, in which all three planes of the embryo can be viewed.¹⁰ Due to the small size the whole embryo fits in one dataset. Acquiring a dataset takes only a couple of minutes, which leads to a reduction of scanning time, compared to 2D ultrasound.¹¹

In combination with high-resolution 3D ultrasound, virtual reality (VR) can be used to visualize the embryo. VR allows the use of all three dimensions of the human embryo to its fullest by visualizing the rendered dataset as a 'hologram'. The I-Space VR system running the V-Scope software can be used to visualize morphology and to quantify biometry and volumetry during first trimester pregnancies.¹²⁻¹⁷

The aim of this prospective longitudinal ultrasound study is to evaluate first trimester growth and development of the cerebellum using two different approaches for analyzing stored 3D datasets: 3D software (4D View) and VR software (V-Scope). These measurements are compared to each other and related to gestational age (GA) and crown-rump length (CRL). We finally test the intraobserver and interobserver reliability and agreement of both methods.

PATIENTS AND METHODS

Patients

A total of 141 healthy volunteering pregnant women were included into our study. These women were recruited via the department of Obstetrics and Gynaecology at the Erasmus MC University Medical Center. A small proportion (around 20%) of the women applied from outside the University hospital. All women gave written informed consent and the regional committee for medical ethics approved the study. In this prospective study a quick 3D ultrasound exam (with a maximum scanning time of 10 minutes) was performed weekly between 6 or 7 weeks' of gestation and 12 weeks' of gestation, during which a series of 3D sweeps

encompassing the whole fetus were obtained. GA was calculated using the first day of the last menstrual period. In case of an unknown date of the last menstruation or in case of a discrepancy of one week or more, GA was determined by the CRL measurements performed in the first trimester. For the IVF/ICSI pregnancies the GA was based on the date of oocyte retrieval.

Exclusion criteria were a non-viable pregnancy, a chromosomal or structural anomaly detected before or after birth, multiple pregnancies and intra-uterine fetal death.

Twenty-nine patients were excluded: 16 patients were diagnosed with a non-viable pregnancy, two patients were diagnosed with a trisomy 21 pregnancy, three patients were diagnosed with a congenital anomaly, three patients carried multiple pregnancies, two pregnant women showed an intra-uterine fetal death and there were three drop-outs (one because of her religious background and two patients were not able to participate on a weekly basis). In the remaining 112 patients 630 3D ultrasound scans were performed between 7+0 and 12+6 weeks GA. Only 3D datasets of the fossa posterior with a clear demarcation of the cerebellum were selected for further analysis and datasets including movement artefacts and a poor quality were excluded. Acquisition of the 3D ultrasound datasets was performed by one examiner (MR), evaluation and analysis was performed off-line by two experienced examiners (MR and IALG). A total of 6 women had adjustments for their GA based on the CRL measured in the first trimester.

Ultrasound equipment

The ultrasound examinations were performed using a GE Voluson E8 (GE, Zipf, Austria) and a 4.5 – 11.9 MHz vaginal probe. The quality of the scans was evaluated off-line using specialized 3D software (4D View, version 7.0, GE Medical Systems). The approved scans were stored as Cartesian volumes, which were later used for VR visualization using the BARCO I-Space at the Department of Bioinformatics.

Measurements

The measurements were performed off-line using two different measuring methods: 3D software (4D view) and VR software (V-Scope). 4D view allows measurement of the cerebellum in 3D ultrasound datasets on a separate personal computer or on the ultrasound machine, which are both using 2D displays. V-Scope is a special volume rendering software application, written for the I-Space, which is an immersive four-walled VR system. V-Scope creates an interactive hologram of the ultrasound image and this hologram can be manipulated by means of a virtual pointer, controlled by a wireless joystick. In both methods the provided length-measuring tools were used (movie 5).

In 4D view the 3D datasets were displayed in the orthogonal multiplanar mode. Cerebellum measurements were performed in a coronal section of the head through the rhombencephalon showing the cerebellum, fourth ventricle and plexus choroideus of the fourth ventricle (figure 1). V-Scope enables visualization of all three planes in just one image. Again, all measurements were performed in a

Movie 5. This 2D movie shows how observer M.R. measures the cerebellum of an embryo of nine weeks' GA. The total cerebellar diameter and left and right hemispherical diameters are measured by using the wireless joystick in the I-Space VR application.

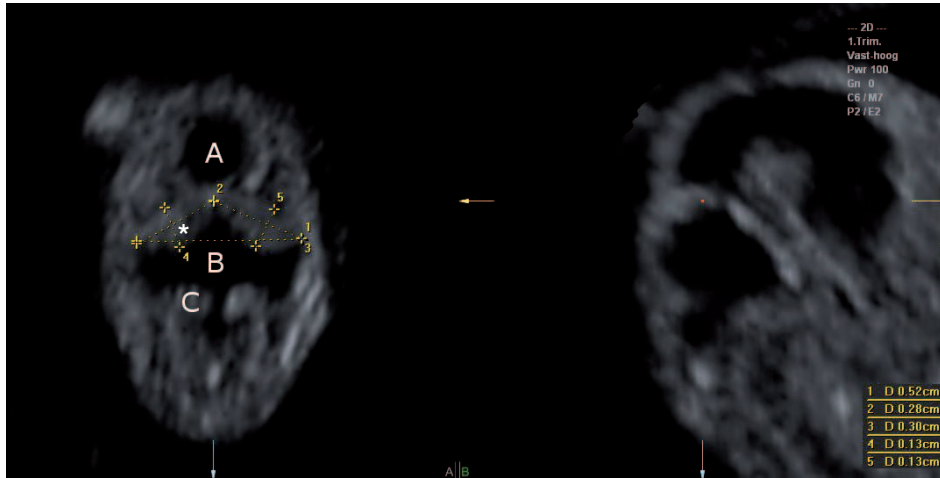


Figure 1. Head of an embryo of 8 weeks and 5 days GA visualized using 4D View software. The cerebellum (*) measurements are performed in the coronal plane (left panel of the image, plane A). In this plane the mesencephalon (A), fourth ventricle (B) and choroid plexus (C) are visible. The total cerebellar diameter (1), individual left (2) and right (3) hemispherical diameter, with the corresponding left (4) and right (5) hemispherical thickness are measured using the 'distance two points' function. The right panel of the image shows the sagittal plane (plane B) of the head.

coronal section through the rhombencephalon (figure 2). The following parameters were determined using both methods: total cerebellar diameter, individual left and right hemispherical diameter, with the corresponding left and right hemispherical thickness (figure 2). The CRL was also determined. Verwoerd-Dikkeboom et al. already showed that both length-measuring methods are reproducible when used for standard biometric measurements in the first trimester of pregnancy.¹⁵ Therefore, the CRL measurements were only performed in VR.

All measurements were performed three times and the mean values were used for analysis.

Reproducibility

The intraobserver and interobserver reliability and agreement was evaluated in 35 randomly chosen datasets of 35 randomly chosen patients. A total of 5 datasets per gestational week were selected. To study the intraobserver and interobserver agreement of the 3D measurements, all cerebellar measurements were performed

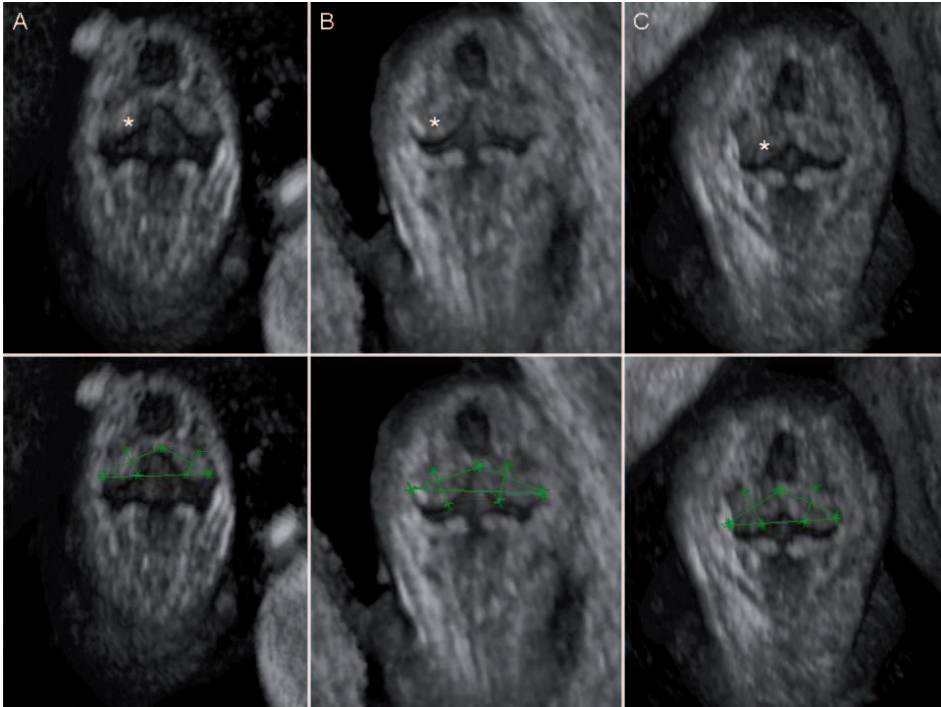


Figure 2. The cerebellum (*) of three different patients is visualized in the I-Space. **A.** This is the same embryo as in figure 1 (8 weeks and 5 days GA). **B.** This is an embryo of 9 weeks and 3 days GA. **C.** This embryo is 10 weeks and 2 days GA. The corresponding cerebellar measurements are displayed in the images below A, B and C.

twice by one observer (IALG) using 3D software and repeated independently by another (MR). For the reproducibility of the VR measurements, all measurements were again performed twice by one observer (MR) and repeated independently by another observer (IALG). The observers were blinded to each others results. To prevent recollection bias the second series of measurements by the same observer were performed at least two weeks after the first series.

Statistical analysis

To assess reliability, the intraclass correlation coefficients (ICC) were calculated in SPSS (Release 17.0 for windows). An ICC value above 0.70 is in general considered to represent a good reliability. To study whether there was a systematic difference between the measurements acquired with the two different methods – 4D view and V-Scope – the mean difference and 95% CI of the mean difference were calculated using repeated measurement analysis. Secondly, for the agreement between and within the two observers we calculated the mean difference and the 95% CI of the mean using the paired t-test. The 95% limits of agreement (mean difference \pm 1.96SD) were calculated as described by Bland and Altman in both cases.¹⁸

Repeated-measurements ANOVA (random coefficient models) analysis was used to examine the longitudinal measurements (SAS PROC MIXED, release 9.2; SAS Institute Inc, Cary, NC, USA) for their relation with GA and with CRL. The association between the cerebellum measurements and the GA and CRL were expressed in figures and in equations. Patients with unreliable GA according to the CRL measurement were excluded from the analysis of the GA data. The possible differences in symmetry of the left and right hemispherical diameter and thickness were evaluated with multilevel analysis.

RESULTS

The median age of the participating women was 32.0 years (range: 18.9 – 42.7 years). Sixty-three percent of the women were nulliparous. Seventy percent of the patients conceived spontaneously, while 28% became pregnant after IVF or ICSI treatment and 2% after IUI. Twenty-six percent had recurrent miscarriages in the past, defined as having two or more miscarriages. Fifty-nine (53%) healthy girls and 53 (47%) healthy boys were born with a median birth weight of 3390 grams and a range from 450 to 4700 grams (SD: 636 grams).

A total number of 630 ultrasound scans were performed in these pregnant women, with a median of 6 datasets and a minimum of 3 and a maximum of 7 datasets per patient. A total of 453 datasets were excluded from further analysis, leaving 177 high quality datasets of the posterior fossa (28%). Reasons for exclusion were movement artifacts (N=81 (13%)) and poor image quality (N=372 (59%)).

All cerebellum measurements performed in 3D were compared to the measurements performed using VR. The ICC values are displayed in table I. The reliability of the 3D and VR measurements is very good. However a small (less than 0.04 mm) systematic difference ($p < 0.05$) between the 3D and VR measurements is present.

The mean difference, the limits of agreement and the ICC values for the intraobserver and interobserver reproducibility of the 3D and VR measurements are displayed in table II. All ICC values are above 0.98, representing very good reliability between the measurements. The Bland-Altman statistics show a good agreement between the measurements as well (table II). There is a small systematic difference ($p < 0.01$) between the two observers measuring the total cerebellar diameter in VR of 0.12 mm, but there is still a very good reliability (ICC=0.996).

There is no systematic difference between 3D and VR measurements and they are both highly reproducible. Because of this, all further reported results are based on the measurements performed using VR.

Table III shows the I-Space measurements per gestational week, with the corresponding mean value and SD value. The total number of datasets available and the total number of datasets used for the measurements per gestational week are also displayed. We were able to measure the cerebellum as early as 7+1 weeks GA (CRL=10.3 mm).

Table I. The mean difference with the corresponding 95% confidence interval (CI), the limits of agreement and the ICC values are displayed comparing the 3D and VR cerebellum measurements.

	N	Mean difference* (mm)	95% CI mean difference (mm)	95% limits of agreement (mm)	ICC
TCD (3D vs. VR)	177	-0.03	-0.05 to 0.00 [§]	-0.31 to 0.25	0.998
LHD (3D vs. VR)	172	-0.04	-0.06 to -0.03 [§]	-0.26 to 0.18	0.993
LCH (3D vs. VR)	164	-0.01	-0.03 to 0.00 [§]	-0.16 to 0.13	0.994
RHD (3D vs. VR)	172	-0.04	-0.06 to -0.02 [§]	-0.27 to 0.19	0.993
RCH (3D vs. VR)	165	-0.03	-0.04 to -0.01 [§]	-0.18 to 0.13	0.993

TCD = total cerebellar diameter; LHD = left hemispherical diameter; LHT = left hemispherical thickness; RHD = right hemispherical diameter; RHT = right hemispherical thickness

[§] Statistically significant ($p < 0.05$).

* Mean differences are calculated as 3D measurement series minus VR measurement series.

Satisfying fits of the repeated measurement models for the cerebellum measurements were obtained by either linear functions or quadratic functions of GA and CRL. The equations for the mean values and the associated SD in relation to GA and CRL are displayed in table IV. A graphical representation of the relationships with GA is shown in figure 3.

There is no significant difference between the left and right hemispherical diameter (mean difference = 0.02 ± 0.01 mm; $p = 0.14$). There is also no difference between the left and right hemispherical thickness (mean difference = -0.004 ± 0.01 mm; $p = 0.70$). Both differences do not significantly change over gestational time.

DISCUSSION

In this study we have shown for the first time that the human cerebellum can be measured *in vivo* as early as seven weeks GA. We measured the total cerebellar diameter, left and right hemispherical diameter, with the corresponding left and right hemispherical thickness in the coronal plane using two different measuring techniques: a 3D technique (4D view) and an innovative VR technique (V-Scope). Intraobserver and interobserver reliability and agreement of both techniques are very good.

V-Scope is an innovative VR application, allowing the observer to get a real impression of the developing cerebellum. Using VR, off-line cerebellum measurements can easily be performed in high quality 3D datasets. VR has also been proven to be a promising tool for future research and clinical practice. In contrast to standard 3D analysis software the third dimension can be used to its fullest as a result of the depth perception offered by the VR system. Small systematic differences are present when the cerebellar parameters performed using 3D and VR are compared, however these are too small to be (clinically)

5.2

Table II. Mean differences between measurements with the corresponding 95% confidence interval (CI), the limits of agreement and the ICC values with the corresponding 95% CI are displayed comparing the 3D and VR cerebellum measurements performed by the same and by the second observer.

	N	Mean difference (mm)	95% CI mean difference (mm)	95% limits of agreement (mm)	ICC	95% CI ICC
TCD (Intraobserver VR)	35	0.02	-0.02 to 0.06	-0.20 to 0.24	0.999	0.998 to 0.999
LHD (Intraobserver VR)	35	-0.03	-0.07 to 0.02	-0.29 to 0.24	0.991	0.981 to 0.995
LHT (Intraobserver VR)	33	0.02	-0.01 to 0.04	-0.12 to 0.15	0.996	0.992 to 0.998
RHD (Intraobserver VR)	35	-0.01	-0.05 to 0.04	-0.25 to 0.24	0.992	0.984 to 0.996
RHT (Intraobserver VR)	34	-0.01	-0.03 to 0.01	-0.14 to 0.12	0.996	0.993 to 0.998
TCD (Interobserver VR)	35	-0.12	-0.18 to -0.06 [§]	-0.45 to 0.22	0.996	0.986 to 0.999
LHD (Interobserver VR)	35	-0.02	-0.06 to 0.02	-0.26 to 0.23	0.992	0.984 to 0.996
LHT (Interobserver VR)	33	-0.04	-0.09 to 0.00	-0.31 to 0.22	0.985	0.968 to 0.992
RHD (Interobserver VR)	35	-0.03	-0.09 to 0.03	-0.37 to 0.31	0.985	0.970 to 0.992
RHT (Interobserver VR)	34	-0.05	-0.09 to 0.00	-0.29 to 0.20	0.986	0.971 to 0.993
TCD (Intraobserver 3D)	35	0.04	0.00 to 0.08	-0.20 to 0.28	0.999	0.997 to 0.999
LHD (Intraobserver 3D)	35	0.03	0.00 to 0.07	-0.16 to 0.23	0.994	0.988 to 0.997
LHT (Intraobserver 3D)	33	0.01	-0.04 to 0.07	-0.30 to 0.33	0.980	0.960 to 0.990
RHD (Intraobserver 3D)	35	0.00	-0.04 to 0.05	-0.27 to 0.28	0.991	0.981 to 0.995
RHT (Intraobserver 3D)	33	0.05	0.00 to 0.10	-0.24 to 0.35	0.981	0.960 to 0.991
TCD (Interobserver 3D)	35	0.00	-0.04 to 0.04	-0.24 to 0.24	0.999	0.998 to 0.999
LHD (Interobserver 3D)	35	0.00	-0.04 to 0.04	-0.21 to 0.21	0.994	0.989 to 0.997
LHT (Interobserver 3D)	33	-0.02	-0.03 to 0.00	-0.12 to 0.09	0.998	0.995 to 0.999
RHD (Interobserver 3D)	35	0.04	0.00 to 0.07	-0.15 to 0.23	0.995	0.989 to 0.997
RHT (Interobserver 3D)	34	-0.03	-0.05 to 0.00	-0.15 to 0.10	0.996	0.991 to 0.998

[§] Statistically significant ($p < 0.01$).

Table III. Measurements performed in the I-Space per gestational week. The corresponding mean and standard deviation (SD) are also shown. In the third row the total number of datasets used for the cerebellum measurements and the total number of datasets available in each gestational week are shown.

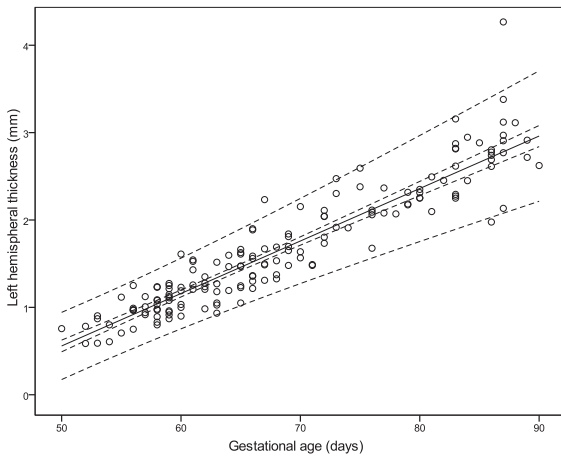
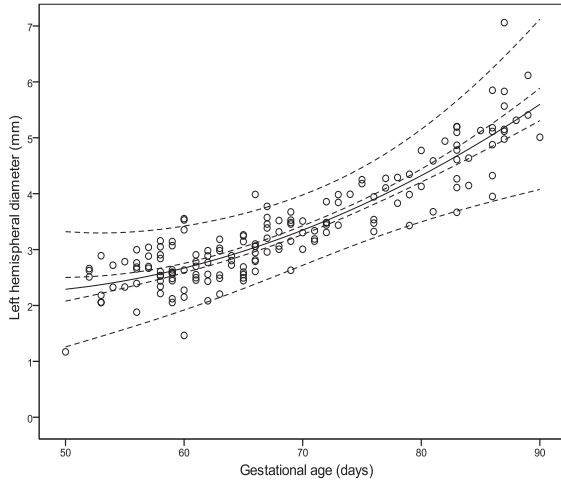
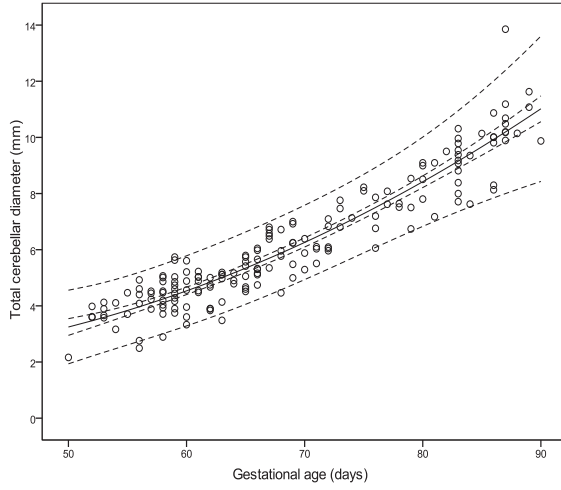
Ultrasound characteristics	Gestational age (complete weeks)		7+0		8+0		9+0		10+0		11+0		12+0	
	Mean (SD)	Mean (SD)	Mean (SD)	Mean (SD)	Mean (SD)	Mean (SD)	Mean (SD)	Mean (SD)	Mean (SD)	Mean (SD)	Mean (SD)	Mean (SD)	Mean (SD)	Mean (SD)
CRL (mm)	12.67 (2.95)	18.94 (3.10)	26.46 (4.03)	36.89 (5.50)	49.27 (6.45)	62.60 (6.71)								
Number of datasets	13 / 102	54 / 103	43 / 107	22 / 109	25 / 108	20 / 101								
TCD (mm)	3.72 (0.58)	4.42 (0.68)	5.52 (0.80)	6.76 (0.89)	8.56 (0.95)	10.17 (1.33)								
LHD (mm)	2.40 (0.47)	2.65 (0.39)	3.04 (0.40)	3.60 (0.36)	4.39 (0.52)	5.20 (0.72)								
LHT (mm)	0.77 (0.17)	1.11 (0.20)	1.48 (0.27)	2.00 (0.33)	2.40 (0.29)	2.84 (0.46)								
RHD (mm)	2.38 (0.50)	2.65 (0.38)	3.04 (0.38)	3.58 (0.41)	4.33 (0.46)	5.11 (0.67)								
RHT (mm)	0.76 (0.14)	1.11 (0.20)	1.49 (0.27)	2.00 (0.34)	2.41 (0.31)	2.85 (0.42)								

5.2

Table IV. Equations for the mean and variance of each cerebellum measurement in relation to GA (in gestational days) and CRL (in mm). In the analysis of these formulae the GA and CRL are centered by subtracting the mean value of GA and CRL, respectively. The total number of datasets (N) used are displayed.

Cerebellum measurements (mm)			N	Line	Formula
Measurement related to GA					
Total cerebellar diameter	169	Mean			$X = GA - 70$ $6.2590 + 0.1943 * X + 0.002183 * X^2$
		Variance*			$0.4565 + 0.006006 * X + 0.000475 * X^2 + 0.000066 * X^3 + 0.000002805 * X^4$
Left hemispherical diameter	164	Mean			$3.3477 + 0.08271 * X + 0.001489 * X^2$
		Variance			$0.1032 - 0.00062 * X + 0.000511 * X^2 + 0.000022 * X^3 + 0.0000008286 * X^4$
Left hemispherical thickness	163	Mean			$1.7596 + 0.06006 * X$
		Variance			$0.06175 + 0.002664 * X + 0.000075 * X^2$
Right hemispherical diameter	164	Mean			$3.3505 + 0.07938 * X + 0.001245 * X^2$
		Variance			$0.11411 - 0.00020 * X + 0.000284 * X^2 + 0.000017908 * X^3 + 0.000001214 * X^4$
Right hemispherical thickness	159	Mean			$1.7628 + 0.06044 * X$
		Variance			$0.05406 + 0.002504 * X + 0.000075 * X^2$
Measurement related to CRL					
Total cerebellar diameter	176	Mean			$6.6245 + 0.1336 * X$
		Variance			$0.37834 + 0.002916 * X + 0.000051 * X^2$
Left hemispherical diameter	171	Mean			$3.5754 + 0.05748 * X$
		Variance			$0.13019 + 0.000017370 * X + 0.000051 * X^2$
Left hemispherical thickness	163	Mean			$1.9132 + 0.04253 * X - 0.0003854 * X^2$
		Variance			$0.05922 + 0.0004206 * X - 0.0001108 * X^2 + 0.000000484 * X^3 + 0.0000001515 * X^4$
Right hemispherical diameter	171	Mean			$3.5536 + 0.05578 * X$
		Variance			$0.12611 - 0.00032 * X + 0.000027 * X^2$
Right hemispherical thickness	165	Mean			$1.9245 + 0.04309 * X - 0.0004002 * X^2$
		Variance			$0.05204 + 0.0011242 * X - 0.00007904 * X^2 - 0.000000084 * X^3 + 0.0000001288 * X^4$

* The standard deviation (SD) at a particular value of X is to be obtained by taking the square root of the variance.



5.2

5.2

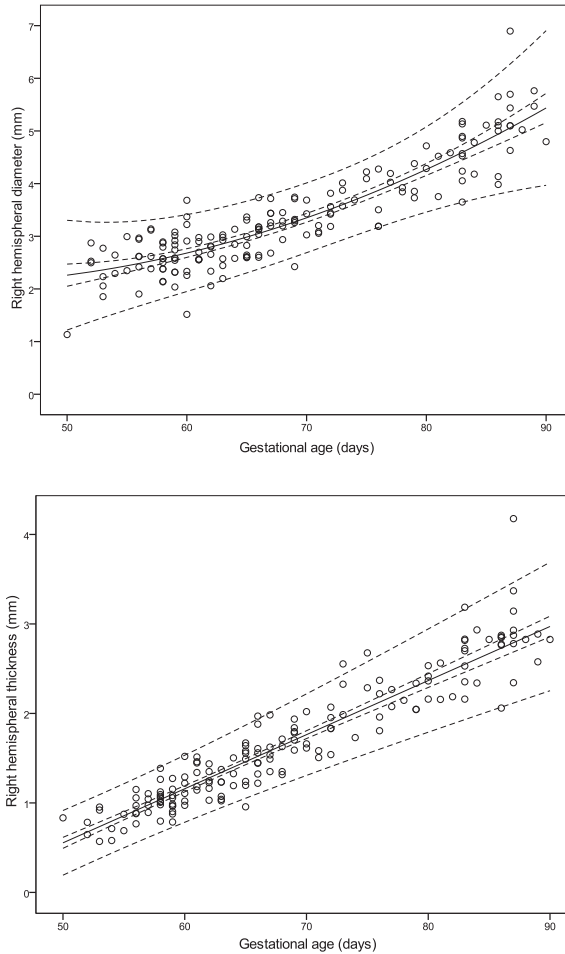


Figure 3. The cerebellar parameters in relation to GA, with the corresponding mean line (solid line), 95% CI of the mean values (dotted inner lines) and the 95% reference intervals (dotted outer lines).

relevant. Therefore we have decided to present only the growth charts and tables using the VR cerebellum measurements.

The 11.9 MHz transvaginal probe used in this study is one of the highest resolution vaginal probes currently available. The use of this probe enabled us to measure the cerebellum already at around seven weeks GA (mean CRL: 13 mm). This is earlier than described by Blaas et al.⁸ Already at around 6+4 weeks' GA (Carnegie stage 14 and 15; approximately 5-7 mm in greatest length) the cerebellar hemispheres and plates appear in the growing embryo.¹⁹ Although high quality images were obtained in the present study, visualization of the cerebellum was only possible in 13% of cases in week seven. The most successful cerebellum

measurements could be performed in gestational week eight (52%), suggesting a preferable anatomical position of the embryo in this gestational week.

In this prospective study, measurements of the cerebellum were performed off-line, on stored 3D datasets. During the weekly ultrasound exams, a 3D sweep of the entire pregnancy was performed, without specifically targeting the cerebellum. This may explain the low overall success rate of 28%. An important point is that although the use of a high frequency transducer produces high-resolution images of the fetal brain, the quality of the images declines rapidly with increasing depth (for instance due to a high BMI). Therefore lack of depth penetration was the main reason for the high exclusion rate. Movement artefacts only accounted for 13% of the exclusion. In a clinical setting a much higher success rate can be achieved by increasing scanning time and targeted imaging of the cerebellum.

There is only one other study by Blaas et al. describing the 2D longitudinal ultrasound development of the cerebellum in the first trimester in 29 pregnant women.⁸ Our results of 177 observations are highly comparable to their results of 93 observations. They also measured the cerebellum in the coronal plane, however only the total cerebellar diameter and the cerebellar thickness was determined. Both in our study and the study of Blaas et al., a square root model was used in relating the total cerebellar diameter to the GA whereas a linear model was used to relate the cerebellar thickness with the GA. Compared to the results of Blaas et al. the total cerebellar diameter in our study was 4% larger (4.8 mm vs. 5.0 mm) at 9+0 weeks GA and 16% larger (8.1 mm vs. 9.4 mm) at 12+0 weeks GA. The cerebellar thickness measured in our study was 5% smaller at 9+0 weeks GA and 4% larger at 12+0 weeks GA.

Anatomical studies show that the two cerebellar hemispheres fuse already around 10 weeks GA (Carnegie stage 23).²⁰ Although it was easy to visualize the separated cerebellar hemispheres we decided not to measure the gap between them, since the small size of it seemed to vary considerably due to imaging artefacts. In contrast to the study of Blaas et al., in our study fusion was already seen in week 10 of pregnancy, and always present in week 11, whereas in their study the two cerebellar hemispheres seemed to meet in the mid-line during weeks 11 and 12.⁸ This may be explained by the increasing quality of the datasets.

We uniquely measured the right and left hemispherical diameter and thickness separately. In a previous study asymmetry of the cerebellar hemispheres has been demonstrated by measuring the left en right hemispherical volume. However, that study had been performed in the second and third trimester.²¹ In our first trimester cerebellum measurements no significant differences between left and right in the diameter or thickness of hemispheres could be demonstrated.

The average growth rate of the total cerebellar diameter over a time period of 40 gestational days (between day 50 and 90) was 0.19 mm per day. The average growth rate between week 16 and week 36 of pregnancy was 0.25 mm per gestational day in the study of Verburg et al., of which the results are widely used

in clinical practice.²² The average growth rate is lower in the first trimester when compared to that in the second and third trimester of pregnancy.

It can be concluded that cerebellar measurements performed using VR are comparable to traditional 3D measurements. In VR, for the first time, all three dimensions can be used to measure cerebellar structures between seven and 12 weeks GA. Reference values are now available for studies on cerebellum development in the early first trimester, as well as for diagnosis of central nervous system defects, which will be the subject of future research.

REFERENCES

1. Becker R, Wegner RD. Detailed screening for fetal anomalies and cardiac defects at the 11-13-week scan. *Ultrasound Obstet Gynecol.* 2006;27:613-8.
2. Ebrashy A, El Kateb A, Momtaz M, El Sheikha A, Aboulghar MM, Ibrahim M, Saad M. 13-14-week fetal anatomy scan: a 5-year prospective study. *Ultrasound Obstet Gynecol.* 2010;35:292-6.
3. Timor-Tritsch IE, Bashiri A, Monteagudo A, Arslan AA. Qualified and trained sonographers in the US can perform early fetal anatomy scans between 11 and 14 weeks. *Am J Obstet Gynecol.* 2004;191:1247-52.
4. Blaas HG, Eik-Nes SH, Vainio T, Isaksen CV. Alobar holoprosencephaly at 9 weeks gestational age visualized by two- and three-dimensional ultrasound. *Ultrasound Obstet Gynecol.* 2000;15:62-5.
5. Becker R, Mende B, Stiemi B, Entezami M. Sonographic markers of exencephaly at 9 + 3 weeks of gestation. *Ultrasound Obstet Gynecol.* 2000;16:582-4.
6. Blaas HG, Eik-Nes SH. Sonoembryology and early prenatal diagnosis of neural anomalies. *Prenat Diagn.* 2009;29:312-25.
7. O'Rahilly R, Muller F. *The embryonic human brain*: Wiley; 2006.
8. Blaas HG, Eik-Nes SH, Kiserud T, Hellevik LR. Early development of the hindbrain: a longitudinal ultrasound study from 7 to 12 weeks of gestation. *Ultrasound Obstet Gynecol.* 1995;5:151-60.
9. Timor-Tritsch IE, Peisner DB, Raju S. Sonoembryology: an organ-oriented approach using a high-frequency vaginal probe. *J Clin Ultrasound.* 1990;18:286-98.
10. Fauchon DE, Benzie RJ, Wye DA, Cairns DR. What information on fetal anatomy can be provided by a single first-trimester transabdominal three-dimensional sweep? *Ultrasound Obstet Gynecol.* 2008;31:266-70.
11. Bhaduri M, Fong K, Toi A, Tomlinson G, Okun N. Fetal anatomic survey using three-dimensional ultrasound in conjunction with first-trimester nuchal translucency screening. *Prenat Diagn.* 2010;30:267-73.
12. Verwoerd-Dikkeboom CM, Koning AH, Hop WC, van der Spek PJ, Exalto N, Steegers EA. Innovative virtual reality measurements for embryonic growth and development. *Hum Reprod.* 2010;25:1404-10.
13. Rousian M, Verwoerd-Dikkeboom CM, Koning AH, Hop WC, van der Spek PJ, Exalto N, Steegers EA. Early pregnancy volume measurements: validation of ultrasound techniques and new perspectives. *BJOG.* 2009;116:278-85.
14. Rousian M, Koning AH, van Oppenraaij RH, Hop WC, Verwoerd-Dikkeboom CM, van der Spek PJ, Exalto N, Steegers EA. An innovative virtual reality technique for automated human embryonic volume measurements. *Hum Reprod.* 2010;25:2210-6.
15. Verwoerd-Dikkeboom CM, Koning AH, Hop WC, Rousian M, Van Der Spek PJ, Exalto N, Steegers EA. Reliability of three-dimensional sonographic measurements in early pregnancy using virtual reality. *Ultrasound Obstet Gynecol.* 2008;32:910-6.
16. Verwoerd-Dikkeboom CM, Koning AH, van der Spek PJ, Exalto N, Steegers EA. Embryonic staging using a 3D virtual reality system. *Hum Reprod.* 2008;23:1479-84.
17. Verwoerd-Dikkeboom CM, van Heesch PN, Koning AH, Galjaard RJ, Exalto N, Steegers EA. Embryonic delay in growth and development related to confined

- placental trisomy 16 mosaicism, diagnosed by I-Space Virtual Reality. *Fertil Steril*. 2008;90:2017.e19-22.
18. Bland JM, Altman DG. Statistical methods for assessing agreement between two methods of clinical measurement. *Lancet*. 1986;1:307-10.
 19. O'Rahilly R, Muller F. Developmental stages in human embryos. Washington: Carnegie Institution of Washington Publication; 1987.
 20. O'Rahilly R, Muller F. The embryonic human brain: An atlas of developmental stages: Wiley; 2006
 21. Rutten MJ, Pistorius LR, Mulder EJ, Stoutenbeek P, de Vries LS, Visser GH. Fetal cerebellar volume and symmetry on 3-d ultrasound: volume measurement with multiplanar and vocal techniques. *Ultrasound Med Biol*. 2009;35:1284-9.
 22. Verburg BO, Steegers EA, De Ridder M, Snijders RJ, Smith E, Hofman A, Moll HA, Jaddoe VW, Witteman JC. New charts for ultrasound dating of pregnancy and assessment of fetal growth: longitudinal data from a population-based cohort study. *Ultrasound Obstet Gynecol*. 2008;31:388-96.

5.2

PART 5

PART 6

PART 7

A SYSTEMATIC TOOL
FOR DIAGNOSING FIRST
TRIMESTER CONJOINED
TWINS



CHAPTER 6.1

DIAGNOSTIC TECHNIQUES AND
CRITERIA FOR FIRST TRIMESTER
CONJOINED TWIN DOCUMENTATION:
a review illustrated by case reports

ABSTRACT

Background Conjoined twins are rare with a live birth rate around 1 in 250 000. Conjoined twins are classified in eight types based on the site of union. Imaging techniques are essential for proper first trimester diagnosis, crucial for adequate obstetrical management. Technological development lead to new imaging techniques like three-dimensional (3D) Virtual Embryoscopy (VE). The aim of the article is to provide a systematic diagnostic tool for first trimester diagnosis of conjoined twins.

Methods A PubMed literature search was performed using the terms *Ultrasound, Doppler, MRI and CT* in combination with *First trimester* and *Conjoined twins*. Three recent cases at our department, a thoracopagus, cephalopagus and parapagus, are reviewed and examined additionally using 3D VE.

Results A brief summary of the different types of conjoined twins is described based on the literature including a table for practical use during ultrasound examination. In the evaluation of conjoined twins two-dimensional (2D) ultrasound is still the golden standard. 3D ultrasound and doppler ultrasonography add anatomical and prognostic information complementary to 2D ultrasound. VE imaging reveals additional findings in our three first trimester cases not seen with routine 2D ultrasound examination.

Conclusions Each case of conjoined twins has its own characteristics and should therefore be evaluated with the best possible imaging techniques. 3D ultrasound and doppler ultrasonography should be added to the evaluation of conjoined twins. MRI is helpful in the second and third trimester of pregnancy. VE imaging may contribute to earlier, more appropriate counseling and management of these pregnancies.

Keywords Conjoined twins; first trimester diagnosis; imaging techniques; Virtual Embryoscopy

Leonie Baken, Melek Rousian, Erwin J.O. Kompanje, Anton H.J. Koning, Peter J. van der Spek, Eric A.P. Steegers, Niek Exalto

Submitted

INTRODUCTION

Conjoined twins are a rare phenomenon. As conjoined twins occur regular in domestic animals and several cases are described in wild mammals¹⁻⁴, most published records concern cases in humans. The prevalence of conjoined twins in humans is approximately 1 in 50 000 pregnancies⁵. Due to the poor prognosis most will die during pregnancy or the pregnancies are terminated by induced abortion. The prevalence in live births is estimated to be around 1 in 250 000 (5). For unknown reasons there is a female predominance with a ratio of 3:1.

There are two hypotheses on the origin of conjoined twins; the fission theory in which a fertilized ovum divides incompletely and the fusion theory explaining secondary fusion of two originally distinct monovular embryos. Spencer argues that all types of conjoined twins can only be explained by secondary fusion⁶⁻⁹. The recent finding of a monochorionic diamniotic conjoined twin pregnancy may further contribute to the fusion theory¹⁰. Others are in favor of the fission theory, maintained by the observation that the incidence of mirror-imaging is higher in conjoined twins than in monozygotic twins¹¹. No matter what theory is correct, conjoined twinning is a rare and random event challenging physicians in making a proper diagnosis, which is essential for considering treatment options. Nowadays conjoined twins are frequently detected during first trimester ultrasound examinations, challenging sophisticated imaging techniques as aids in making a proper diagnosis. Ultrasound criteria for the diagnosis of conjoined twins in the second and third trimester are well defined. Detailed first trimester analysis and diagnosis, however, are more difficult. False positive first trimester diagnosis of conjoined twins have been described in literature¹²⁻¹³. Both monochorionic monoamniotic twins in close proximity and an intra-amniotic hematoma near the embryo can be mistaken for a conjoined twin pregnancy¹⁴. Well defined first trimester ultrasound criteria for diagnosing conjoined twins are therefore desirable and should be discussed.

First trimester diagnosis of conjoined twins and therefore early evaluation of the different management options assures the best possible outcome for both mother and affected infants. After appropriate diagnosis and counseling the first decision is whether to continue or terminate the pregnancy. Offering earlier termination of pregnancy is associated with minimal maternal morbidity and has less psychological impact on the parents compared to performing this procedure later in pregnancy¹⁵⁻¹⁶. In a continuing conjoined twins pregnancy with one relatively normal and one abnormal twin selective feticide may be another management option, especially in early pregnancy and in cases with minimal fusion, resulting in the birth of a healthy infant¹⁷. Exceptionally rare cases are conjoined twins in a triplet pregnancy¹⁸⁻²³. Early recognition of this extreme rare event and selective reduction of the co-existing conjoined twin provides better survival chances of the third child^{18-19, 21-23}.

Associated risks in conjoined twins pregnancy are intrauterine growth retardation, polyhydramnion, pre-eclampsia, cord entanglement and intrauterine

fetal death²⁴. After correct first trimester diagnosis of conjoined twins and continuation of pregnancy these risks can be monitored.

As described above proper first trimester diagnosis of conjoined twins is important for many different reasons. Schmidt et al. already advocated for first trimester routine ultrasound screening to allow diagnosis of severe congenital abnormalities, like conjoined twins, in 1982²⁵. At the end of the last century serial ultrasound scanning in case of monozygotic twin pregnancies and conjoined twins was recommended in a few other studies²⁶⁻²⁷. Follow-up scans in first trimester diagnosis of conjoined twins are advocated by Lam et al. in order to visualize the fetal anatomy and the extend of fusion more clearly²⁸.

The aim of the article is to explore the imaging techniques used in the diagnosis of conjoined twins and provide a systematic diagnostic tool for obstetricians who face themselves challenged with first trimester diagnosis of a conjoined twin.

METHODS

Literature search

Articles were identified through a PubMed database search retrieving articles on the first trimester diagnosis of conjoined twins. The literature search was performed on the 1st of December 2010 for all available papers written in English. References of all relevant articles were hand-searched for additional citations. The free text search terms 'ultrasound', 'Doppler', 'MRI' and 'CT' in combination with 'first trimester' and 'conjoined twins' were used. Papers on parasitic conjoined twins were excluded.

Diagnostic process of recent cases

In the past four years three cases of conjoined twins were diagnosed in the Erasmus MC University Medical Center Rotterdam. All three cases were initially examined using two-dimensional (2D) and three-dimensional (3D) ultrasound. For consecutive analysis using Virtual Embryoscopy (VE) the 3D images made on the GE Voluson E8 system (GE, Zipf, Austria) were converted to cartesian volumes, using specialized 3D software (4D View, GE Medical Systems), and transferred to the BARCO I-Space. The volumes were screened in the I-Space for quality and completeness of the embryos. The volumes were resized, turned and clipped in different planes to obtain the best possible images for evaluation. The evaluation of the three cases with Virtual Reality was done by a different examiner than the sonographer who did the initial ultrasound exams.

The diagnostic findings during 2D and 3D ultrasound were extrapolated from the medical records. All features seen with the VE imaging technique were written down and compared to the 2D/3D ultrasound findings.

RESULTS

History of the depiction of conjoined twins









The history of printed descriptions and illustrations of conjoined twins is long and extensive. The oldest known printed illustration of a pair of conjoined twins is in the 1499 book by Jacob Locher, *Carmen heroicum de partu monstrifero*²⁹. From the end of the seventeenth century, the first scientific journals appeared in which all sorts of congenital malformations, both real and imagined, were depicted and described. Before these, a series of books on monsters, which were extremely popular, were published. Authors often copied the fantasy cases from each other. Explanations, as devilish conception or the result of witnessing evil by the pregnant women, often fueled the fear of the lay public. From the mid 18th century onwards, only real depictions and descriptions appeared in the scientific literature. Illustration techniques in these books and articles were copper engravings, steel engravings and lithographs, offering a very realistic picture of both the external appearance and the internal anatomy of the malformations described. In the first half of the 19th century very detailed descriptions and illustrations of conjoined twins were published, as the 1832 monograph and atlas on the well-known parapagus dicephalus conjoined twins Ritta and Christina by Etienne Serres (1787-1868)³⁰. Other detailed accounts on conjoined twins have been given by the Dutch anatomist *Willem Vrolik* (1801-1863)³¹. The first photographic images of conjoined twins were used in publications after the mid nineteenth century. In 1906, the first volume of one of the most important works on teratology, *Ernst Schwalbe's 'Die Morphologie der Missbildungen des Menschen und der Tiere'*, was published³². The last volumes were published as late as 1960. For this work 'modern' imaging techniques of the skeletal anatomy were used for illustrations. In the second volume many radiographic imaging of all sort of conjoined twins were depicted. Also angiography was used to study the blood vessel connections between the twins. The first CT images of the internal anatomy of conjoined twins appeared in the late 1970's.

Classification of conjoined twins

Each set of conjoined twins is unique with respect to the site and extent of union and their complex anatomy. The most complex anatomy is situated at the site of union³³. Description of conjoined twins is made easier with a simple classification into eight types, advocated by Spencer^{7, 34}. These eight types are named cephalopagus, thoracopagus, omphalopagus, ischiopagus, parapagus, craniopagus, rachipagus and pyopagus. The suffix pagus means fixed.

The first differentiation in this classification of conjoined twins is made in ventral versus dorsal union. Further differentiation is made by the site of union. The eight types of conjoined twins with their characteristics, incidence and vitality are described below and are summarized in table I.

Table 1: Types of conjoined twins and their characteristics (**Bold:** always present)

Types*	Ventral					Dorsal				
	Cephalo	Thoraco	Omphalo	Ischio	Para	Cranio	Rachi	Pyo		
										
	rostral	rostral	rostral	lateral	caudal					
Incidence	11%	19%	18%	11%	28%	5%	<1%	6%		
Extent of union	Head to umbilicus	Thorax to umbilicus	Umbilicus	Lower abdomen and pelvis	Lower abdomen and pelvis	Cranium (never foramen magnum/ skull base)	Vertebral column	Sacrum and perineum		
Varieties	Symmetrical/ asymmetrical	-	Fusion from sternum to umbilicus	End-to-end fusion/twins facing each other	Dicephalus/ di-prosopus	Orientation in any position	Fusion into occiput	-		
Head/ face	Fused, 2 faces on opposite sides of head	2	2	2	1 or 2 heads, 2 faces	Fused skull, 2 faces	2 faces	2		
CNS	2	-	-	-	Anencephaly	Fused meninges separate brains	2	Fused dura/ spinal cords		
Vertebral column	2	2	2	2	2	2	Fused spinal cords	2		
Shoulders	4	4	4	4	2-3	4	4	4		
Upper limbs	4	4	4	4	2-4	4	4	4		

6.1

Thorax	Fused	Fused	Fused	Fused	Fused	2	2	2	2	2
Heart	2	1 con-joined/2 fused	2	2	1 or 2	2	2	2	2	2
Abdomen	1	Fused	Fused	2	1	2	2	2	2	2
Umbilicus	1	1	1	1	1	2	2	2	2	2
Liver	2	Shared	Shared	Minimal fusion	Shared	2	2	2	2	2
GI-tract	1 upper GI	2	Shared	1 lower GI	1 lower GI	2	2	2	2	2
Genitalia	2	2	2	Shared	2	2	Unknown	2	2	Fused
Pelvis	2	2	2	Fused	1	2	2	2	2	Fused
Lower limbs	4	4	4	3-4	2	4	4	4	4	3-4
Viability	No	Rare	Yes	Yes	Yes	Yes	Yes	Yes	Yes	Yes
Separability	No	Not likely	Yes	Yes	Not likely	Not likely	Not likely	Not reported	Not reported	Yes

*All words have the extent 'pagus'

Ventral union

Ventrally conjoined twins are fused rostral (cephalopagus, thoracopagus, omphalopagus), caudal (ischiopagus) or lateral (parapagus). Ventral union always includes the umbilicus and the abdomen. Extensive fusion including the thorax, the head or the pelvis and perineum may be present³³. All share a common yolk sac and, as a consequence, all share some part of the gastrointestinal tract.

The *cephalopagus* twin is also called Janiceps twins after the Roman god Janus with the two faces. These are fused from the head to the umbilicus. Each twin contributes to half of the head, thorax and abdomen. This extensive fusion complicates correct diagnosis; cephalopagus conjoined twins are often referred as a singleton pregnancy with the inconclusive finding of an enlarged head³⁵⁻³⁶. There are always two vertebral columns, two sets of genitalia, four upper and four lower limbs. Cephalopagus twins are symmetrical with two complete faces or asymmetrical with one relatively normal face and one reduced face. Two hearts are formed which are united in the plane of fusion. In the asymmetrical cephalopagus the posterior heart can be very small and functionless. The upper gastrointestinal tract is always shared, with one esophagus, stomach and small intestine. The trachea is also shared which provides a main bronchus for a lung of each twin. This type of conjoined twins is non viable.

In many *thoracopagus* a shared cardiac anatomy is the most prominent feature. The complexity of the shared cardiac anatomy covers a wide range from a channel between the two atria to complete fused hearts (75%); though nearly all of these hearts are inseparable. Livers are almost invariably fused in thoracopagus conjoined twins; if the fusion is extensive this also precludes separation.

The *omphalopagus* is characterized by a fusion from the sternum to the umbilicus. Since both thoracopagus and omphalopagus may have an union of thorax and abdomen it may be difficult to differentiate between the two. The omphalopagus twins, however, have two separate hearts, while the thoracopagus share their hearts to some extent. In 25% of cases there are cardiac anomalies, ranging from minor to severe, influencing the prognosis. In case of normal hearts the chances of survival are high. There is a single umbilical cord artery present, and due to this associated anomalies may be present. Twenty-five percent of omphalopagus cases an omphalocele is present. Shared intestines (17%) are associated with stillborn twins in half of the cases.

The liver is shared in most omphalopagus and this is associated with the extent of union of the abdominal wall. The possibility of surgical separation depends on the vasculature of the conjoined livers. Separation is often possible with a success rate of 82%⁷.

The *ischiopagus* twins are fused at the pelvis and lower abdomen in the cloacal membrane. This fusion can be end to end or, rarely, with the twins facing each other. As the ischiopagus twins are fused in the cloacal membrane, the two sets of external genitalia are located laterally. The lower gastrointestinal tract is shared in 70% of cases. Ischiopagus may be tetrapus (having four legs), tripus (three legs) or bipus (two legs). Separation may be possible with a success rate of about 63%⁷.

The most common type of conjoined twins is the *parapagus* with an incidence of 28%. In case of a parapagus there may be a parapagus dicephalus (having two heads) or a parapagus diprosopus (having two faces on the same side of a single head). Parapagus twins are united in the lower abdomen and pelvis and the fusion may extend even to the cranium. Parapagus have two lower limbs and have two, three or four upper limbs. There is always one lower abdomen with one gastrointestinal tract and one pelvis, but there may be two separate thoraxes. Either one or two hearts may be present. The diagnosis of parapagus dicephalus is in most cases made by the observation of two distinct heads and one fetal body³⁷⁻³⁹. In parapagus diprosopus twins there is a high incidence of anencephaly. Also forking of the cervical spine is an additional distinctive finding⁴⁰. Most cases of parapagus diprosopus die in utero or die during the neonatal period. Parapagus dicephalus die in most cases due to anomalies of the heart. The survival into adulthood is rarely accomplished. However, this is more often by choice than clinical impossibility. The well known Hensel twins, who were born March 1990, have now reached adulthood. Both graduated from high school in 2008 and are now university students. Separation is only possible when there are two separate hearts but will inevitably lead to severely handicapped children.

Dorsal union

In dorsally fused twins the cranium and/or the vertebrae are always part of the fusion. The face and both thoracic and abdominal organs however are never involved in this fusion (33). There are three types of dorsally conjoined twins: craniopagus, rachipagus and pyopagus.

Craniopagus conjoined twins (5%) are fused at the cranium, but never at the foramen magnum or the base of the skull. The face, neck, thorax and abdomen are never involved in the union. The orientation of the twins fused at the cranium may be in any position. Skull, meninges and venous sinuses are always fused. Brains are separate in most cases and fusion of the cortex is present in 30% of cases. Separation without further residual handicaps for the twins is unlikely.

An extremely rare type of conjoined twins is the *rachipagus*, which has been described only twice in the literature⁴¹⁻⁴³. Since only two cases are known, it is highly favorable to investigate these cases with the best possible imaging techniques and preserve them⁴⁴. The limited information makes description and generalization of this type of conjoined twins difficult. *Rachipagus* are joined dorsally with fused vertebral columns. The fusion may involve fusion in the occiputs. Surgical separation is impossible.

Pyopagus conjoined twins are joined at the sacrum and the perineum. Each twin has a separate abdomen and therefore the gastrointestinal tract is not involved with the exception of the rectums. There are two sets of genitalia which are united dorsally. When the vertebral canals are continuous the dura and/or spinal cord may be joined which has severe implications for surgery. Separation is likely to be possible since the conjunction does not involve critical organ systems, sometimes only compromising soft tissue⁴⁵⁻⁴⁶. A separation success rate of 68% has been reported⁷.

The prognosis always depends on the final diagnosis of the specific type using the above classification and includes detailed evaluation of the complex anatomy, usually by puzzling and using additional imaging techniques. Surgical separation is very likely to fail with the loss of both children in conjoined twins with a single heart and in conjoined twins with a single QRS-complex on the electrocardiogram (ECG)³³.

Clues for diagnosis

Suspicion of conjoined twinning should be raised in a twin pregnancy with a single placenta, when it is not possible to demonstrate a separating amniotic membrane or when there is only one yolk sac present. Signs of possible conjoined twins are also more than three vessels in the umbilical cord, no change in relative positions of twins after movement or follow-up scans, fewer limbs than would be expected, hyperflexion of the spine and bifid appearance of the fetal pole^{5, 47-49}. Also increased nuchal translucency thickness can be seen in conjoined twins, especially in thoracopagus due to hemodynamic disturbances⁵⁰. When fetal activity increases, at around eight weeks gestational age, it becomes easier to differentiate between monoamniotic twins and conjoined twins⁵¹.

In case of first trimester detection of a conjoined twin detailed first trimester imaging is essential in accurate counseling of the parents and planning opportune obstetric management.

Imaging techniques

Ultrasound

The introduction of ultrasound in 1960 led to a new revolution in diagnostic imaging, although diagnostic ultrasound was already developed in the early 1950s⁵². Sonography is widely used in the obstetrical field and is the most important and primary imaging technique in prenatal diagnosis of conjoined twins⁵. The first diagnosis of conjoined twins using ultrasound was in 1976⁵³. The first diagnosis of conjoined twins in the first trimester, at 12 weeks of gestational age, was reported by Schmidt et al. in 1981⁵⁴. The earliest diagnosis of conjoined twins has been reported at seven weeks of gestation using transvaginal ultrasound⁵⁵.

Most diagnoses of conjoined twins are established using two-dimensional (2D) ultrasound, especially when fusion of body parts is obvious. Ultrasound is the preferred investigation modality since it is non-ionizing, non-invasive, has low costs and broad availability. It also permits real-time examination that is very useful in conjoined twins since conjoined twins do not switch their relative position to each other when fetal movements are present. Minimally conjoined omphalopagus twins can be an exception to this rule; changes in relative position have been reported⁵⁶⁻⁵⁷.

The introduction of the transvaginal ultrasonography provides ultrasound images with high resolution and therefore makes it possible to visualize and quantify the early pregnancy⁵⁸. This has led to advances in first trimester diagnosis of abnormalities in the fetal anatomy⁵⁹, like in the extent of fusion in conjoined twins⁴⁷.

Three-dimensional (3D) ultrasound

3D ultrasound became available with the advances made in computer technology and has shown to be helpful in the detection of congenital abnormalities⁶⁰⁻⁶¹. In conjoined twins 3D ultrasound is used to exactly define the extent of fusion and to obtain more precise anatomic information⁶²⁻⁶⁴. Nowadays, in many cases of conjoined twins 3D ultrasound helped to confirm the presence of anomalies and improved diagnostic confidence⁶³⁻⁶⁹. Especially facial features, like in parapagus or cephalopagus conjoined twins, are better studied in detail using 3D ultrasound^{65,70}. 3D images provide overall assessment of the fetuses; an example is the number of upper and lower extremities which can be important in the definitive classification of conjoined twins. 3D surface rendered images also help the future parents to understand the complex anomalies in their fetuses⁶³⁻⁶⁴.

Since ultrasound and 3D ultrasound are not always successful in providing all detailed information of the complex anatomy in conjoined twins other imaging techniques should also be considered.

Doppler ultrasound

Doppler ultrasound has expanded its application in obstetrics, also in the evaluation of conjoined twin pregnancy by showing vascular communications^{17, 64, 71}. The prognosis of conjoined twins largely depends on the conjunction of the cardiovascular system. Especially the differentiation between thoracopagus and omphalopagus for the definitive classification and prognosis can be facilitated by Doppler ultrasound of the heart^{55, 67, 72}. Doppler ultrasound is an excellent tool in the evaluation of the vasculature of conjoined vital organs to determine prognosis and separability^{15, 71, 73}. In several cases Doppler ultrasound provided additional information like the finding of conjoined livers which is important to determine the possibility and the chance of success of separation surgery⁷¹.

Furthermore, Doppler ultrasound may reveal a characteristic 'double layer' umbilical arterial velocity waveform⁷⁴⁻⁷⁵. This specific pattern is observed in the case of two separate arterial supplies in a single umbilical cord. Such a distinctive Doppler ultrasound pattern can be used as an extra diagnostic sign in conjoined twins as proposed by Woo et al⁷⁴.

Computed tomography (CT)-Scan

Since the discovery of X-rays in 1895 by Wilhelm Conrad Roentgen⁷⁶, diagnostic imaging has made enormous progress. Only 50 years later 1 in 10 hospital patients underwent some sort of diagnostic imaging⁷⁷. The first prenatal diagnosis of conjoined twins performed with the use of X-rays was performed in 1934⁷⁸. Around 1970, CT was introduced in the medical field as the first digital imaging technique.

We only found two publications, published in 1984 and 1990 respectively, on the use of CT for antenatal diagnosis of conjoined twins; both in the third trimester of pregnancy⁷⁹⁻⁸⁰.

X-rays, used in CT-scanning, are potentially dangerous for the fetus and fetal movements will disturb the image quality. Therefore CT imaging in pregnancy is

limited to very specific congenital abnormalities, like skeletal malformations⁸¹. CT may also offer better lung and hollow viscus details⁸². In case of conjoined twins CT is mainly used postpartum as a diagnostic tool to evaluate separability.

Magnetic resonance imaging (MRI)

MRI entered the medical scene in the early 1980s. Fetal MRI has already proven to be complementary to conventional obstetrical ultrasound. Especially in case of complex anatomical anomalies a MRI may provide additional information in evaluating conjoined twins pregnancy⁸³⁻⁸⁶.

With MRI high resolution images of fetal organs, like the brain and liver, show the extent of fusion of internal organs in conjoined twins⁸⁴. MRI provides excellent contrast between cerebrospinal fluid and the brain and spinal cord and is therefore useful in the detection of central nervous system anomalies⁸⁷, as is also shown in several conjoined twin cases^{83, 88-90}.

In the past long MRI acquisition times lead to deteriorated image quality as a result of fetal motions. Ultrafast MRI imaging is available since the early 1990s⁸⁸. With single-shot fast spin-echo MR sequence (SSFSE) artefacts by fetal movements are minimized resulting in good imaging quality⁹¹⁻⁹².

In MRI there is no ionizing radiation and there are no known adverse effects to the fetuses. The disadvantages of MRI are the costs, availability and the lack of real-time imaging possibilities^{85, 93}. The literature does not provide cases of conjoined twins diagnosed in the first trimester with MRI. The earliest prenatally diagnosed conjoined twins using MRI was at 16 weeks of gestation⁸⁴.

In summary MRI is a good imaging technique to provide detailed anatomical information, precisely define the extension of fusion of the conjoined twins⁸⁴ and explore vascular anomalies⁹⁴. MRI can precisely define neuroanatomical anomalies and can for example be very useful in depicting whether there is fusion of the spinal cord in pyopagus or fusion of the meninges in craniopagus. This information is especially useful to predict prognosis and viability and in planning possible separating surgery⁹⁵. When conjoined twins are presented late in pregnancy MRI overcomes the limitations of ultrasound, like in the case of obesity and because of the decreasing amount of amniotic fluid. MRI provides overall assessment of the pregnancy, also in late pregnancy.

Virtual Embryoscopy (VE)

Virtual Embryoscopy is a new technique that enhances the 3D US modality. It is a 3D imaging technique that actually uses all three dimensions, in contrast to traditional 3D reconstructions viewed on a 2D screen. At our department we use a transvaginal probe of the GE Voluson 730 expert and E8 system (GE, Zipf, Austria) for the first trimester ultrasound examinations. The department of Bioinformatics of the Erasmus MC operates a fully immersive virtual reality system: the BARCO I-Space. It allows the viewers to perceive depth and interact with 3D volumes in an intuitive manner. The V-Scope volume rendering application creates a 'hologram' of the 3D ultrasound volume in order to provide VE; stereoscopic imaging allows the discernment of fine details and understanding of 3D structures in the volumes.

We refer to previous articles for a detailed explanation of the BARCO I-Space and V-Scope⁹⁶. The innovative VE technique has already successfully been applied in prenatal medicine⁹⁷⁻¹⁰⁵.

Due to the improved depth perception and 3D interaction the I-Space enables better assessment of embryonic and fetal structures. A combination of 2D and 3D ultrasound examination and VE may improve the detailed morphological description and diagnosis.

As seen in our cases (below) VE provides additional diagnostic information in evaluating complex anatomical structures in conjoined twins.

CASE REPORTS

Case 1

A 30-year-old G4P2 was referred to the Erasmus MC University Medical Center Rotterdam at 10+6 weeks of gestation for prenatal diagnosis because of conjoined twins detected with routine ultrasound. 2D and 3D transvaginal and abdominal ultrasound examinations revealed a thoracopagus with fused thorax and abdomen, sharing one heart and liver (table II, figure 1A,B). The conjoined twins appeared to have two separate heads, shoulder girdles, pelvises and four lower extremities. Fetal hydrops was also noticed. Only three upper extremities could be visualized using regular ultrasound. Fetal karyotype revealed a normal male genotype. The parents were informed about the prognosis and decided to terminate the pregnancy. Pregnancy was terminated at 11+5 weeks gestational age using misoprostol. Intact conjoined twins were born and macroscopic examination confirmed the diagnosis thoracopagus. The parents refused autopsy.

Using the I-Space VE system, the thoracopagus with fetal hydrops was confirmed (figure 1C). In addition 4 arms and 4 legs could be distinguished easily as well as severe scoliosis, an abdominal defect and an abnormal ulnar deviation of one of the hands.

Case 2

A 28 year-old G2P1 was referred to our center because of conjoined twins diagnosed at 13+1 weeks gestational age with routine 2D ultrasound. 2D and 3D ultrasound examination revealed a cephalopagus with fusion of the heads, both thorax and part of the abdomens (table II, figure 2A,B). Two heartbeats, one stomach, 4 arms and 4 legs and one shared umbilical cord and placenta were visualized. The fetal karyogram showed a normal female genotype.

The parents were informed about the lethal prognosis and they decided to have the pregnancy terminated at 14 weeks gestational age by induction. Intact conjoined twins were born and the diagnosis of cephalopagus was confirmed by macroscopic examination (figure 2D). In this case the parents did not give permission for an autopsy.

Table II: 2D/3D ultrasound and VR findings in presented cases (bold: only seen in VE)

Case	1			2			3			
Type	Thoracopagus			Cephalopagus			Parapagus			
GA	10w6d			13w1d			11w6d			
	Ref.	2D/3D	VE	Ref.	2D/3D	VE	Ref.	2D/3D	VE	
Head	2	2	2	1	Fused	Fused	2	2	2	
Frontal bossing	-	-	No	-	-	Yes	-	-	Yes R>L	
Face	2	2	2	1/2	?	1	2	-	2	
Vertebral column	2	-	2, scoliosis	2	-	2	2	2	2	
Shoulders	4	4	4	4		4	2-4		3	
Upper limbs	4	3	4	4	4	4	2-3	2	2	
Hands			Ulnar deviation							
Thorax	Fused	Fused, hydrothorax	Fused, hydrothorax	Fused	Fused	Fused	Fused	Fused	Fused	
Heart	1/2	1	1	2	2	?	1/2	1	?	
Abdomen	Fused	Fused	Defect	Fused	Fused	Fused	Fused	Fused	Fused	
Umbilicus	1	-	1	1	1	1	1	1	1	
Omphalocele	-	-	No	-	-	Yes	-	-	Yes, small	
Stomach	2	-	?	1	-	1	1/2	1	?	
Liver	Shared	1	?	2	-	?	Shared	1	?	
Pelvis	2	-	2	2	-	2	1	-	1	
Lower limbs	4	4	4	4	4	4	2	2	2	
General		Hydrops	Hydrops					Hydrops	Hydrops	
Chromosomal		46, XX			46, XX			46, XY		
Viability		Rare			No			Yes		
Separability		Not likely			No			Not likely		

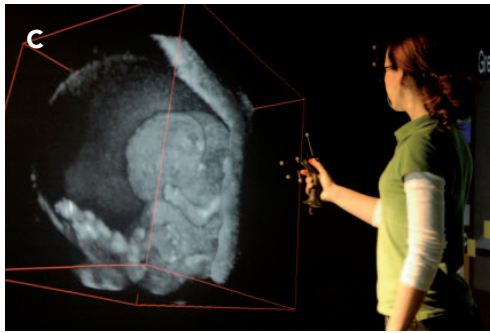
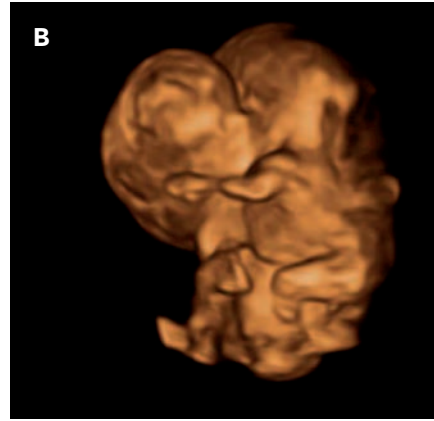


Figure 1. Case 1: Thoracopagus. **A.** A conventional 2D US image clearly showing fusion of the thorax and abdomen. Since one heart was seen during 2D US the diagnosis thoracopagus was made. **B.** A 3D US image showing fetuses 'embracing' each other. **C.** I-Space rendering of the conjoined twins. The operator is visible with the 3D volume of the twins. With VE the fourth arm was discovered as well as an abdominal defect, abnormal ulnar deviation and severe scoliosis, which were not seen during 2D/3D US. It is important to remember that on paper, a picture of an I-Space rendering is nothing more than a 2D picture, since depth cannot be put on paper or on a computer screen. This figure therefore does not capture the full potential of the I-Space. **D.** Ex vivo picture showing the union of both thorax and abdomen.

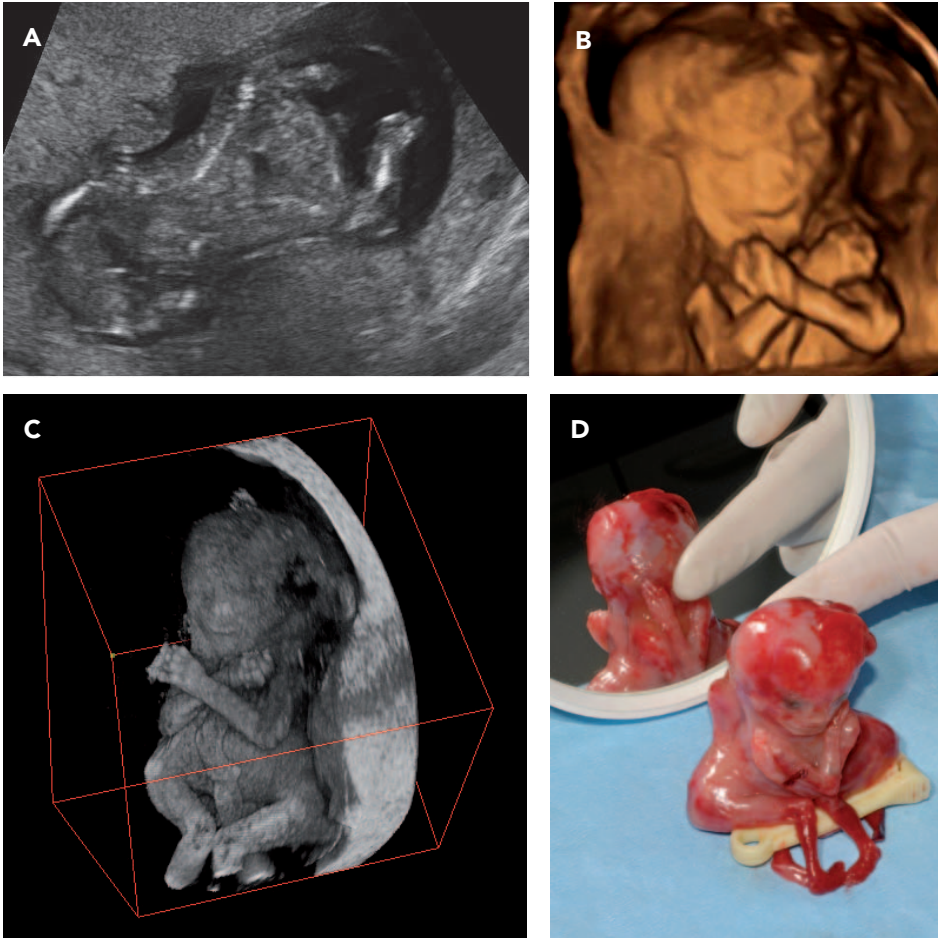


Figure 2. Case 2: Cephalopagus. **A.** 2D US image showing two vertebral columns and one single head. **B.** 3D US image showing the profile of the fused face. **C.** I-space volume clearly showing the two fetuses situated in front of each other (each arm belongs to one of the twins) with the faces fused laterally. With VE it was possible to visualize the back of the head, indicating this as an asymmetrical cephalopagus. **D.** *Ex vivo* picture showing the four upper extremities. The absence of a second face, already seen in VE, was confirmed.

A cephalopagus can either be symmetrical (two identical faces on opposite sides of the head) or asymmetrical (one 'normal' face and one reduced face). In our case the back of the head could not be visualized with 2D and 3D ultrasound and therefore it could not be determined whether the fetus was a symmetrical or an asymmetrical.

Intuitive orientation in the dataset with 3D VE allows for detailed evaluation of anatomical structures (figure 2C). With this technique it was possible to show that only one face was present as well as 4 shoulders and an omphalocele.

Case 3

A 22-years-old G3P2 was presented at 11+6 weeks gestational age at our department of Obstetrics and Prenatal Medicine after detection of conjoined twins during routine ultrasound. Two-dimensional and 3D transvaginal and abdominal ultrasound examination revealed conjoined twins with fetal hydrops (figure 3A,B). Two separate heads and two separate spines were seen. The twins were fused at the level of the thorax and the abdomen sharing one heart, liver and stomach. Two arms and two legs could be visualized. The fetuses were diagnosed as a parapagus dicephalus (table II). Karyotyping by chorionic villus sampling revealed a normal male genotype.

After counseling, the parents decided to have the pregnancy terminated at 14+4 weeks gestational age using misoprostol. Autopsy findings correlated with the diagnosis parapagus dicephalus (figure 3E). There were three lungs, one heart, one set of kidneys, a shared gastro-intestinal tract and two equal, normal sized brains present. The internal genitalia were male.

During 3D VE examination two faces were seen with marked frontal bossing. There were 3 shoulders with two arms and additionally a small omphalocele was discovered (figure 3C,D).

6.1

DISCUSSION

Accurate prenatal imaging is crucial in diagnosing the rare cases of conjoined twins. Eight types of conjoined twins are known, all with their own characteristics (table I). Even though this classification, each conjoined twins is unique with respect to the site and extent of union and their complex anatomy. Prognosis, especially vitality and separability, should therefore be evaluated individually for each individual case with the best possible imaging techniques. First trimester accurate evaluation of conjoined twins allows for early counseling of the parents to discuss the prognosis and management options.

Ultrasound is the main imaging modality used in diagnosing conjoined twins. In many cases the diagnosis can be performed using conventional ultrasound, especially when the conjunction between the twins is obvious. 3D ultrasound can add anatomical information in several cases of conjoined twins, especially regarding facial features. 3D ultrasound should always be included in the evaluation of conjoined twins since the spatial relationships are complex and understanding them is essential for a proper diagnosis. The surface rendered images of 3D ultrasound facilitate counseling of the parents. Additional ultrasound scans in the second trimester may be necessary to make a definitive evaluation of the anatomic relationships. Doppler ultrasound imaging is important for the determination of viability and separability by visualizing vascular communications and by determining the number of hearts. The lack of articles on MRI in first trimester conjoined twin pregnancies may indicate that there is no indication of this imaging technique in these particular pregnancies. MRI has emerged to be

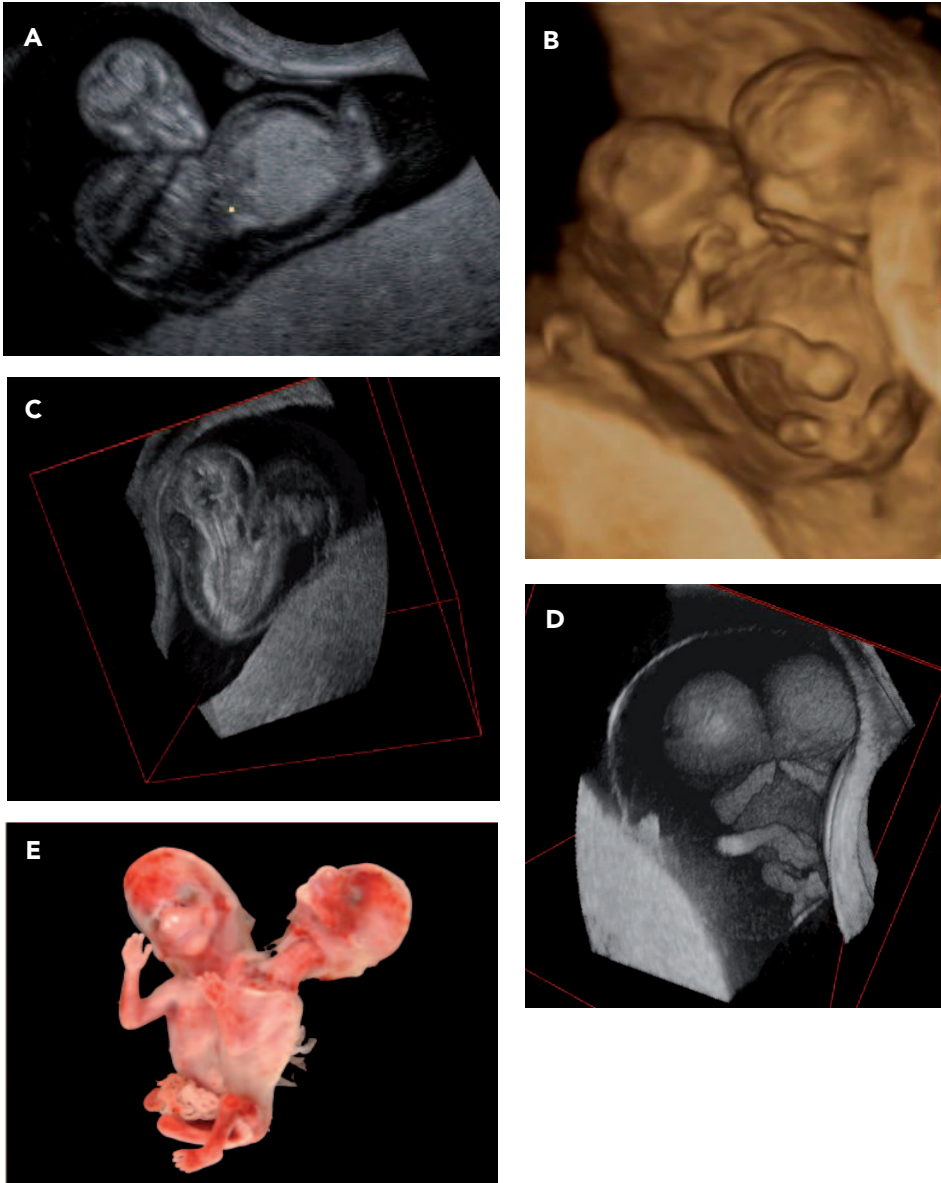


Figure 3. Case 3: Parapagus dicephalus. **A.** 2D US image showing hydrothorax and two separate heads. **B.** 3D US image showing fusion in thorax and abdomen and a single umbilical cord. **C.** I-Space volume showing hydrothorax. Two vertebral columns are visualized. **D.** I-Space volume showing the fusion in thorax and abdomen. VE also showed the presence of only one pelvis. Furthermore frontal bossing and a small omphalocele were visualized. **E.** *Ex vivo* picture confirming that only two upper and two lower extremities were present.

a complementary imaging technique in conjoined twins after the first trimester. In several situations MRI has proved to be superior to ultrasound in that period of pregnancy. MRI is superior in evaluating possible neuroanatomical anomalies crucial in determining whether separation surgery is possible in for example craniopagus and pyopagus conjoined twins. Therefore, the superiority of MRI as compared to ultrasound in the second and third trimester might also apply to the first 12 weeks of pregnancy. The excellent resolution of tissue composition perceived with MRI makes it a potential useful complementary tool in first trimester diagnosis of conjoined twins. A thorough evaluation of this possible diagnostic effect could change our view on the diagnostic process of congenital abnormalities like conjoined twins. The VE technique can also be applied to MRI to provide even more information.

There was no support in the literature on the use of CT in first trimester diagnosis of conjoined twins.

In the three cases of conjoined twins referred to our clinic we demonstrated that 3D VE has the potential to add more precise and extra anatomic information (table II). In all cases new anatomic information came to light when evaluating the twins in the BARCO I-Space. A combination of 2D and 3D ultrasound examination and 3D VE improves the detailed morphological description and diagnosis.

We conclude that 3D VE provides additional diagnostic information in evaluating complex anatomical structures, especially when depth perception is needed, as in case of conjoined twins. This may contribute to earlier, more appropriate counseling and management of these pregnancies. As this is the first article on VE in the diagnosis of conjoined twins, more research is needed to evaluate the implementation of VE in the diagnostic process of conjoined twins and congenital malformations in general.

REFERENCES

1. Kompanje EJ, Hermans JJ. Cephalopagus conjoined twins in a leopard cat (*Prionailurus bengalensis*). *J Wildl Dis.* 2008;44:177-80.
2. Kompanje EJO. A case of symmetrical conjoined twins in a bottlenose dolphin *Tursiops truncatus* (Mammalia, Cetacea). *DEINSEA.* 2005;11:147-50.
3. Kompanje EJO. Two cases of asymmetrical conjoined twins in wild mammals from the Netherlands. *DEINSEA.* 2005;11:139-45.
4. Kompanje EJO, Moeliker K. Vier lammeren, twee preparaten. *Straatgras.* 2010;22.
5. McHugh K, Kiely EM, Spitz L. Imaging of conjoined twins. *Pediatr Radiol.* 2006;36:899-910.
6. Spencer R. Theoretical and analytical embryology of conjoined twins: part I: embryogenesis. *Clin Anat.* 2000;13:36-53.
7. Spencer R. *Conjoined Twins.* Baltimore: Johns Hopkins University Press; 2003.
8. Spencer R. Theoretical and analytical embryology of conjoined twins: part II: adjustments to union. *Clin Anat.* 2000;13:97-120.
9. Spencer R. Conjoined twins: theoretical embryologic basis. *Teratology.* 1992;45:591-602.
10. Destephano CC, Meena M, Brown DL, Davies NP, Brost BC. Sonographic diagnosis of conjoined diamniotic monochorionic twins. *Am J Obstet Gynecol.* 2010;203:e4-6.

11. Kaufman MH. The embryology of conjoined twins. *Childs Nerv Syst.* 2004;20:508-25.
12. Usta IM, Awwad JT. A false positive diagnosis of conjoined twins in a triplet pregnancy: pitfalls of first trimester ultrasonographic prenatal diagnosis. *Prenat Diagn.* 2000;20:169-70.
13. Weiss JL, Devine PC. False positive diagnosis of conjoined twins in the first trimester. *Ultrasound Obstet Gynecol.* 2002;20:516-8.
14. Castro-Aragon I, Levine D. Ultrasound detection of first trimester malformations: a pictorial essay. *Radiol Clin North Am.* 2003;41:681-93.
15. Hubinont C, Kollmann P, Malvaux V, Donnez J, Bernard P. First-trimester diagnosis of conjoined twins. *Fetal Diagn Ther.* 1997;12:185-7.
16. Fontanarosa M, Bagnoli G, Ciolini P, Spinelli G, Curiel P. First trimester sonographic diagnosis of diprosopus twins with craniorachischisis. *J Clin Ultrasound.* 1992;20:69-71.
17. Lam YH, Lee CP, Tang MH, Lau E. Thermocoagulation for selective reduction of conjoined twins at 12 weeks of gestation. *Ultrasound Obstet Gynecol.* 2000;16:267-70.
18. Goldberg Y, Ben-Shlomo I, Weiner E, Shalev E. First trimester diagnosis of conjoined twins in a triplet pregnancy after IVF and ICSI: case report. *Hum Reprod.* 2000;15:1413-5.
19. Sepulveda W, Munoz H, Alcalde JL. Conjoined twins in a triplet pregnancy: early prenatal diagnosis with three-dimensional ultrasound and review of the literature. *Ultrasound Obstet Gynecol.* 2003;22:199-204.
20. Suzumori N, Kaneko S, Nakanishi T, Yamamoto T, Tanemura M, Suzuki Y, Suzumori K. First trimester diagnosis of conjoined twins in a triplet pregnancy. *Eur J Obstet Gynecol Reprod Biol.* 2006;126:132-3.
21. Boulot P, Deschamps F, Hedon B, Laffargue F, Viala JL. Conjoined twins associated with a normal singleton: very early diagnosis and successful selective termination. *J Perinat Med.* 1992;20:135-7.
22. Hill LM. The sonographic detection of early first-trimester conjoined twins. *Prenat Diagn.* 1997;17:961-3.
23. Solt I, Lowenstein L, Okopnik M, Sheinin O, Drugan A. Malformed pygopus conjoined twins in a spontaneous triplet pregnancy. *Harefuah.* 2005;144:590-2, 6.
24. Machin GA, Keith LG, Bamforth F. An atlas of multiple pregnancy: biology and pathology. New York: CRC Press, Parthenon; 1999.
25. Schmidt W, Kubli F. Early diagnosis of severe congenital malformations by ultrasonography. *J Perinat Med.* 1982;10:233-41.
26. Coleman BG, Grumbach K, Arger PH, Mintz MC, Arenson RL, Mennuti M, Gabbe SG. Twin gestations: monitoring of complications and anomalies with US. *Radiology.* 1987;165:449-53.
27. Sebire NJ, Souka A, Skentou H, Geerts L, Nicolaides KH. First trimester diagnosis of monoamniotic twin pregnancies. *Ultrasound Obstet Gynecol.* 2000;16:223-5.
28. Lam YH, Sin SY, Lam C, Lee CP, Tang MH, Tse HY. Prenatal sonographic diagnosis of conjoined twins in the first trimester: two case reports. *Ultrasound Obstet Gynecol.* 1998;11:289-91.
29. Locher J. *Carmen heroicum de partu monstrofero.* Ingolstadt: Johann Kachelofen; 1499.
30. Serres ERA. *Recherches d'anatomie transcendante et pathologique; theorie des formations et des deformations organiques, applique a l'anatomie de Ritta-Christina, et de la duplicite monstrueuse.* Paris: Ballieure; 1832.
31. Vrolik W. *Tabulae ad illustrandum embryogenesis hominis et mammalium, tam naturalem quam abnormen.* Amsterdam: G.M.P. Londonck; 1849.
32. Schwalbe E. *Die morphologie der missbildungen des menschen und der tiere.* Jena, Germany: Gustav Fisher Verlag; 1906-1960.
33. McMahon CJ, Spencer R. Congenital heart defects in conjoined twins: outcome after surgical separation of thoracopagus. *Pediatr Cardiol.* 2006;27:1-12.
34. Spencer R. Anatomic description of conjoined twins: a plea for standardized terminology. *J Pediatr Surg.* 1996;31:941-4.
35. Khanna PC, Pungavkar SA, Patkar DP. Ultrafast magnetic resonance imaging of cephalothoracopagus janiceps dysymmetros. *J Postgrad Med.* 2005;51:228-9.
36. Kuroda K, Kamei Y, Kozuma S, Kikuchi A, Fujii T, Unno N, Baba K, Taketani Y. Cephalopagus conjoined twins. *Ultrasound Obstet Gynecol.* 2000;16:293.

37. van Eyndhoven HW, ter Brugge H. The first-trimester ultrasonographic diagnosis of dicephalus conjoined twins. *Acta Obstet Gynecol Scand.* 1998;77:464-6.
38. Vural F, Vural B. First trimester diagnosis of dicephalic parapagus conjoined twins via transvaginal ultrasonography. *J Clin Ultrasound.* 2005;33:364-6.
39. Daskalakis G, Pilalis A, Tourikis I, Mouloupoulos G, Karamoutzos I, Antsaklis A. First trimester diagnosis of dicephalus conjoined twins. *Eur J Obstet Gynecol Reprod Biol.* 2004;112:110-3.
40. Bulbul Y, Drummond CL, Hillion Y, Bidat L, Ville Y. Diprosopus associated with neural tube defect and facial cleft in the first trimester. *Fetal Diagn Ther.* 2004;19:246-50.
41. Bétoulières P, Caderas de Kerleau J, Gevaudand L. Etude radiologique de squelette d'un monstre double janicéphale-rachipage. *Montpellier Med J.* 1960;58:30-9.
42. Durin L, Hors Y, Jeanne-Pasquier C, Barjot P, Herlicoviez M, Dreyfus M. Prenatal diagnosis of an extremely rare type of conjoined twins: cranio-rachi-pygopagus twins. *Fetal Diagn Ther.* 2005;20:158-60.
43. Spencer R. Rachipagus conjoined twins: they really do occur! *Teratology.* 1995;52:346-56.
44. Kompanje EJ. Very rare congenital malformations: responsibilities of scientists. The case of rachipagus conjoined twins. *Fetal Diagn Ther.* 2006;21:319-20.
45. Hockley AD, Gornall P, Walsh R, Nishikawa H, Lam H, MacPherson L, Bissenden J, Downey G, Spitz L. Management of pyopagus conjoined twins. *Childs Nerv Syst.* 2004;20:635-9.
46. Ogutu D, Anastasakis E, Chi C, Kadir RA. First trimester diagnosis of conjoint (pygopagus) twins: A case report of successful prenatal and postnatal management. *J Obstet Gynaecol.* 2008;28:340-2.
47. Tongsong T, Chanprapaph P, Pongsatha S. First-trimester diagnosis of conjoined twins: a report of three cases. *Ultrasound Obstet Gynecol.* 1999;14:434-7.
48. Koontz WL, Herbert WN, Seeds JW, Cefalo RC. Ultrasonography in the antepartum diagnosis of conjoined twins. A report of two cases. *J Reprod Med.* 1983;28:627-30.
49. Maggio M, Callan NA, Hamod KA, Sanders RC. The first-trimester ultrasonographic diagnosis of conjoined twins. *Am J Obstet Gynecol.* 1985;152:833-5.
50. Maymon R, Mendelovic S, Schachter M, Ron-El R, Weinraub Z, Herman A. Diagnosis of conjoined twins before 16 weeks' gestation: the 4-year experience of one medical center. *Prenat Diagn.* 2005;25:839-43.
51. Luchinger AB, Hadders-Algra M, van Kan CM, de Vries JI. Fetal onset of general movements. *Pediatr Res.* 2008;63:191-5.
52. Goldberg BB. Obstetric US imaging: the past 40 years. *Radiology.* 2000;215:622-9.
53. Wilson RL, Cetrulo CL, Shaub MS. The prepartum diagnosis of conjoined twins by the use of diagnostic ultrasound. *Am J Obstet Gynecol.* 1976;126:737.
54. Schmidt W, Heberling D, Kubli F. Antepartum ultrasonographic diagnosis of conjoined twins in early pregnancy. *Am J Obstet Gynecol.* 1981;139:961-3.
55. Sherer DM, Dalloul M, Kheyman M, Zigalo A, Nader I, Sokolovski M, Abulafia O. Transvaginal color Doppler imaging diagnosis of thoracopagus conjoined twins at 7 weeks' gestation. *J Ultrasound Med.* 2006;25:1485-7.
56. Huisman TA, Arulrajah S, Meuli M, Brehmer U, Beinder E. Fetal MRI of conjoined twins who switched their relative positions. *Pediatr Radiol.* 2010 Mar;40(3):353-7.
57. Neilson JP. Prenatal diagnosis in multiple pregnancies. *Curr Opin Obstet Gynecol.* 1992;4:280-5.
58. Timor-Tritsch IE, Farine D, Rosen MG. A close look at early embryonic development with the high-frequency transvaginal transducer. *Am J Obstet Gynecol.* 1988;159:676-81.
59. Dugoff L. Ultrasound diagnosis of structural abnormalities in the first trimester. *Prenat Diagn.* 2002;22:316-20.
60. Merz E, Bahlmann F, Weber G. Volume scanning in the evaluation of fetal malformations: a new dimension in prenatal diagnosis. *Ultrasound Obstet Gynecol.* 1995;5:222-7.
61. Sladkevicius P, Campbell S. Advances in ultrasound assessment in the establishment and development of pregnancy. *Br Med Bull.* 2000;56:691-703.
62. Maymon R, Halperin R, Weinraub Z, Herman A, Schneider D. Three-dimensional transvaginal sonography of conjoined twins at 10 weeks: a case report. *Ultrasound Obstet Gynecol.* 1998;11:292-4.

63. Bega G, Wapner R, Lev-Toaff A, Kuhlman K. Diagnosis of conjoined twins at 10 weeks using three-dimensional ultrasound: a case report. *Ultrasound Obstet Gynecol.* 2000;16:388-90.
64. Fang KH, Wu JL, Yeh GP, Chou PH, Hsu JC, Hsieh CT. Ischiopagus conjoined twins at 9 weeks of gestation: three-dimensional ultrasound and power Doppler findings. *Ultrasound Obstet Gynecol.* 2005;25:309-10.
65. Kuroda K, Kamei Y, Kozuma S, Kikuchi A, Fujii T, Unno N, Baba K, Taketani Y. Prenatal evaluation of cephalopagus conjoined twins by means of three-dimensional ultrasound at 13 weeks of pregnancy. *Ultrasound Obstet Gynecol.* 2000;16:264-6.
66. Suzumori N, Nakanishi T, Kaneko S, Yamamoto T, Tanemura M, Suzuki Y, Suzumori K. Three-dimensional ultrasound of dicephalus conjoined twins at 9 weeks of gestation. *Prenat Diagn.* 2005;25:1063-4.
67. Bonilla-Musoles F, Raga F, Bonilla F, Jr., Blanes J, Osborne NG. Early diagnosis of conjoined twins using two-dimensional color Doppler and three-dimensional ultrasound. *J Natl Med Assoc.* 1998;90:552-6.
68. Bornstein E, Santos R, Timor-Tritsch IE, Monteagudo A. "Brothers in arms": 3-dimensional sonographic findings in a first-trimester thoraco-omphalopagus conjoined twin pair. *J Ultrasound Med.* 2009;28:97-9.
69. Abu-Rustum RS, Adra AM. Three-dimensional sonographic diagnosis of conjoined twins with fetal death in the first trimester. *J Ultrasound Med.* 2008;27:1662-3.
70. Maruotti GM, Paladini D, Napolitano R, Mazzarelli LL, Russo T, Quarantelli M, D'Armiento MR, Martinelli P. Prenatal 2D and 3D ultrasound diagnosis of dipropopus: case report with post-mortem magnetic resonance images (MRI) and review of the literature. *Prenat Diagn.* 2009;29:992-4.
71. Basgul A, Kavak ZN, Sezen D, Gokaslan H. Thoraco-omphalopagus conjoined twins detected at as early as 9 weeks of gestation: transvaginal two-dimensional ultrasound, color Doppler and fetoplacental Doppler velocity waveform findings. *Fetal Diagn Ther.* 2006;21:477-80.
72. Ohkuchi A, Minakami H, Sato I, Nakano T, Tateno M. First-trimester ultrasonographic investigation of cardiovascular anatomy in thoracoabdominally conjoined twins. *J Perinat Med.* 2001;29:77-80.
73. Sen C, Celik E, Vural A, Kepkep K. Antenatal diagnosis and prognosis of conjoined twins--a case report. *J Perinat Med.* 2003;31:427-30.
74. Woo JS, Liang ST, Lo R. Characteristic pattern of Doppler umbilical arterial velocity waveform in conjoint twins. *Gynecol Obstet Invest.* 1987;23:70-2.
75. Blickstein I, Keith LG. Multiple pregnancy: epidemiology, gestation & perinatal outcome. 2 ed. London: Informa UK Ltd; 2005.
76. Assmus A. Early History of X Rays. 1995; Available from: <http://www.slac.stanford.edu/pubs/beamline/25/2/25-2-assmus.pdf>.
77. Daffner RH. *Clinical Radiology, the essentials.* Third edition ed. Baltimore: Lippincott Williams & wilkins; 2007.
78. Hansmann M, Schlachter H, Foedisch HJ. Prapartale diagnosis eines thoracopagus mittels ultrasonographie. *Gynakologe.* 1979;12.
79. Siegel HA, Seltzer SE, Miller S. Prenatal computed tomography: are there indications? *J Comput Assist Tomogr.* 1984;8:871-6.
80. Barth RA, Filly RA, Goldberg JD, Moore P, Silverman NH. Conjoined twins: prenatal diagnosis and assessment of associated malformations. *Radiology.* 1990;177:201-7.
81. Werner H, dos Santos JR, Fontes R, Daltro P, Gasparetto E, Marchiori E, Campbell S. Additive manufacturing models of fetuses built from three-dimensional ultrasound, magnetic resonance imaging and computed tomography scan data. *Ultrasound Obstet Gynecol.* 2010;36:355-61.
82. Grassi R, Esposito V, Scaglione M, Cirillo M, Cappabianca S, Guglielmi G, Sasso FS, Rotondo A. Multi-detector row CT for depicting anatomic features of cephalothoracopagus varieties: revised approach. *Radiographics.* 2004;24:e21.
83. Unal O, Arslan H, Adali E, Bora A, Yildizhan R, Avcu S. MRI of omphalopagus conjoined twins with a Dandy-Walker malformation: prenatal true FISP and HASTE sequences. *Diagn Interv Radiol.* 2010;16:66-9.
84. Hu LS, Caire J, Twickler DM. MR findings of complicated multifetal gestations. *Pediatr Radiol.* 2006;36:76-81.

85. Turner RJ, Hankins GD, Weinreb JC, Ziaya PR, Davis TN, Lowe TW, Gilstrap LC. Magnetic resonance imaging and ultrasonography in the antenatal evaluation of conjoined twins. *Am J Obstet Gynecol.* 1986;155:645-9.
86. Spielmann AL, Freed KS, Spritzer CE. MRI of conjoined twins illustrating advances in fetal imaging. *J Comput Assist Tomogr.* 2001;25:88-90.
87. Pugash D, Brugger PC, Bettelheim D, Prayer D. Prenatal ultrasound and fetal MRI: the comparative value of each modality in prenatal diagnosis. *Eur J Radiol.* 2008;68:214-26.
88. Ozkur A, Karaca M, Gocmen A, Bayram M, Sirikci A. Cephalopagus conjoined twins presented with encephalocele: diagnostic role of ultrafast MR imaging. *Diagn Interv Radiol.* 2006;12:90-2.
89. Kantarci M, Alper F, Eren S, Onbas O, Ceviz N, Tastekin A, Durur I, Okur A. Omphalopagus conjoined twins: ultrafast MR imaging findings. *Diagn Interv Radiol.* 2006;12:187-9.
90. Huppert BJ, Brandt KR, Ramin KD, King BF. Single-shot fast spin-echo MR imaging of the fetus: a pictorial essay. *Radiographics.* 1999;19:S215-27.
91. Chen Q, Levine D. Fast fetal magnetic resonance imaging techniques. *Top Magn Reson Imaging.* 2001;12:67-79.
92. Yamashita Y, Namimoto T, Abe Y, Takahashi M, Iwamasa J, Miyazaki K, Okumara H. MR imaging of the fetus by a HASTE sequence. *AJR Am J Roentgenol.* 1997;168:513-9.
93. Benson RC, Colletti PM, Platt LD, Ralls PW. MR imaging of fetal anomalies. *AJR Am J Roentgenol.* 1991;156:1205-7.
94. McAdams RM, Milhoan KA, Hall BH, Richardson RG. Prenatal and postnatal imaging of thoracopagus conjoined twins with a shared six-chamber heart. *Pediatr Radiol.* 2004;34:816-9.
95. Singla V, Singh P, Gupta P, Gainer S, Garg M, Khandelwal N. Prenatal diagnosis of thoracopagus fetus: a case report with brief review of literature. *Arch Gynecol Obstet.* 2009;280:1025-7.
96. Koning AH, Rousian M, Verwoerd-Dikkeboom CM, Goedknegt L, Steegers EA, van der Spek PJ. V-scope: design and implementation of an immersive and desktop virtual reality volume visualization system. *Stud Health Technol Inform.* 2009;142:136-8.
97. Rousian M, Koning AH, van Oppenraaij RH, Hop WC, Verwoerd-Dikkeboom CM, van der Spek PJ, Exalto N, Steegers EA. An innovative virtual reality technique for automated human embryonic volume measurements. *Hum Reprod.* 2010;25:2210-6.
98. Rousian M, Verwoerd-Dikkeboom CM, Koning AH, Hop WC, van der Spek PJ, Exalto N, Steegers EA. Early pregnancy volume measurements: validation of ultrasound techniques and new perspectives. *BJOG.* 2009;116:278-85.
99. Rousian M, Verwoerd-Dikkeboom CM, Koning AH, van der Spek PJ, Exalto N, Steegers EA. Innovative three-dimensional imaging: opportunities for virtual embryology. *Ned Tijdschr Geneesk.* 2010;154:A1606.
100. Verwoerd-Dikkeboom CM, Koning AH, Groenenberg IA, Smit BJ, Brezinka C, Van Der Spek PJ, Steegers EA. Using virtual reality for evaluation of fetal ambiguous genitalia. *Ultrasound Obstet Gynecol.* 2008;32:510-4.
101. Verwoerd-Dikkeboom CM, Koning AH, Hop WC, Rousian M, Van Der Spek PJ, Exalto N, Steegers EA. Reliability of three-dimensional sonographic measurements in early pregnancy using virtual reality. *Ultrasound Obstet Gynecol.* 2008;32:910-6.
102. Verwoerd-Dikkeboom CM, Koning AH, Hop WC, van der Spek PJ, Exalto N, Steegers EA. Innovative virtual reality measurements for embryonic growth and development. *Hum Reprod.* 2010;25:1404-10.
103. Verwoerd-Dikkeboom CM, Koning AH, van der Spek PJ, Exalto N, Steegers EA. Embryonic staging using a 3D virtual reality system. *Hum Reprod.* 2008;23:1479-84.
104. Verwoerd-Dikkeboom CM, van Heesch PN, Koning AH, Galjaard RJ, Exalto N, Steegers EA. Embryonic delay in growth and development related to confined placental trisomy 16 mosaicism, diagnosed by I-Space Virtual Reality. *Fertil Steril.* 2008;90:2017.e19-22.
105. Groenenberg IA, Koning AH, Galjaard RJ, Steegers EA, Brezinka C, van der Spek PJ. A virtual reality rendition of a fetal meningomyelocele at 32 weeks of gestation. *Ultrasound Obstet Gynecol.* 2005;26:799-801.

PART 6

PART 7

PART 8

GENERAL DISCUSSION

The aim of this thesis is to assess *in vivo* growth and development in first trimester pregnancies using 3D ultrasound datasets, in an innovative virtual reality (VR) application, which we tentatively describe as 'virtual embryoscopy'. We focus on four topics:

1. The reproducibility of new embryonic biometric and volumetric measurements performed using VR.
2. The construction of growth charts in relation to GA and the CRL for newly introduced biometric and automated volumetric measurements.
3. *In vivo* staging based on internal and external morphologic characteristics and the relation of the stages to GA, CRL, embryonic volume and brain ventricle volume.
4. The applicability of VR for diagnosing complex congenital anomalies such as first trimester conjoined twins.

After discussing the design of the study, these four topics will be further elaborated on.

Study design: a longitudinal cohort study

Growth is a keyword in this thesis. Growth of an embryo or early fetus can be compared using longitudinally collected data. For repeated measurements during pregnancy, appropriate reference ranges must be derived from longitudinal studies¹⁻². It is possible to analyze longitudinal data as if they came from a cross-sectional study, which enables one to study size charts and age assessment charts². We have to be aware that the sample size has to be large enough and appropriate statistics have to be used for this purpose. In this thesis all patients - a cohort of first trimester pregnant women - had 3D ultrasound examinations performed weekly between six and 12 weeks GA.

At this moment, the study is embedded in a larger project, which aims to analyze growth and development during and after pregnancy (childhood) and the influences on these processes; like lifestyle, general health and genetics. This cohort study is called the PREDICT study. For the patients that will be included in the future, this means that in addition to the weekly 3D ultrasound examinations between six and 12 weeks GA, patients have to fill out several questionnaires (including a Food Frequency Questionnaire) at their first visit, at 24 weeks pregnancy, at birth and at the first birthday of the newborn. Furthermore, blood samples are taken in the first trimester of pregnancy, and where possible umbilical cord samples are taken at birth.

Reproducibility of VR measurements

When new visualization techniques (including their applications) are introduced, it must be demonstrated that the results obtained with this new technique are reproducible, which covers the accuracy and reliability. The first new function introduced to the VR software, was the tracing application. This function enables

the measurement of the length of structures – like embryonic structures - precisely in three dimensions. Actually, it enables the measurement of embryonic structures requiring 3D interaction, like the length of the arm, leg or umbilical cord, for the first time as far as we know. In 2008, Verwoerd-Dikkeboom et al.³ compared (standard and non-standard) biometric measurements performed using 4D View (a program present on the ultrasound machine which enables 2D measurements in a 3D dataset) and VR software (in the I-Space). The yolk sac diameter, CRL, biparietal diameter, head circumference and abdominal circumference were measured using both visualization techniques. The conclusion of the study was that length measurements performed using VR, were reliable.

Secondly, the volume measuring tool was introduced and evaluated. This tool enables (semi) automated volume measurements of hypoechoic and hyperechoic structures. However, the study was limited to the measurement of *in vitro* and *in vivo* hypoechoic structures (balloons and yolk sacs), since they were the only structures that could be measured by all four available techniques, of which VOCAL is seen as the 'golden standard'. V-Scope was as accurate and reliable as the 'golden standard'. V-Scope was also the fastest measuring technique in the *in vivo* part. The main factor influencing the reproducibility of the volume measurements, but also of the length measurements, was the image quality.

The measurement of structures which would enable us to monitor the embryonic growth and development more accurately and precisely was the next step. Examples of these structures are the gestational sac, the amniotic sac, the yolk sac, the embryonic volume and brain cavity volume, which are not all presented in this thesis. This also includes the volumetric growth parameters used for more precise monitoring of growth in the second and third trimester of pregnancy⁴⁻⁶. These structures are not only hypoechoic or simple shaped structures as studied in the reproducibility study (**part 3.1**), but since the technique is automated, the reproducibility of the hypoechoic structures can be extrapolated to hyperechoic structures as well (like the embryonic body volume).

Non-standard biometric measurements

After studying the reproducibility of the two measurement tools in V-Scope, we measured two structures of vital importance to embryogenesis: the umbilical cord and vitelline duct. These structures are not measured routinely due to their complex shape and morphology, requiring 3D interaction for their measurement.

The measurement of these structures might be important, since for instance abnormalities of the umbilical cord, are associated with intrauterine demise, fetal malformations and chromosomal abnormalities⁷⁻¹⁰, which makes early detection clinically valuable¹¹. Therefore, knowledge of the development of these structures in the first trimester may eventually serve as a background for early detection of abnormal fetal development (**part 4.1**). In **part 4.1** a linear relation is found between the umbilical cord length and the CRL and GA, which is also the case for the vitelline duct length measurements. Image quality greatly affects the ability of measuring different parts of the umbilical cord and vitelline duct, and because

of that it was not possible to measure these structures successfully in all cases. We believe that in the future, equipment offering better image quality in the first trimester will help to overcome this limitation.

In **part 4.2** examples of other non-standard measurements like the length of the arm¹² and legs are illustrated; which are structures requiring 3D interaction for their measurement as well. In future studies these measurements have to proof their ability to discriminate between normal and abnormal development.

Volume measurements

Using 2D ultrasound, volume estimations of symmetric and (near) spherical structures can be achieved using three orthogonal diameters and applying the volume formula of an ellipsoid shape. Although this gives a reasonable approximation for symmetrical structures, the technique is inappropriate for complex structures and shapes¹³. With the development of 3D ultrasound transducers accurate volume measurements were introduced, even in organs that are irregular or asymmetrical in shape¹⁴⁻¹⁵.

The ability to perform volume measurements of different structures facilitates visualization of the (spatial) relationships and sizes, besides the already used length, width, depth or circumference measurements. This makes the measurement more informative, because it reflects the real size, instead of taking a derivative, like the CRL for growth.

When we are interested in the growth of an embryo (as a whole), the measurement of the embryonic volume seems superior to the CRL measurement, since the whole embryo is taken into account and the measurement does not depend on factors like the position or movement of an embryo¹⁶. In **part 5.1** of this thesis the relationship between the CRL and embryonic volume in the first trimester and birth weight is studied, resulting in a non significant relationship, which might be a power problem due to the limited number of measurements included. In a recently published study the late first trimester fetal volume measurements and CRL measurements significantly correlated with birth weight, and the fetal volume even better than the CRL¹⁷.

The gestational sac volume is another example of a volume measurement that may have a predictive value for adverse pregnancy outcomes¹⁸⁻²⁰, although this has to be studied more extensively in the future. To facilitate this research, new charts were constructed in this thesis as well, using VR.

Brain development: volume and cerebellum

In **part 5** of this thesis we mainly focus on the development of the embryonic brain and especially the brain ventricle and cerebellar development. Normal development of both structures is of vital importance.

The shape and size of the brain cavities are important diagnostic markers for the detection of central nervous system disorders in very early pregnancy. Therefore it may be expected that holoprocencephaly is the first condition

that can be recognized with ultrasound in the developing embryo²¹. In several case studies it has been demonstrated that holoprocencephaly can already be diagnosed at 9 weeks GA²²⁻²³. The brain ventricle volume measurements of these cases showed that the volumes were different in comparison to normal developing brain ventricles²². Acrania is another example of a central nervous system disorder, characterized by an altered appearance of the brain cavities with decreased fluid content, which can be recognized as early as 9 weeks GA²⁴⁻²⁵.

In aqueductal stenosis, the Sylvian aqueduct is wide throughout the first trimester, so one can expect that an early diagnosis is possible. However it is unknown when exactly the stenosis develops.

In the second trimester of pregnancy the cerebellum is measured routinely²⁶, but in this thesis we show that the cerebellum can already be measured at 7 weeks GA using VR. Diagnosing embryonic brain anomalies ultrasonographically is possible already in the first trimester. Reference values of the brain ventricle volumes and cerebellum length measurements, to compare findings in high risk patients, are therefore necessary. The charts constructed in this thesis provide quantitative and accurate information and may be useful in the differentiation between early normal and abnormal brain development.

The reported relatively low success rate is a point of debate, but may be explained by the fact that at the time these 3D ultrasound examinations were performed, the focus was on the embryo as a whole, and no separate brain scans were recorded. Targeted scanning of the brain will result in a much higher success rate.

Using VR for *in vivo* staging

An accurate description of *in vivo* embryonic growth and development can be achieved by adequate staging. The Carnegie Staging system describes the human embryonic growth by using *in vitro* samples²⁷⁻²⁸. As the I-Space allows us to see depth and the 3D ultrasound datasets collected in our studies are high resolution samples, it is possible to stage embryos (**part 5.1**) using the internal and external morphological characteristics. In our study it was not possible to use the histological characteristics or *in vitro* verification, as was the case in the Carnegie Staging system²⁷. Still the ability of staging the embryos, with good correlation with the CRL and GA, shows us that the development of a living human embryo, can be monitored using VR, next to the separate measurements of different structures. In this way, the whole embryo can be used to get an accurate description of its growth and development.

Abnormal growth and development: Conjoined twins and miscarriages

Previously, we described the visualization and quantification possibilities of the VR application for normal growing and developing human embryos and early fetuses. In addition we studied the value of VR in the description of conjoined twins in **part 6**. This is a group of high risk pregnancies in which accurate diagnostics is

crucial for prognosis purposes. Ultrasound is the main diagnostic tool, and the depth perception and 3D interaction offered by VR provides additional information in the evaluation of the complex anatomical structures. Since this is a review and case study, many more cases will have to be studied before we can state that VR contributes to earlier and more appropriate counseling and management of these cases.

To illustrate the potential clinical value of embryonic volumetry, series of recently obtained embryonic volume measurements of four pregnancies ending in a miscarriage are presented. Two of the miscarriages occurred at eight weeks GA and two at ten weeks GA. Figure 1 shows the embryonic growth of the additional four miscarriage cases. In two out of four cases (case one and four) embryonic volume measurements are below the 2.5th percentile whilst the corresponding CRL measurements are normal. The embryonic volume measurements are abnormal from the beginning in three out of four cases ending in a miscarriage, whereas the CRL measurements are less indicative of an abnormal outcome. The four cases show that different growth patterns may already exist in first trimester pregnancies subsequently ending as a miscarriage. As has been shown by abnormal first trimester growth and adverse obstetric outcomes from CRL studies²⁹⁻³¹, it is to be expected that embryonic volume measurements are more accurate in prediction models. Embryonic volume measurements may therefore be implemented in routine clinical practice in the nearby future. However, more research is needed to validate the assumption that abnormal volume measurements can be successfully used to predict a miscarriage.

Future perspectives and general applicability

Before VR can be implemented into clinical practice for the visualization and detection of congenital abnormalities in the first trimester of pregnancy, additional research has to be performed. One of our ongoing studies will compare the detection rate of congenital abnormalities in first trimester pregnancies using a VR system (movie 6) and the regularly used ultrasound machines. Blinded observers will score and describe the congenital abnormalities they see and the time needed for the detection will be registered. Finally, a questionnaire will be filled out, comparing the opinion of the different observers using both systems about topics such as the quality of the images, the user interface and the offered depth perception.

The I-Space VR system, located at the Erasmus MC, is the only Cave-like system in the world used for growth and developmental analysis of the early pregnancy. As explained in several parts of this thesis, a desktop alternative for the fully immersive system exists (figure 2). The V-Scope application can be run on this desktop system, which uses a low-cost 3D screen and a similar tracking system as used in the I-Space. Such a display system on the desk of a doctor or added to an ultrasound machine will not only greatly benefit a doctor or technician in coming up with a diagnosis, but also aid in the counseling of patients by clearly illustrating embryonic and early fetal anatomy. We foresee a future where 3D displays will

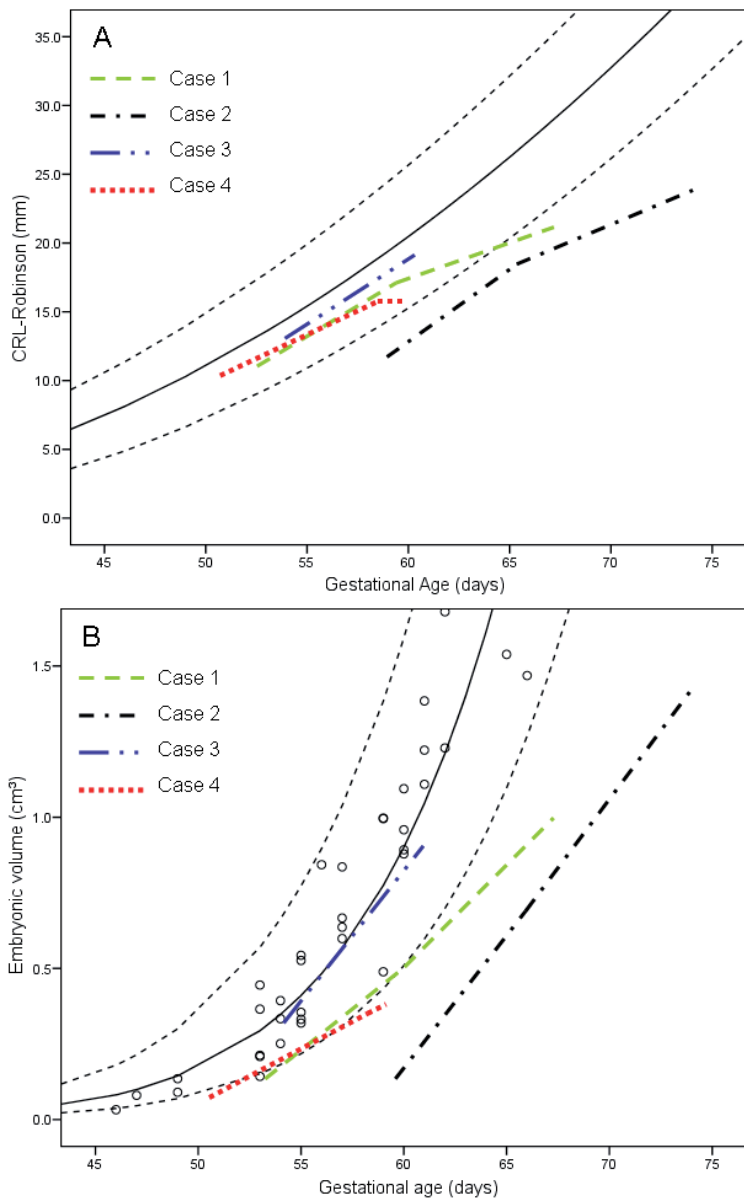


Figure 1. A. Crown-rump length measurements of four miscarriage cases are plotted against gestational age. The mean value and the 95% reference interval for the Robinson and Fleming growth chart are indicated by the solid and dotted lines, respectively. **B.** The whole-body volume measurements of the four miscarriage cases are plotted against gestational age. The mean value and the 95% reference interval are again indicated by the solid and dotted lines, respectively.

Movie 6. This movie shows a fetus at 12 weeks GA in the I-Space. The fetus has an omphalocele, radius dysplasia, a single umbilical artery, spina bifida and exencephaly, and was finally diagnosed with trisomy 18.

be as common as 2D displays in hospital settings. Until that day, our department offers the possibility to send first trimester 3D datasets to our research center by using the following webpage: <https://png3dvr.erasmusmc.nl>. These 3D datasets are loaded in the I-Space and checked using V-Scope software. The outcome of this 'virtual consult' is sent to the requesting doctor and can be shared with the patient.

In conclusion we can state that virtual reality offers an impressive new way of looking *in vivo* at an embryo, presenting information in all three human dimensions and making it possible to measure structures which could not be measured before. The combination of staging, biometry and volumetry, called 'Virtual Embryoscopy', enables us to study normal and abnormal **embryonic development**; which will eventually offer earlier and more accurate diagnosis of abnormal growth and development and contribute to a shift from second and third trimester fetal analysis to the first trimester. Being able to do so will bring 'embryonic medicine' a step closer.

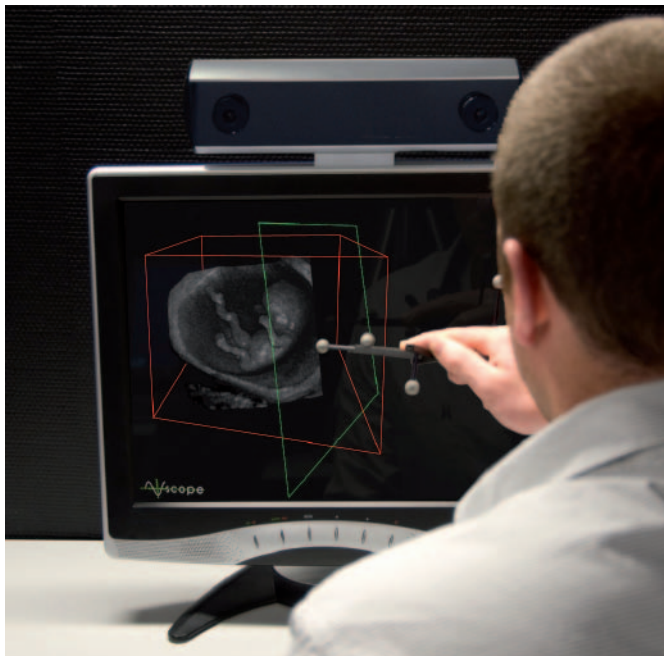


Figure 2. Desktop version running the V-Scope application as the I-Space. An embryo of 10 weeks' GA is displayed on the screen. The observer is interacting with the hologram.

REFERENCES

1. Johnsen SL, Wilsgaard T, Rasmussen S, Sollien R, Kiserud T. Longitudinal reference charts for growth of the fetal head, abdomen and femur. *Eur J Obstet Gynecol Reprod Biol.* 2006;127:172-85.
2. Altman DG, Chitty LS. Design and analysis of studies to derive charts of fetal size. *Ultrasound Obstet Gynecol.* 1993;3:378-84.
3. Verwoerd-Dikkeboom CM, Koning AH, Hop WC, Rousian M, Van Der Spek PJ, Exalto N, Steegers EA. Reliability of three-dimensional sonographic measurements in early pregnancy using virtual reality. *Ultrasound Obstet Gynecol.* 2008;32:910-16.
4. Lee W, Balasubramaniam M, Deter RL, Hassan SS, Gotsch F, Kusanovic JP, Goncalves LF, Romero R. Fractional limb volume--a soft tissue parameter of fetal body composition: validation, technical considerations and normal ranges during pregnancy. *Ultrasound Obstet Gynecol.* 2009;33:427-40.
5. Lee SM, Jun JK, Lee EJ, Lee JH, Park CW, Park JS, Syn HC. Measurement of fetal urine production to differentiate causes of increased amniotic fluid volume. *Ultrasound Obstet Gynecol.* 2010;36:191-5.
6. Prendergast M, Rafferty GF, Davenport M, Persico N, Jani J, Nicolaides K, Greenough A. Three-dimensional ultrasound fetal lung volumes and infant respiratory outcome: a prospective observational study. *BJOG* 2011;118:608-14.
7. Hill LM, DiNofrio DM, Guzick D. Sonographic determination of first trimester umbilical cord length. *J Clin Ultrasound.* 1994;22:435-8.
8. Nyberg DA, Mahony BS, Luthy D, Kapur R. Single umbilical artery. Prenatal detection of concurrent anomalies. *J Ultrasound Med.* 1991;10:247-53.
9. Saller DN, Jr., Keene CL, Sun CC, Schwartz S. The association of single umbilical artery with cytogenetically abnormal pregnancies. *Am J Obstet Gynecol.* 1990;163:922-5.
10. Sepulveda W, Gutierrez J, Sanchez J, Be C, Schnapp C. Pseudocyst of the umbilical cord: prenatal sonographic appearance and clinical significance. *Obstet Gynecol.* 1999;93:377-81.
11. Deurloo KL, Kist WJ, Vugt JMG. Three dimensional ultrasound: an overview of its clinical use. *Fetal Matern Med Rev.* 2007;18:145-79.
12. Verwoerd-Dikkeboom CM, Koning AH, Hop WC, van der Spek PJ, Exalto N, Steegers EA. Innovative virtual reality measurements for embryonic growth and development. *Hum Reprod.* 2010;25:1404-10.
13. Ioannou C, Sarris I, Salomon LJ, Papa-georghiou AT. A review of fetal volumetry: the need for standardisation and definitions in measurement methodology. *Ultrasound Obstet Gynecol.* 2011;doi:10.1002/uog.9074.
14. Riccabona M, Nelson TR, Pretorius DH. Three-dimensional ultrasound: accuracy of distance and volume measurements. *Ultrasound Obstet Gynecol.* 1996;7:429-34.
15. Riccabona M, Nelson TR, Pretorius DH, Davidson TE. In vivo three-dimensional sonographic measurement of organ volume: validation in the urinary bladder. *J Ultrasound Med.* 1996;15:627-32.
16. Falcon O, Peralta CF, Cavoretto P, Auer M, Nicolaides KH. Fetal trunk and head volume in chromosomally abnormal fetuses at 11+0 to 13+6 weeks of gestation. *Ultrasound Obstet Gynecol.* 2005;26:517-20.
17. Antsaklis A, Anastasakis E, Komita O, Theodora M, Hiridis P, Daskalakis G. First trimester 3D volumetry. Association of the gestational volumes with the birth weight. *J Matern Fetal Neonatal Med* 2011;24:1055-9.
18. Falcon O, Wegrzyn P, Faro C, Peralta CF, Nicolaides KH. Gestational sac volume measured by three-dimensional ultrasound at 11 to 13 + 6 weeks of gestation: relation to chromosomal defects. *Ultrasound Obstet Gynecol.* 2005;25:546-50.
19. Figueras F, Torrents M, Munoz A, Comas C, Antolin E, Echevarria M, Carrera JM. Three-dimensional yolk and gestational sac volume. A prospective study of prognostic value. *J Reprod Med.* 2003;48:252-6.
20. Babinszki A, Nyari T, Jordan S, Nasser A, Mukherjee T, Copperman AB. Three-dimensional measurement of gestational and yolk sac volumes as predictors of pregnancy outcome in the first trimester. *Am J Perinatol* 2001;18:203-11.

21. O'Rahilly R, Muller F. Prenatal ages and stages-measures and errors. *Teratology*. 2000;61:382-4.
22. Blaas HG, Eik-Nes SH, Vainio T, Isaksen CV. Alobar holoprosencephaly at 9 weeks gestational age visualized by two- and three-dimensional ultrasound. *Ultrasound Obstet Gynecol*. 2000;15:62-5.
23. Timor-Tritsch IE, Monteagudo A, Santos R. Three-dimensional inversion rendering in the first- and early second-trimester fetal brain: its use in holoprosencephaly. *Ultrasound Obstet Gynecol*. 2008;32:744-50.
24. Machado RA, Brizot ML, Carvalho MH, Waissman AL, Bunduki V, Zugaib M. Sonographic markers of exencephaly below 10 weeks' gestation. *Prenat Diagn*. 2005;25:31-3.
25. Becker R, Mende B, Stiemer B, Entezami M. Sonographic markers of exencephaly at 9 + 3 weeks of gestation. *Ultrasound Obstet Gynecol*. 2000;16:582-4.
26. Verburg BO, Steegers EA, De Ridder M, Snijders RJ, Smith E, Hofman A, Moll HA, Jaddoe VW, Witteman JC. New charts for ultrasound dating of pregnancy and assessment of fetal growth: longitudinal data from a population-based cohort study. *Ultrasound Obstet Gynecol*. 2008;31:388-96.
27. O'Rahilly R, Muller F. *Developmental stages in human embryos*. Washington: Carnegie Institution of Washington Publication 1987.
28. O'Rahilly R, Muller F. *Developmental stages in human embryos: revised and new measurements*. *Cells Tissues Organs*. 2010;192:73-84.
29. Bukowski R, Smith GC, Malone FD, Ball RH, Nyberg DA, Comstock CH, Hankins GD, Berkowitz RL, Gross SJ, Dugoff L, Craigo SD, Timor-Tritsch IE, Carr SR, Wolfe HM, D'Alton ME. Fetal growth in early pregnancy and risk of delivering low birth weight infant: prospective cohort study. *BMJ*. 2007;334:836.
30. Mukri F, Bourne T, Bottomley C, Schoeb C, Kirk E, Papageorghiou AT. Evidence of early first-trimester growth restriction in pregnancies that subsequently end in miscarriage. *BJOG* 2008;115:1273-8.
31. Smith GC, Smith MF, McNay MB, Fleming JE. First-trimester growth and the risk of low birth weight. *NEJM*. 1998;339: 1817-22.

PART 7

PART 8

PART 9

SUMMARY
SAMENVATTING

SUMMARY

The overall aim of this thesis is to establish an accurate and reliable description of new *in vivo* biometric and volumetric measurements in the first trimester of pregnancy using 3D ultrasound datasets, analyzed using an innovative VR system. These new measurements, which make optimal use of all three dimensions, will form a basis for follow-up studies describing the abnormal development of embryonic and early fetal life.

In **part 1, chapter 1.1** the introduction of the research performed in this thesis is briefly described. **Chapter 1.2** is an overview of the application of 3D ultrasound during embryonic and early fetal life. In addition, the I-Space VR system and V-Scope volume rendering application are described; explaining functionality such as the measurement of old and new biometric parameters, the measurement of new automated volumetric parameters and the possibility of embryonic staging. Finally, the possible use of VR in the detection of abnormal growth and development is introduced.

In **part 2** the accuracy and reliability of the V-Scope volume measuring function is tested in an *in vivo* and *in vitro* setting. Three-dimensional ultrasound datasets of first trimester yolk sacs were used for the *in vivo* part of the study. For the *in vitro* part, small water filled balloons with a known volume were used. In addition to the semi-automatic V-Scope method, the volume measurements of the hypoechoic parts were performed using three other techniques: VOCAL, Inversion mode and SonoAVC. VOCAL is a manual segmentation method, which makes volume measurements of hypoechoic and hyperechoic structures possible. Inversion mode and SonoAVC are semi-automated volume measuring methods, allowing only measurements of hypoechoic structures. In the *in vitro* and *in vivo* part of the study VOCAL and V-Scope proved to be the most reliable. The intraobserver and interobserver reproducibility of all four techniques proved to be good. As V-Scope is an automated, less time-consuming method, it offers great potential for the estimation of different embryonic structures in an accurate way.

In **part 3** non-standard volume measurements of different embryonic structures are described. Growth charts are constructed and parameters are related to GA and CRL, and to other parameters as well. In **chapter 3.1** the use of VR for the measurement of the embryonic body, including the limbs, and the yolk sac is evaluated in normal, healthy pregnancies. VR allows us to obtain unique information about the size of the embryo using all three dimensions. The interobserver reproducibility of the irregularly shaped human body volume measurements proved to be excellent. In **chapter 3.2**, the gestational sac diameter (GSD), gestational sac fluid volume (GSFV) and gestational sac volume (GSV) were measured using VR and new charts were constructed according to GA, CRL and GSD. The GSD formula constructed in our study was significantly different from the commonly clinically used formula. The GSV measured in our study was on average 20% smaller when compared to the GSV calculated by using the ellipsoid formula.

The description of normal growth of the first trimester umbilical cord and vitelline duct by length measurements are presented in **chapter 4**. The *in vivo* measurement of these structures during the first trimester of pregnancy is only possible when the measuring application offers depth perception and 3D interaction. VR enables the measurement of multi-planar structures, like the umbilical cord, which contains loops already in the early pregnancy.

In **chapter 5** the study of neurosonographic parameters and the construction of charts relating the growth of the brain structures to GA and CRL are presented. **Part 5.1** introduces the possibility of measuring the volume of the brain cavities (semi-)automatically. The visualization of the cavities allows embryonic staging using some internal morphological criteria of the Carnegie Staging system, in addition to the external morphological criteria. In the second part, **part 5.2**, the development of the cerebellum during the first trimester is described in detail. Next to the total cerebellar diameter, the length of the left and right hemispheres and the corresponding heights were measured and related to GA and CRL. The measurements were performed in two different settings: on the ultrasound machine and using the I-Space VR system. Both methods proved to be highly reproducible and comparable to each other. The use of VR allows easy localization of the cerebellum, providing a realistic impression of the developing hemispheres.

In **chapter 6**, the applicability of VR to provide a systematic diagnostic tool for diagnosing first trimester conjoined twins is described. In this overview study all possible imaging techniques are evaluated. Three cases of first trimester conjoined twins are described in detail using 2D and 3D ultrasound examination, as well as examination using the VR system. VR provided additional information in our first trimester cases, and therefore may contribute to earlier, more appropriate counseling and management of conjoined twin cases.

In the last chapter, **chapter 7**, the general discussion, the results of all studies are combined and discussed in a broader perspective. Our goal was to discuss the use of a VR application in the study of **embryonic growth and development** in an *in vivo* setting. The I-Space VR system and the V-Scope application allow the exploration of all three dimensions, and therefore offers visualization and quantification of structures that cannot be shown or measured in one or two dimensions. Since abnormalities and/or developmental problems in the embryonic period have major consequences for fetal and neonatal life, it is important to check these structures and their growth as early and precisely as possible. Early diagnosis of abnormalities may eventually lead to new antenatal strategies and interventions, opening up a new field of 'embryonic medicine'.

SAMENVATTING

Dit proefschrift heeft als doel het accuraat en betrouwbaar beschrijven van nieuwe *in vivo* uitgevoerde biometrische lengte- en volumemetingen in het eerste trimester van de zwangerschap aan de hand van drie-dimensionale (3D) echoscopie datasets, geanalyseerd met behulp van een innovatief virtuele realiteit (VR) systeem. Deze nieuwe metingen, uitgevoerd met optimaal gebruik van alle drie de dimensies, zullen een basis vormen voor vervolgstudies waarin abnormale ontwikkeling in de embryonale en vroege foetale periode centraal zullen staan.

Deel 1, **hoofdstuk 1.1** is de algemene introductie van het proefschrift. In **hoofdstuk 1.2** wordt de mogelijkheid beschreven om 3D echoscopie tijdens de embryonale en vroege foetale periode toe te passen. Tevens worden het I-Space VR systeem en de V-Scope applicatie beschreven; waarbij de functionaliteit, zoals het meten van bestaande en nieuwe biometrische parameters, het meten van nieuwe automatische volumetrische parameters en stagering van het embryo, wordt toegelicht. Tenslotte wordt het gebruik van VR in de detectie van abnormale groei en ontwikkeling geïntroduceerd.

In **deel 2** van het proefschrift wordt de nauwkeurigheid en betrouwbaarheid van volumemetingen met V-Scope getest in een *in vivo* en *in vitro* setting. Voor het *in vivo* gedeelte werden 3D echoscopie datasets van eerste trimester dooierzakken gebruikt en voor het *in vitro* gedeelte kleine, met watergevulde ballonnen waarvan de hoeveelheid ingebrachte water bekend was. Naast het meten van de hypoechogene inhoud van structuren met V-Scope, werden de metingen ook uitgevoerd gebruikmakend van drie andere technieken: VOCAL, Inversion mode en SonoAVC. Bij de VOCAL methode wordt gebruik gemaakt van manuele segmentatie om volumemetingen te verrichten in zowel hypoechogene als hyperechogene structuren. Inversion mode en SonoAVC zijn semi-automatische volumemetingmethoden, die alleen de mogelijkheid bieden om volumes te meten van hypoechogene structuren. In het *in vitro* en *in vivo* gedeelte van de studie bleken VOCAL en V-Scope het meest betrouwbaar. De intra-onderzoeker en inter-onderzoeker reproduceerbaarheid van alle vier de technieken was goed. Omdat bij V-Scope een geautomatiseerde methode wordt gebruikt, heeft deze techniek, mede door de snelheid ervan, grote potentie voor het accuraat en efficiënt meten van verschillende embryonale structuren.

In de kliniek niet standaard uitgevoerde volumemetingen van verschillende embryonale structuren worden beschreven in **deel 3**. Tevens worden groeicurven beschreven die de gemeten parameters relateren aan de zwangerschapsduur en kop-stuit lengte (CRL), en aan enkele andere parameters. In **hoofdstuk 3.1** worden de metingen van het embryonale volume, inclusief de ledematen, en van het volume van de dooierzak beschreven in een normale populatie gezonde zwangeren. VR maakt het mogelijk om unieke informatie te verkrijgen over het embryonale volume, gebruikmakend van alle drie de dimensies. De inter-onderzoeker reproduceerbaarheid van het embryonale volume bleek goed te zijn, ondanks de onregelmatige en complexe vorm van het embryo. In het

volgende hoofdstuk, **hoofdstuk 3.2**, werden een aantal structuren gemeten met behulp van VR: de diameter van de vruchtzak, het volume van de totale vruchtzak en het volume van het vocht in de vruchtzak. Nieuwe curven zijn geconstrueerd, waarbij de gemeten parameters zijn gerelateerd aan de zwangerschapsduur, CRL en vruchtzakdiameter. De in deze studie geconstrueerde formule, die de vruchtzakdiameter vergelijkt met de zwangerschapsduur in dagen, is significant verschillend van de in de kliniek gebruikte formule. Het vruchtzakvolume gemeten in onze studie was gemiddeld 20% kleiner vergeleken met het volume berekend met behulp van de formule voor een ellipsoïde figuur, zoals gebruikelijk in de klinische praktijk.

De normale eerste trimester lengtegroei van de navelstreng en ductus vitellinus worden beschreven in **deel 4**. De *in vivo* meting van deze structuren tijdens het eerste trimester van de zwangerschap is alleen mogelijk wanneer de meetmethode diepteperceptie biedt in combinatie met 3D interactie. VR biedt de mogelijkheid om structuren die zich niet in één vlak bevinden, zoals de navelstreng met meerdere windingen, al vroeg in de zwangerschap te meten.

In **deel 5** wordt een veelbelovende ontwikkeling beschreven: het bepalen van neurosonografische parameters en de constructie van curven waarmee deze parameters worden gerelateerd aan de zwangerschapsduur en CRL. In **hoofdstuk 5.1** wordt de mogelijkheid van het (semi-)automatisch meten van het hersenventrikel volume geïntroduceerd. Een bijkomend voordeel van het visualiseren van de hersenventrikels is de mogelijkheid om *in vivo* te studeren op basis van enkele interne morfologische criteria, die beschreven worden in het Carnegie Stadiersysteem, naast de criteria beschreven voor de externe morfologische kenmerken. In het tweede gedeelte, **hoofdstuk 5.2**, wordt in detail de ontwikkeling van het cerebellum tijdens het eerste trimester beschreven. De volgende structuren zijn gemeten en gerelateerd aan de zwangerschapsduur en CRL: de totale cerebellaire diameter, de lengte van de linker en rechter hemisfeer en de hoogte van de linker en rechter hemisfeer. De metingen zijn uitgevoerd op het echoscopie apparaat en in de I-Space VR systeem. De metingen konden met beide methoden reproduceerbaar worden gemeten. De waarden, verkregen met de verschillende meetmethoden, waren vergelijkbaar met elkaar. Met behulp van VR kan het cerebellum gemakkelijk worden gelokaliseerd en wordt een realistische impressie geboden van de zich ontwikkelende cerebellaire hemisferen.

VR kan gebruikt worden als een methode om eerste trimester Siamese tweelingen systematisch te diagnosticeren. Deze mogelijkheid van de I-Space wordt beschreven in **deel 6**, aan de hand van drie casus van eerste trimester Siamese tweelingen. Er wordt hierbij gebruik gemaakt van twee-dimensionale, 3D en VR technieken. VR biedt additionele informatie bij de diagnostiek van eerste trimester Siamese tweelingen, en kan als zodanig bijdragen aan een betere counseling en behandeling.

In de algemene discussie, het laatste deel van dit proefschrift (**deel 7**), worden de resultaten uit alle studies gecombineerd en geplaatst in een breder perspectief. Het doel was het bediscussiëren van het gebruik van VR in de studie

naar *in vivo* **embryonale groei en ontwikkeling**. Het I-Space VR systeem en de V-Scope applicatie bieden de mogelijkheid om alle drie de dimensies optimaal te gebruiken. Het is dan ook mogelijk om bepaalde embryonale structuren te visualiseren en kwantificeren, die niet goed te visualiseren en kwantificeren zijn wanneer maar een of twee dimensies beschikbaar zijn. Het is belangrijk om deze structuren en hun groei zo vroeg en precies mogelijk te volgen, omdat abnormale groei en/of ontwikkeling in de embryonale periode vergaande consequenties heeft voor de foetale en postnatale periode. Vroege diagnostiek van abnormale ontwikkeling zal mogelijk uiteindelijk kunnen leiden tot nieuwe strategieën in aangedane patiënten en patiënten met een hoog risico op zwangerschapsgerelateerde complicaties.

PART 8

PART 9

AUTHORS AND AFFILIATIONS
PUBLICATIONS AND AWARDS
PORTFOLIO
WORD OF THANKS/DANKWOORD

AUTHORS AND AFFILIATIONS

From the Department of Obstetrics and Gynecology, Division of Obstetrics and Prenatal Medicine, Erasmus MC, University Medical Center Rotterdam, The Netherlands

Eric A.P. Steegers,
Niek Exalto,
Irene A.L. Groenenberg,
Robbert H.J. van Oppenraaij,
Christine M. Verwoerd-Dikkeboom

From the Department of Bioinformatics, Erasmus MC, University Medical Center Rotterdam, The Netherlands

Peter J. van der Spek,
Anton H.J. Koning

From the Department of Biostatistics, Erasmus MC, University Medical Center Rotterdam, The Netherlands

Wim C. Hop

From the Department of Intensive care, Erasmus MC, University Medical Center Rotterdam, The Netherlands & Curator collection human and non-human dysmorphology at the Natural History Museum Rotterdam, The Netherlands

Erwin J.O. Kompanje



PUBLICATIONS, AWARDS AND INVITED PRESENTATIONS

Scientific publications and awards related to this thesis

Chapter 1.2

Rousian M, Verwoerd-Dikkeboom CM, Koning AHJ, Van der Spek PJ, Exalto N, Steegers EAP. Innovative three-dimensional imaging: opportunities for virtual embryoscopy. *Ned Tijdschr Geneeskd.* 2010;154:A1606.

Chapter 2.1

Rousian M, Verwoerd-Dikkeboom CM, Koning AHJ, Hop WC, Van der Spek PJ, Exalto N, Steegers EAP. Early pregnancy volume measurements: validation of ultrasound techniques and new perspectives. *BJOG.* 2010;116:278-85.

Chapter 3.1

Rousian M, Koning AHJ, Van Oppenraaij RHF, Hop WC, Verwoerd-Dikkeboom CM, Van der Spek PJ, Exalto N, Steegers EAP. An innovative virtual reality technique for automated human embryonic volume measurements. *Hum Reprod.* 2010;25:2210-6.

Chapter 3.2

Rousian M, Koning AHJ, Hop WC, Van der Spek PJ, Exalto N, Steegers EAP. Gestational sac fluid volume measurements in virtual reality. *Ultrasound Obstet Gynecol.* 2011 doi 10.1002/uog.9033

Chapter 4.1

Rousian M, Verwoerd-Dikkeboom CM, Koning AHJ, Hop WC, Van der spek PJ, Steegers EAP, Exalto N. First trimester umbilical cord and vitelline duct measurements using virtual reality. *Early Hum Dev.* 2011;87:77-82.

Chapter 4.2

Rousian M, Koning AHJ, Van der Spek PJ, Steegers EAP, Exalto N. Virtual reality for embryonic measurements requiring depth perception. *Fertil Steril.* 2011;95:773-4.

Chapter 5.1

Rousian M, Hop WC, Koning AHJ, Van der Spek PJ, Exalto N, Steegers EAP. First trimester embryonic brain development and volumetry using virtual reality. Submitted.

* The Georgio Pardi Foundation President's Presenter Award for outstanding research in the study of the fetal brain (Society for Gynecologic Investigation (SGI) congress, March 26th, 2010).

* The SGI President's Presenter Award (SGI Congress, March 17th, 2011)

Chapter 5.2

Rousian M, Groenenberg IAL, Hop WC, Koning AHJ, Van der Spek PJ, Exalto N, Steegers EAP. Human embryonic growth and development of the cerebellum using three-dimensional ultrasound and virtual reality. Submitted.

Chapter 6.1

Baken L, **Rousian M**, Kompanje EJO, Koning AHJ, Van der Spek PJ, Exalto N, Steegers EAP. Diagnostic techniques and criteria for first trimester conjoined twin documentation. Submitted.

Other scientific publications

Spekknijder L, **Rousian M**, Steegers EAP, Van der Spek PJ, Koning AHJ, Steensma AB. Reproducibility of pelvic floor measurements in contraction using three-dimensional pelvic floor ultrasound and virtual reality. *Ultrasound Obstet Gynecol*. In press.

Reus AD, El-Hamichi H, **Rousian M**, Exalto N, Hop WC, Steegers-Theunissen RPM, Steegers EAP. Early first trimester trophoblast volume measurements using 3D ultrasonography and VOCAL technique. Submitted.

Koning AHJ, **Rousian M**, Verwoerd-Dikkeboom CM, Goedknecht L, Steegers EAP, Van der Spek PJ. V-Scope: design and implementation of an immersive and desktop virtual reality volume visualization system. *Stud Health Technol Inform*. 2009;142:136-8.

Verwoerd-Dikkeboom CM, Koning AHJ, Hop WC, **Rousian M**, Van der Spek PJ, Exalto N, Steegers EAP. Reliability of three-dimensional sonographic measurements in early pregnancy using virtual reality. *Ultrasound Obstet Gynecol*. 2008;32:910-6.

Rousian M, Koning AHJ, Van der Spek PJ, Exalto N, Steegers EAP. Het embryo in virtual reality. *NVOG*. 2009;10:314-5 (invited).

Invited presentations

Rousian M. Three dimensional virtual reality imaging of the early pregnancy. ESHRE annual meeting, June 27th, 2010, Rome, Italy.

Rousian M. Embryonic brain ventricle development and volumetry in virtual reality. Symposium: The fetal brain: in memory of Giorgio Pardi, April 30th, 2010, Milan, Italy.

Rousian M. Three dimensional virtual reality imaging of the early pregnancy. University of Chicago, March 22th, 2010, Chicago, United States.

PORTFOLIO

Summary of PhD training and teaching

Name PhD candidate	Melek Rousian
Erasmus MC Department	Obstetrics and Gynaecology, Division of Obstetrics and Prenatal Medicine
Research School	Netherlands Institute for Health Sciences (NIHES)
PhD period	March 2008 - December 2010
Promotors	Prof. dr. Eric Steegers Prof. Peter van der Spek
Copromotors	Dr. Niek Exalto Dr. Anton Koning

General courses	Year
Biomedical English Writing and Communication, Erasmus MC, Rotterdam, The Netherlands	2009
PhD introduction day, Erasmus MC, Rotterdam, The Netherlands	2009
Master of Science in Clinical Epidemiology, NIHES, Rotterdam, The Netherlands	2009
Public Health Studies, Harvard University, Boston, United States. Courses: 'Society and Health' and 'Ethical Basis: Health Care'	2008

International conferences

International Society of Ultrasound in Obstetrics and Gynecology (ISUOG) congress, Chicago, United States. Poster presentation	2008
WFUMB congress, Sydney, Australia. Oral presentation	2009
European Society of Human Reproduction and Embryology (ESHRE) annual meeting, Amsterdam, The Netherlands. Oral presentation	2009
Society for Gynecologic Investigation (SGI) congress, Glasgow, Scotland. Poster presentation	2009
ESHRE wintercourse, Rotterdam, The Netherlands. Oral presentation	2009
SGI congress, Orlando, United States. Award winning oral presentation	2010
ESHRE annual meeting, Rome, Italy. Invited oral presentation	2010
Symposium: The fetal brain: in memory of Giorgio Pardi, Milan, Italy. Invited oral presentation	2010
ISUOG congress, Prague, Czech Republic. Three oral presentations	2010
University of Chicago, Chicago, United States. Invited presentation	2010
SGI congress, Miami, United States. Award winning oral presentation	2011

National conferences

NIHES Master of Science Symposium, Rotterdam, The Netherlands. Oral presentation	2008
Bo Hjelt Foundation meeting, Rotterdam, The Netherlands. Oral presentation	2009
Symposium Jonge Zwangerschap, Utrecht, The Netherlands. Oral presentation	2009
Symposium: Nederlands Vereniging voor Obstetrie en Gynaecologie, Gynaecongres, Arnhem	2009
Wladimiroff Wetenschapsdag, Erasmus MC, Rotterdam, The Netherlands. Oral presentation	2009

PNDT symposium St. Radboud University, Nijmegen,
The Netherlands. Oral presentation 2010

Grant applications and reviewing papers

ZonMW: Virtual reality echoscopie in het 1e trimester als alsternatief
voor prenatale diagnostiek van structurele aangeboren afwijkingen 2009

Review paper Archives of Gynecology and Obstetrics 2010

Review paper Fertility and Sterility 2010

Teaching activities

Lunchbijeenkomst Financiële Vrienden Erasmus MC, Rotterdam,
The Netherlands 2009

IMC Weekendschool, Kindergeneeskunde-dag, Erasmus MC,
Rotterdam, The Netherlands 2010

Workshop 'Three-dimensional live ultrasound', University of
Chicago, Chicago, United States 2010

NIHES day program for Master of Science students, Erasmus MC,
Rotterdam, The Netherlands 2010

Vriendendag, Erasmus MC-Vriendenfonds, Rotterdam,
The Netherlands 2010

Supervising students and colleagues

Nikki Otte, Keuzeonderzoek Student, Erasmus MC 2009

Jet Wilbers, Keuzeonderzoek Student, Erasmus MC 2010

Leonie Baken, Master's thesis, Erasmus MC 2010

Yentl Gondrie, Keuzeonderzoek Student, Erasmus MC 2010

Averil Reus, PhD project, Erasmus MC 2010

Hakkima el-Harbach, Keuzeonderzoek Student, Erasmus MC 2010

WORD OF THANKS/DANKWOORD

Mijn eerste dag als 18-jarige geneeskundestudent kan ik me nog heel goed herinneren (het is dan ook nog niet zo lang geleden). Ik had toen nooit kunnen bedenken dat een aantal jaar later mijn proefschrift af zou zijn. Het was een bijzonder pad, waarin ik met veel verschillende persoonlijkheden heb mogen samenwerken: een goede leerweg.

Allereerst wil ik alle deelnemers die bereid waren om iedere week een echo te laten maken in het begin van hun zwangerschap bedanken voor hun tijd, inzet en moeite.

Professor Eric Steegers, mijn eerste promotor. Beste professor, als 2^e jaars geneeskundestudent en net Master of Science student werd ik voor mijn onderzoeksstage ingedeeld binnen uw afdeling. U was ontzettend enthousiast over een nog niet lang geleden gestart onderzoek over een virtuele ruimte, genaamd de I-Space. Toentertijd kon ik me er nog niet zoveel bij voorstellen, maar door dit onderzoek heb ik niet alleen veel geleerd, maar het is ook een geweldige periode geweest. Ik ben u dankbaar voor uw enthousiasme en inspirerende begeleiding binnen het onderzoek, en ik zal altijd met een glimlach op mijn gezicht denken aan onze samenwerking.

Dr. Niek Exalto, mijn copromotor. Beste Niek, bij u moet ik altijd denken aan uw volgende woorden: 'Plezier in je werk komt op nummer 1'. Het werken als onderzoeker, u hebbende als mijn dagelijkse begeleider, leverde niet alleen mooie onderzoeksresultaten op, maar was vooral ook plezierig. Ik kan dan ook terugkijken op een tijd waarbij we samen meerdere malen in de I-Space datasets hebben bekeken, ideeën hebben uitgewisseld en manuscripten hebben doorgenomen. Het was mij een genoegen om met u samen te mogen werken!

Dr. Anton Koning, mijn tweede copromotor. Beste Anton, hartelijk dank voor je betrokkenheid bij het project en het bedenken van vele ingewikkelde algoritmen om het gebruik van de I-Space te vergemakkelijken, waarbij ik je helaas alleen maar kon 'helpen' met mijn mening over de nieuwe functie... Verder kwam ik niet. Ik wil je tevens bedanken voor alle tips en trics om te overleven in de elektronica wereld, en voor de ultrasnelle correcties van mijn manuscripten.

Professor Peter van der Spek, mijn tweede promotor. Beste Peter, hartelijk dank voor de mogelijkheid die uw afdeling heeft geboden om dit onderzoek tot stand te brengen en draaiend te houden. Het naar Rotterdam halen van de I-Space was een zeer goede beslissing!

Wim Hop, wij hebben meerdere uren zitten mind-breaken over de statistiek die we hebben losgelaten op onze datasets om tot de resultaten van dit proefschrift te komen. Hartelijk dank voor al je adviezen en hulp!

Irene Groenenberg, zo enthousiast en toegewijd; daar bewonder ik je om. Naast het mooie onderzoek, hebben we het vooral gehad over fashion, sporten, eten en nog veel meer leuke dingen! Hartelijk dank voor deze goede tijd.

De 'jonge garde' van het onderzoek in de I-Space: Robbert vO, Evelien vU, Hein B, Averil R, Manon G, Stephanie E, Leonie S en in het bijzonder Christine VD (als mijn 'voorgangster') en Leonie B (als mijn 'opvolgster'): Dank voor alle hulp tijdens het onderzoek en heel veel succes met het vervolg van jullie onderzoek en opleidingen! Ik zal de goede tijd die we samen hebben doorgebracht missen.

In mijn dankwoord kan in natuurlijk alle personeel van de afdeling Obstetrie en Prenatale geneeskunde niet vergeten. Ik wil jullie bedanken voor alle ondersteuning, maar vooral voor de gezellige en leerzame tijd.

In het bijzonder wil ik Anneke S, Peter vH en Frederique vD bedanken voor al hun adviezen en goede gesprekken over het onderzoek, maar ook privé! Ik zal jullie zeker missen.

De afdeling Bioinformatica kan ik ook niet vergeten: bedankt voor alle hulp en moeite bij de totstandkoming van dit proefschrift en de website!

Lieve onderzoekers: kamers HE111, 115 en 117, kamer HS508, kamers op de 22^e en recent toegevoegd kamers op de Westzeedijk: bedankt voor de gezellige lunches, borrels, etentjes, congressen (MIAMI BEACH): I always had great fun spending time with you!

Mijn paranimfen: Anneke en Christianne. Lieve An, wij zaten in dezelfde studiegroep in jaar 1 en samen hebben wij ons opgegeven voor de Master of Science opleiding: we hebben een fantastische tijd doorgemaakt, de zomers samen doorgekomen, roommates in de USA, we hebben altijd hele lange, kritische gesprekken: Gracias tibi ago! Tanne: lief, behulpzaam, gezellig, kritisch, avontuurlijk, VWO, bordenwisper, vakantie, zon, skiën, Bursa, Spanje: er zijn zoveel woorden die in mij opkomen als ik aan jou denk, wat maar weer illustreert hoeveel wij al samen hebben meegemaakt en hopelijk nog zullen meemaken! Tu eres especial!

Zey, Hasret en Cawai: wij als de onafscheidelijke vierling: jullie zijn al heel erg lang in mijn leven, vooral Zey (lees kleutertijd): jullie staan echt ALTIJD klaar voor mij: grote bewondering en liefde, dank jullie wel. Bij de mensen die voor mij klaarstaan, horen ook Fatma, Hossei, Zohra, Zeynep, Serap, Serpil, Melissa, Gerthe, Sylvia, Pinar, Yasemin, Burcu: Stuk voor stuk verschillende persoonlijkheden, maar echt SUPER vrouwen. Bedankt voor alle fantastische momenten! Ik houd van jullie! Lieve Zeynep: tijdens onze studietijd waren jij, PP en ik vaak onafscheidelijk samen, waarbij wij ontelbare momenten hebben meegemaakt waar ik dagelijks nog aan terugdenk. Dank je voor je vriendschap.

Alle andere vrienden van de studietijd, die ik ontmoet heb tijdens de geneeskunde en de Master of Science opleiding (I will not forget the USA), tijdens mijn tijd bij de IFMSA, en tenslotte als laatst toegevoegd aan mijn leven als student mijn cogroep (1) wil ik hartelijk danken voor hun aanwezigheid en gezelligheid.

Aan alle familie en schoonfamilie: Bedankt voor jullie aanwezigheid, steun en begrip, maar vooral voor alle gezellige momenten die wij samen tijdens deze periode hebben meegemaakt.

Lieve mama en papa: jullie zijn er altijd voor mij, onvoorwaardelijke liefde! Dat hebben jullie ons ook altijd bijgebracht. Baba, ik ben enorm trots op hoe u samen met Anne het leven heeft opgebouwd waarin wij zijn opgegroeid: vol liefde en respect, want dat staat op nummer één in ons gezin. Anne, al woon ik niet meer thuis, u waakt nog altijd over mij. Ik wil u bedanken voor al uw steun en warmte die u mij heeft gegeven.

Mijn 3 zussen: stuk voor stuk geweldige en heel verschillende persoonlijkheden. Cagla, als kleine zussen speelden we niet vaak samen, vanwege onze verschillende interesses. Ik speelde met poppen, puzzels en turnde. Jij klom in bomen en hield van voetballen. Hoe ouder we werden, hoe meer raakvlakken we kregen. Ik ben dan ook erg blij dat je mijn zus bent, ook al plaag ik je soms nog graag ☺. Bedankt dat je me op moeilijke momenten uit de brand hebt geholpen. Ik hoop dat we snel weer samen op vakantie kunnen!

Merve en Ece, toen jullie werden geboren waren Cagla en ik ontzettend blij. Als grote zussen voelden wij ons ook een beetje mama geworden. Ondertussen zitten jullie allebei op de middelbare school, en ben ik erg trots op jullie prestaties! Het is altijd super gezellig als jullie langskomen of als we samen leuke dingen doen! Zussen, ik houd van jullie...

En dan als laatste, sevgilim Ilim. Wie had ooit gedacht dat de macho en meest populaire jongen van de middelbare school met Melek zou trouwen? Gelukkig is het wel gebeurd! Ik wil je hemelsbreed bedanken voor de goede zorgen, steun, liefde en vooral geduld; wat er toe heeft geleid dat het combineren van alle dingen in mijn leven lukt! Je bent een top vent! Seni seviyorum.

